

DESIGN AND MANUFACTURE OF A SCALABLE PROSTHETIC HAND THROUGH THE  
UTILIZATION OF ADDITIVE MANUFACTURING

A Major Qualifying Project Report:

Submitted to the Faculty

of the

WORCESTER POLYTECHNIC INSTITUTE

in partial fulfillment of the requirements for the

Degree of Bachelor of Science

By

**Sean Greene**

**Daniel Lipson**

**Abimael Mercado**

**Aung Heain Soe**

Date:

Approved By:

---

Prof. David C. Planchard, Project Advisor

---

Prof. Glenn R. Gaudette, Project Co-Advisor

## Table of Contents

Table of Figures .....	5
List of Tables .....	9
Nomenclature .....	11
Abstract.....	13
Introduction .....	14
Background .....	16
Rapid Prototyping.....	17
Physiology .....	19
Components of a 3D Prosthetic Hand .....	21
e-NABLE Group and Designs.....	24
Previous MQPs .....	25
Design of a Powered Hand Orthosis .....	25
Design of a Powered Hand Orthosis 2 .....	25
Intelligent Robotic Hand Design .....	26
Design of a Human Hand Prosthesis .....	26
Design of a Prosthetic Robotic Hand.....	28
Benchmarking .....	29
Cyborg Beast.....	30
Talon Hand .....	31
Odysseus Hand .....	32
Flexy Hand.....	33
Flexy Hand 2.....	34
Raptor Hand .....	35
Raptor-Reloaded Hand .....	36
Dextrus Hand.....	37
Osprey Hand.....	38
Phoenix Hand .....	39
K-1 Hand.....	40
Methods and Procedure.....	41
Design Specifications .....	41
Weighted Decision Matrix.....	43
Decision Matrix Scaling weights .....	45

Weight .....	45
Max capable load.....	45
Range of motion.....	45
Cost .....	45
Time to assemble.....	45
Durability.....	45
Operating temperature .....	46
Time to print.....	46
Scalability.....	46
Cosmetics .....	46
Safety .....	46
Serviceability.....	46
Determination of Decision Matrix Scores .....	47
Material .....	47
Number of Joints.....	48
Tensioning Device .....	49
Printer Information .....	52
Infill .....	54
Design Methodology.....	55
Hand base .....	57
Fingers, Thumb, and Pins .....	62
Gauntlet .....	72
Tensioning Device .....	78
Global Variables .....	82
Testing Procedure .....	84
Kinematic Analysis .....	86
Mobility .....	86
Design Analysis .....	88
Experiences with Additive Manufacturing.....	97
Instron Testing .....	102
Assembly Instructions .....	118
Conclusion .....	130
Prototype Assessment.....	130

Future Work.....	131
Appendices .....	132
Appendix A: An Overview of Rapid Prototyping Processes.....	132
SLA.....	132
SLS.....	132
LOM.....	132
FDM.....	132
3D Printing.....	132
MJP .....	133
Appendix B: How to Change Hand Sizing and Save STL Files.....	134
Step 1: Open the Assembly. ....	134
Step 2: Opening the Equations Dialogue .....	135
Step 3: Opening the Equations Text File.....	135
Step 4: Editing the Input Dimension .....	136
Step 5: Save the Parts as STL Files.....	137
Step 6: Fixing Scaling Issues (Not Always Applicable) .....	137
Appendix C: Brochure .....	139
Appendix D: Mathcad Calculations .....	141
Works Cited .....	151

# Table of Figures

Figure 1: Bones in the Hand.....	19
Figure 2: Types of Wrist Movements.....	19
Figure 3: Prototype Hand (Two-Segment Finger) Exploded View.....	21
Figure 4: Prototype Hand (Three-Segment Finger) Exploded View.....	21
Figure 5: Two-Segment Finger Exploded View.....	22
Figure 6: Three-Segment Finger Exploded View.....	22
Figure 7: Thumb Exploded View.....	22
Figure 8: First Generation Hand Exploded View.....	23
Figure 9: First Generation Finger Exploded View.....	23
Figure 10: Ratcheting Tensioning Mechanism Exploded View.....	23
Figure 11: FBD Example from MQP.....	25
Figure 12: Force vs Cable Angle.....	26
Figure 13: Hand Cover Designs.....	27
Figure 14: Cable Tension Mechanism.....	28
Figure 15: Cyborg Beast.....	30
Figure 16: Odysseus Hand.....	32
Figure 17: Flexy Hand 1.....	33
Figure 18: Flexy Hand 2.....	34
Figure 19: Raptor Hand.....	35
Figure 20: Raptor-Reloaded Hand.....	36
Figure 21: Dextrus Hand.....	37
Figure 22: Osprey Hand.....	38
Figure 23: Phoenix Hand.....	39
Figure 24: K-1 Hand.....	40
Figure 25: ABS.....	47
Figure 26: PLA.....	48
Figure 27: Two-Segment Finger.....	48
Figure 28: Three-Segment Finger.....	49
Figure 29: Ratchet System.....	49
Figure 30: Pin System.....	50
Figure 31: Screw System.....	50
Figure 32: XYZ da Vinci 1.0 AiO.....	52
Figure 33: Dimension SST 1200es.....	53
Figure 34: MakerBot Replicator 2.....	53
Figure 35: Sindoh 3DWOX.....	53
Figure 36: Hand Assembly 1.....	55
Figure 37: Hand Assembly 2.....	55
Figure 38: Hand Assembly 3.....	55
Figure 39: Hand Assembly 4.....	56
Figure 40: Hand Assembly 5.....	56
Figure 41: Concept Hand Base with Adjustable Thumb.....	57
Figure 42: Concept Hand Base with Two Ratchet Systems.....	57
Figure 43: Gen 1 Hand Base; Isometric View.....	58

Figure 44: Gen 1 Hand Base; Alternate View .....	58
Figure 45: Gen 1.1 Hand Base.....	58
Figure 46: Gen 2 Hand Base; Isometric View.....	59
Figure 47: Gen 2 Hand Base; Bottom View.....	59
Figure 48: Gen 3 Hand Base; Isometric View.....	59
Figure 49: Gen 3 Hand Base; Back View .....	59
Figure 50: Gen 4 Hand Base; Side View.....	60
Figure 51: Gen 4 Hand Base; Isometric View.....	60
Figure 52: Gen 5.1 Hand Base; Isometric View.....	61
Figure 53: Gen 5.1 Hand Base with Velcro Attachment Screws .....	62
Figure 54: Concept Finger .....	62
Figure 55: Concept Thumb.....	62
Figure 56: Gen 1 Finger; Assembly.....	63
Figure 57: Gen 1 Finger; Proximal Phalange .....	63
Figure 58: Gen 1 Finger; Middle Phalange.....	63
Figure 59: Gen 1 Finger; Distal Phalange .....	63
Figure 60: Gen 1 Finger; Distal Phalange; Isometric View .....	63
Figure 61: Gen 1 Thumb; Proximal Phalange .....	63
Figure 62: Gen 1 Thumb; Distal Phalange; Alternate View.....	64
Figure 63: Gen 1 Thumb; Distal Phalange; Bottom View.....	64
Figure 64: Gen 2 Finger; Middle Phalange Bottom.....	64
Figure 65: Gen 2 Finger; Middle Phalange Top.....	64
Figure 66: Gen 2 Finger; Middle Phalange Top Design 2.....	65
Figure 67: Gen 2 Finger; Middle Phalange Top Design 3.....	65
Figure 68: Gen 2 Finger; Top Design Print Failure .....	65
Figure 69: Gen 2 Finger; Snap Pin Failed Tolerance .....	65
Figure 70: Gen 2 Finger; Distal Phalange; Side View.....	66
Figure 71: Gen 2 Finger; Assembly; Side View .....	66
Figure 72: Single Piece Proximal Fingers.....	66
Figure 73: Gen 3 Finger Assembly.....	67
Figure 74: Gen 3 Finger; Middle Phalange; End View .....	67
Figure 75: Gen 3.1 Finger Assembly.....	67
Figure 76: Gen 3.2 Finger; Assembly; Isometric View .....	67
Figure 77: Gen 3.2 Finger; Assembly; Side View .....	67
Figure 78: Gen 2 Thumb; Assembly.....	67
Figure 79: Generation 3.3 Finger, Proximal; Isometric View.....	68
Figure 80: Generation 3.3 Finger, Middle; Isometric View .....	68
Figure 81: Generation 3.4 Finger, Proximal; End View.....	69
Figure 82: Generation 3.5 Finger, Proximal; Isometric View.....	69
Figure 83: Generation 3.5 Finger, Proximal; Side Cross-Sectional View .....	69
Figure 84: Two-Joint Finger; Assembly .....	70
Figure 85: Two-Joint Finger; Sub-Assembly.....	70
Figure 86: Two-Joint Finger; Sub-Assembly; Front View.....	71
Figure 87: Two-Segment Finger; Sub-Assembly; Bottom View .....	71

Figure 88: Finger Pin Gen 1 .....	71
Figure 89: Finger Pin Gen 2 .....	71
Figure 90: Leather Gauntlet Attachment Concept Sketch.....	72
Figure 91: Leather Gauntlet Attachment Concept Assembly .....	73
Figure 92: Gen 1 Gauntlet with Holes for Tensioning Pins .....	73
Figure 93: Gen 2 Gauntlet with Holes for Ratchet Tensioning Mechanism .....	74
Figure 94: Gen 3 Gauntlet with Mounting Space for Tensioning System.....	74
Figure 95: Gen 4 Gauntlet with Sliding Mechanism.....	75
Figure 96: Gen 5 Gauntlet with Sliding Mechanism and Cable Bridge.....	76
Figure 97: Gen 6 Gauntlet with Cable Bridge .....	76
Figure 98: Gen 7 Gauntlet with Sliding Mechanism and Cable Bridge.....	77
Figure 99: Gen 7.1 Gauntlet with Sliding Cover.....	77
Figure 100: Sketch of Early Concept Ratchet Tensioning Device.....	78
Figure 101: Gen 1 Tensioning Mechanism; Front View .....	78
Figure 102: Gen 1 Tensioning Mechanism; Exploded View .....	79
Figure 103: Gen 1 Tensioning Mechanism; Isometric View .....	79
Figure 104: Gen 1.1 Gauntlet Tensioning Mechanism; Isometric View.....	79
Figure 105: Gen 1.2 Gauntlet Tensioning Mechanism; Isometric View.....	80
Figure 106: Snap Pin; Front View .....	80
Figure 107: Top “T Shape” Locking Device - Isometric View .....	81
Figure 108: Locking Device Test piece - Isometric View .....	81
Figure 109: Gen 2 Gauntlet Tensioning Mechanism; Top View.....	81
Figure 110: Gen 2 Gauntlet Tensioning Mechanism; Isometric View.....	81
Figure 111: Global Variables and Equations .....	82
Figure 112: Each dimension is inserted into global variable or equation .....	83
Figure 113: Mobility of Two-Segment Finger-Hand Design .....	86
Figure 114: Mobility of Three-Segment Finger-Hand Design.....	87
Figure 115: Representation of Print Layers .....	88
Figure 116: Cross Section View of the Finger Assembly .....	89
Figure 117: Distal Phalange Displacement Analysis .....	90
Figure 118: Distal Phalange Von Mises Stress Analysis .....	90
Figure 119: Middle Phalange Displacement Analysis.....	90
Figure 120: Middle Phalange Von Mises Stress Analysis.....	90
Figure 121: Proximal Phalange Displacement Analysis.....	90
Figure 122: Proximal Phalange Von Mises Stress Analysis.....	90
Figure 123: Old Pin Design .....	91
Figure 124: New Pin Design.....	91
Figure 125: Previous Design .....	91
Figure 126: Improved Design .....	91
Figure 127: Free Body Diagram of Gauntlet.....	92
Figure 128: Old Wrist Pin Von Mises Analysis (left) and Deformation Analysis (right) .....	93
Figure 129: New Wrist Pin Von Mises Analysis .....	94
Figure 130: Old Wrist Joint (left) and Updated Wrist Joint (right) of a Gauntlet.....	95
Figure 131: Free Body Diagram of a Gauntlet.....	95

Figure 132: Gauntlet Von Mises Analysis (left) & Deformation Analysis (right) .....	96
Figure 133: Program Generated Supports .....	99
Figure 134: Added Supports in Gauntlet Design .....	99
Figure 135: Failed Distal Phalange with Ratchet System .....	100
Figure 136: Failed Ratchet Mechanism System Spool .....	100
Figure 137: Failed Ratchet Mechanism System Shaft.....	100
Figure 138: Printing Multiple Components.....	100
Figure 139: Example of De-Lamination .....	101
Figure 140: Instron Testing Setup .....	102
Figure 141: Instron Testing Results for 4 Samples in Tensile for Three-Segment Fingers .....	103
Figure 142: Instron Testing Results for 4 Samples in Tensile for Two-Segment Fingers .....	104
Figure 143: Testing Results for 4 Samples in Compression for Two-Segment Fingers .....	107
Figure 144: Instron Testing Results for 4 Samples in Cyclic for Two-Segment Fingers.....	107
Figure 145: Safety Factor Calculation for Two-Segment Fingers in Tensile .....	110
Figure 146: Safety Factor Calculation for Two-Segment Fingers in Cyclic .....	111
Figure 147: Safety Factor Calculation for Two-Segment Fingers in Compression .....	111
Figure 148: Safety Factor Calculation for Three-Segment Fingers in Tensile.....	112
Figure 149: Instron Setup for Force to Close Hand .....	113
Figure 150: Mathcad for Gen2 (Two-Segment) Model.....	114
Figure 151: Mathcad for Gen2 (Two-Segment) Model Force to Close.....	115
Figure 152: Mathcad for Gen3 (Two-Segment) Model Force to Close.....	116
Figure 153: Mathcad for Gen3 (Two-Segment) Model Force to Close.....	117
Figure 154: Exploded view of hand showing all the parts labeled with numbers.....	118
Figure 155: Parts comprising finger.....	121
Figure 156: Completed finger for comparison .....	121
Figure 157: Completed set of fingers .....	121
Figure 158: Parts needed for finger to hand base .....	122
Figure 159: Completed finger and hand base .....	122
Figure 160: Parts needed for hand base to gauntlet.....	122
Figure 161: Complete 3D hand without tension.....	123
Figure 162: Return cable through finger.....	123
Figure 163: Return cable pair.....	123
Figure 164: Pair of fingers tied together .....	124
Figure 165: All the return cables tied.....	124
Figure 166: Tension cable fed through top channel.....	124
Figure 167: Tension cable tied to finger with clinch knot .....	125
Figure 168: All the fingers tied.....	125
Figure 169: Tension cables through hand base and gauntlet .....	125
Figure 170: Example of pitch angle for gauntlet .....	126
Figure 171: Tensioning the hand.....	126
Figure 172: Tension hand with primary and secondary screws .....	126
Figure 173: Added Cover .....	127
Figure 174: Hand base and gauntlet with foam added .....	127
Figure 175: Hand base with leather option .....	127



Figure 176: Hand with gel finger tips .....	128
Figure 177: Hand with Velcro on gauntlet.....	128
Figure 178: Completed 3D prosthetic hand .....	128
Figure 179: Final Prototype .....	130
Figure 180: Full assembly of 2 Segment Hand.....	134
Figure 181: Step 1; Changing the Configuration.....	134
Figure 182: Step 2; Open the Equations Dialogue. ....	135
Figure 183: Step 3; Open the Equations Text File.....	135
Figure 184: Step 4; Editing the Input Dimension .....	136
Figure 185: New Hand Size! .....	136
Figure 186: Step 5; Save as an STL .....	137
Figure 187: Fixing Potential Scaling Issues.....	138
Figure 188: Outside Page of Brochure .....	139
Figure 189: Inside Page of Brochure.....	140
Figure 190: Nomenclature.....	141
Figure 191: Calculations of Factor of Safety.....	142
Figure 192: Calculations of Factor of Safety of Tensile Strength; Continued .....	143
Figure 193: Calculations of Factor of Safety and Mean of Tensile Strength .....	144
Figure 194: Calc. of Standard Deviation of Tensile Strength and Data of Cyclic Loading .....	145
Figure 195: Calculations of Factor of Safety of Cyclic Loading.....	146
Figure 196: Calc. of Factor of Safety, Mean and Standard Deviation of Cyclic Loading .....	147
Figure 197: Compression Testing of Two-Segment Fingers.....	147
Figure 198: Compression Testing of Two-Segment Finger: Specimen #5.....	148
Figure 199: Data and Calculations of Factor of Safety of Compression Testing .....	148
Figure 200: Calc. of Factor of Safety, Mean and Standard Deviation of Compression Testing .....	149
Figure 201: Data of Compression Testing .....	149
Figure 202: Calc. of Factor of Safety, Mean and Standard Deviation of Tensile Strength.....	150

## List of Tables

Table 1: Nomenclature.....	11
Table 2: Nomenclature; Continued.....	12
Table 3: Wrist Flexion Angles.....	20
Table 4: Muscle Dynamics in the Hand .....	20
Table 5: Bill of Materials of Prototype Hand Assembly (Two-Segment Finger) .....	21
Table 6: Bill of Materials of Prototype Hand Assembly (Three-Segment Finger) .....	21
Table 7: Bill of Materials of Two-Segment Finger .....	22
Table 8: Bill of Materials of Three-Segment Finger .....	22
Table 9: Bill of Materials of Thumb Assembly.....	22
Table 10: Bill of Materials of First Generation Hand Assembly .....	23
Table 11: Bill of Materials of First Generation Finger Assembly .....	23
Table 12: Bill of Materials of Ratcheting Tension Mechanism Assembly .....	23
Table 13: Design Specifications .....	41
Table 14: Design Specifications; Continued .....	42

Table 15: Weighted Decision Matrix.....	43
Table 16: Weighted Decision Matrix; Continued.....	44
Table 17: Instron Testing Results for 4 Samples in Tensile for Three-Segment Fingers.....	103
Table 18: Instron Testing Results for 4 Samples in Tensile for Two-Segment Fingers .....	104
Table 19: Testing Results for 4 Samples in Tensile for Two-Segment Fingers; Continued.....	105
Table 20: Testing Results for 4 Samples in Tensile for Two-Segment Fingers; Continued.....	106
Table 21: Testing Results for 4 Samples in Cyclic for Two-Segment Fingers.....	108
Table 22: Results for 4 Samples in Cyclic for Two-Segment Fingers; Continued .....	109

# Nomenclature

Table 1: Nomenclature

Symbol	Definition	Symbol	Definition	Symbol	Definition
$m$ (grams)	Mass	$\epsilon$ (dimensionless)	Strain	PIP	Proximal Interphalangeal (Joint)
kg	Kilograms	$E$ (N/m <sup>2</sup> )	Elastic Modulus	DIP	Distal Interphalangeal (Joint)
$g$ (9.81m <sup>2</sup> /s)	Gravitational acceleration	$J$ (°)	Compliance	MP	Metacarpophalangeal (Joint)
$A$ (in <sup>2</sup> )	Area	Oz.	Ounces	CM	Carpometacarpal (Joint)
$r$ (in)	Radius	$\pi$	Pi: ~3.14159	IC	Intercarpal (Joint)
Pa	Pascals	N	Newtons	RC	Radiocarpal (Joint)
$\mu$	Coefficient of friction	$F_r$ (Newtons)	Frictional Force	GM	Greater Multangular
h	Hours	$\rho$ (g/mL <sup>3</sup> )	Density	LM	Lesser Multangular
L x W x H (in)	Length, Width, Height	W (grams)	Weight	FP	First Phalangeal (Series)
$g$	Grams	F (Newtons)	Force	SP	Second Phalangeal (Series)
(') (ft)	Feet	s	Seconds	TP	Third Phalangeal (Series)
(") (in)	Inches	d (in)	Distance	FDS	Flexor Digitorum Sublimis
m	Meter	$\tau$ (N*m)	Torque	FDP	Flexor Digitorum Profundus
cm	Centimeter	t (seconds)	Time	FCU	Flexor Carpi Ulnaris
mm	millimeter	ABS	Acrylonitrile Butadiene Styrene	FCR	Flexor Carpi Radialis

Table 2: Nomenclature; Continued

Symbol	Definition	Symbol	Definition	Symbol	Definition
$\sigma$	Stress (N/m <sup>2</sup> )	PLA	Polylactic Acid	FPL	Flexor Pollicis Longus
APL	Abductor Pollicis Longus	PL	Palmaris Longus	EDC	Extensor Digitorum Communis
ECU	Extensor Carpi Ulnaris	ECRL	Extensor Capri Radialis Longus	ECRB	Extensor Carpi Radialis Brevis
EIP	Extensor Indicis Proprius	EPL	Extensor Pollicis Longus	ECRL	Extensor Carpi Radialis Longus
FPB	Flexor Pollicis Brevis	I	Interosseus	L	Lumbricalis
OP	Opponens Pollicis				

# Abstract

The objective of this project was to create a freely-available, scalable, 3-Dimensional (3D) printable prosthetic hand. Current 3D printed prosthetic hand designs are openly available and inexpensive to produce with a 3D printer; however, these prosthetics are also prone to failure. Tolerance issues, printing errors, and poor instructions lead to a significant number of prosthetics that cannot be assembled, do not work correctly, or break with light use. We aim to provide a solution to these problems through the use of equation based scaling and proper instructions. Resizing available 3D printed prosthetics does not always work, as holes and joints will scale with the rest of the device by the same amount, reducing functionality when larger or smaller than the initial design. Our design scales using equations to scale different features at different rates, and a provided text file allows for variable editing. It is also as reliable and easy to assemble as currently available hands.

There are two main methods of operation for these prosthetics: wrist powered and elbow powered. A decision was made to focus on wrist powered devices, as they are more common and provide another joint of movement. These devices work by the wearer bending down their wrist, allowing the tensioning cables to pull the fingers closed. Releasing the wrist allows elastics to return the fingers to a resting state. This specific prosthetic is intended for users with a moving wrist that has at least part of their palm to attach the device to.

# Introduction

With the emerging field of 3D printing, inexpensive 3D printed prosthetics are continually being developed to replace commercially developed prosthetics. High end prosthetics can cost thousands of dollars, which is unfortunately not affordable for many of those in need of prosthetic hands. As children grow, they need new prosthetics to fit their growing arms, which would cost more than a fully grown arm. One of the main advantages of 3D printed prosthetic hands is that they allow for custom prosthetics at a fraction of the price. While low income families may not be able to afford a new traditional prosthetic at the cost of several thousand dollars, there is a much greater chance of being able to afford a 3D printed prosthetic at the cost of approximately \$50 dollars.

While low cost 3D printed prosthetics are currently available, many fail due to scaling files below the printer's capable resolution, depending on the model of the printer. These prosthetics are difficult to assemble, do not scale properly, and will not stand up to day-to-day use for a significant period of time.

There are many benefits to 3D printed prosthetics such as cost, versatility, speed, growth, and comfort<sup>1</sup>. Prosthetics that are commercially made can cost between \$5,000 and \$50,000. A 3D printed prosthetic can cost approximately \$50 from e-NABLE. A commercially made prosthetic can take up to months to both produce and calibrate and a 3D printed prosthetic takes about one day to print. 3D printed prosthetics are very versatile and customizable. The prosthetics can be designed to fit the specific user as well as various activities. In terms of growth, children who are in need of a prosthetic constantly grow out of their prosthetic until they have finished developing. Being able to print inexpensive 3D prosthetics allows users to frequently replace outgrown devices without paying for more expensive commercially made products. In terms of comfort, many sockets that are made commercially are uncomfortable compared to 3D printed alternatives.

As a primary goal, the team aimed to produce a functioning 3D printed prosthetic hand that is capable of scaling based on user driven dimensions. Using imported dimensions through the use of a text file; the SolidWorks Models can be customized to fit the user. The 3D printed hand is available for the same cost as other models featured on e-NABLE while increasing the functionality, reliability, and ease of assembly. Through the optimization of previous e-NABLE hand models as well models developed by the team a functional prosthetic was developed.

## Background

The purpose of this project was to build a low cost 3D printed mechanical prosthetic hand with the design intent of reliability, scalability, and ease of assembly. 3D printing is an additive manufacturing process that allows individuals to model parts utilizing computer aided software and fabricate physical models using 3D printers. This allows a wide variety of individuals and communities with limited resources to have otherwise much more expensive prosthetics without an engineering background or hands on abilities. There are currently many types of 3D printed prosthetic hands with different functionalities, appearances, and requirements, and a large portion of the designs are open-source and available for public users to download, modify, and print. One of the most well-known groups in the 3D printed prosthetic community is e-NABLE, which was founded by Professor Jon Schull from Rochester Institute of Technology and Ivan Owen. It was started from 2011, when Ivan Owen designed a mechanical hand device and posted a video of it to YouTube. A carpenter named Richard from South Africa had lost four of his fingers saw Ivan's YouTube video, and reached out for help. Ivan developed a set of fingers for Richard based on a 19th century prosthetic design<sup>ii</sup>, and they began working together to improve the design. Soon after, they began working on a prosthetic for a five year old child named Liam, who was born without a thumb or fingers on his right hand<sup>iii</sup>. When Ivan realized the need to design a device that would scale as Ivan grew, he invented the 3D printed prosthetic hand to accomplish the task. In 2013, Professor Jon Schull and Ivan Owen created a Google+ community, e-NABLE to help out individuals in need. The community quickly grew and is now at over 7000 members and volunteers that have printed and gifted thousands of devices across the world. Ever since the community was founded, it has been very active at not only helping others print their own hands, but also modifying and improving existing designs.



## Rapid Prototyping

Rapid Prototyping (RP) can be defined as a group of techniques used to quickly fabricate a scale model of a part or assembly using 3D computer aided design (CAD) data<sup>iv</sup>. The concept of RP was developed in the early 1980s in order to provide quicker, cheaper prototypes. Without the need for tooling setups or skilled model makers, modeling prototypes could be done in a fraction of the time for a fraction of the cost<sup>v</sup>. RP began with Stereo lithography (SLA), a process patented in 1986 by 3D systems company founder, Charles (Chuck) W. Hull. <sup>vi,vii</sup> SLA is a process where an Ultraviolet (UV) light cures a liquid photopolymer one layer at a time to produce a 3D object. Since then, more rapid prototyping technologies have been developed. The new RP technologies currently available are Selective Laser Sintering (SLS), Laminated Object Manufacturing (LOM), Fused Deposition modeling (FDM)<sup>viii</sup>, Multi-jet printing (MJP)<sup>ix</sup>, and 3D printing. Each technology has its own advantages and disadvantages, and are each used for unique applications. A brief overview of the different types of RP is available in Appendix A: An Overview of Rapid Prototyping Processes.

With the help of CAD software, a 3D model is created and converted into an STL file, which is currently the standard format in the RP industry. STL files provide a 'triangular representation of the 3D surface geometry' in the form of text<sup>x</sup>. For current processes, these files are typically sent to another software package that converts them into another file type, such as G-Code, which is readable in RP machines. The software package can either send this data directly to an RP machine, or be saved to a portable device to be used by the RP machine itself.

Rapid prototyping is an additive process, and is alternatively known as additive manufacturing. Typical manufacturing processes, such as milling or turning, are subtractive processes. In a subtractive manufacturing process, a large stock material is cut or drilled into a smaller piece (or pieces) of the desired form. In additive manufacturing, many small pieces of stock, which can come in several forms including powder and filament, are combined to form the desired shape. The main advantages, in general, of additive manufacturing are that complexity can be added at

no cost, no tooling is required, waste is reduced, less operator skill is required, and some assemblies can be made already put together.

On the other hand, additive manufacturing generally requires post processing, results in parts with reduced mechanical properties, limited and relatively expensive selection of materials, and is much more difficult to scale as a process<sup>xi</sup>. Part geometry play an important role in how they are printed. This is also true when trying to reduce the amount material wasted due to the raft and support material. The geometry of the parts printed require a flat surface in order to minimize the material wasted.

For this project, we will be using one of the RP processes, 3D printing, for fabricating our prototypes and final design. 3D Printing has become widely used in multiple industrial sectors of industries ranging from airplane components<sup>xii</sup> to medical devices<sup>xiii</sup>. In today's market, 3D printers are available for both personal and professional use. The cost of 3D printers depends on their resolutions and material usage, and can range from approximately \$100<sup>xiv</sup> to millions of dollars<sup>xv</sup>. For this project, we will be using an XYZ Da Vinci 1.0, Dimension SST 1200es, Makerbot Replicator 2, and Sindoh 3D printer to fabricate our designs.

## Physiology

The human hand consists of five different sets of bones. The carpal bones consists of the greater multangular (GM), navicular (N), lunate (L), triquetrum (T), pisiform (P), lesser multangular (LM), capitate (C), and hamate (H) bones. The metacarpal bones consist of the M-I, II, III, IV, and V bones. The first phalangeal (FP) bones consist of FP-I, II, III, IV, V. The second phalangeal series consists of SP-II, III, IV, and V. The third phalangeal series consists of TP-I, II, III, IV, V. The different joints in the hand consist of the radiocarpal (RC), intercarpal (IC), carpometacarpal (CM), metatarsophalangeal (MP), proximal interphalangeal (PIP), distal interphalangeal (DIP)<sup>xvi</sup>. Figure 1 below indicates the bones located within the human hands with the bones and joints abbreviated as discussed in this section.

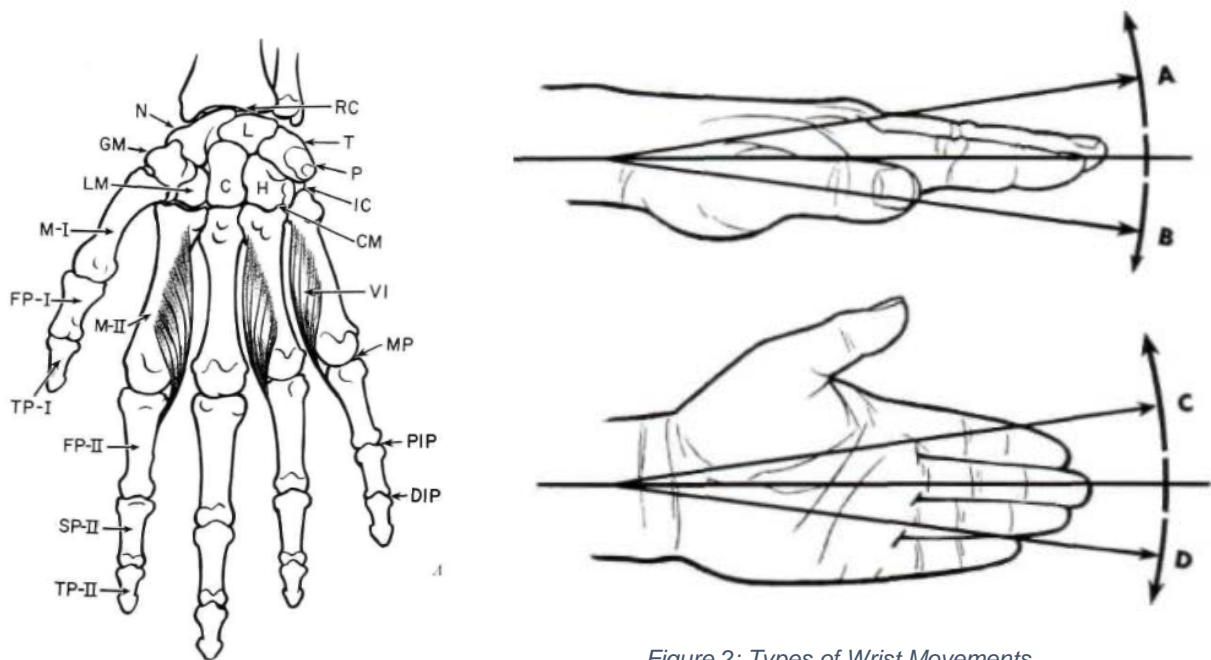


Figure 1: Bones in the Hand

Figure 2: Types of Wrist Movements

Figure 2 indicates the angles of rotation about the wrist. Dorsiflexion or extension is indicated by angle *A*, flexion or volar flexion is indicated by angle *B*, radial flexion is indicated by angle *C*, and ulnar flexion is indicated by angle *D*.

Table 3: Wrist Flexion Angles

ANGULAR EXTENT OF WRIST FLEXIONS						
Articulation	Dorsal Flexion (deg.)	Volar Flexion (deg.)	Total (deg.)	Ulnar Flexion (deg.)	Radial Flexion (deg.)	Total (deg.)
Capitate-radius	78	44	122	28	17	45
Capitate-lunate.	34	22	56	15 <sup>b</sup>	8 <sup>b</sup>	23 <sup>b</sup>
Lunate-radius	44	22	66	13 <sup>c</sup>	9 <sup>c</sup>	22 <sup>c</sup>

In Table 3: Wrist Flexion Angles, the hand muscle dynamics are clearly displayed. The values are based upon the average of 15 young males at the University of California.

Table 4: Muscle Dynamics in the Hand

HAND MUSCLE DYNAMICS			
Action	Muscles	Total Fick Forces <sup>a</sup> (lb.)	Measured Force (lb.)
Hand-on wrist:			
Volar Flexion	FDS, FDP,FCU, FCR, FPL, APL,	730 <sup>b</sup>	50.0 <sup>c</sup>
Dorsal Flexion	PL, EDC, ECU, ECRL, ECRB,	367	30.0 <sup>c</sup>
Radial Flexion	EIP, EPL, ECRL, APL, EIP,	244	38.0 <sup>c</sup>
Ulnar Flexion	ECRB, FCR,	227	29.5 <sup>c</sup>
Prehension:	FCU, ECU		
Palmar			21.5
Tip	FDS, FPL, FDP, L, FPB, OP		21.0
Lateral	FDS, FPL, FDP, L, FPB, OP FPB, OP, FPL, I		23.0

The types of flexion denoted by A, B, C or D in Figure 2 also relate to the forces in Table 3 and Table 4 as denoted using the superscript.

## Components of a 3D Prosthetic Hand

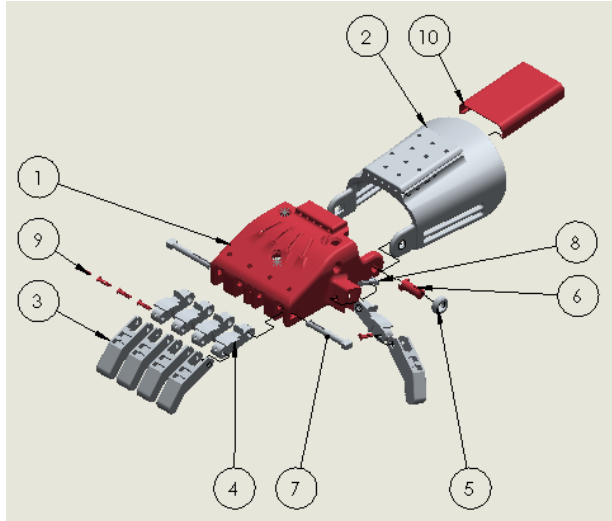


Figure 3: Prototype Hand (Two-Segment Finger)  
Exploded View

Table 5: Bill of Materials of Prototype Hand Assembly  
(Two-Segment Finger)

ITEM NO.	DESCRIPTION	QTY.
1	Hand base	1
2	Gauntlet	1
3	Distal Finger	5
4	Proximal Finger	5
5	wrist pin cap	2
6	wrist pin long	2
7	Knuckle Pin	2
8	Thumb To Hand Pin	1
9	Distal to Proximal Pin	5
10	Gauntlet_cover	1

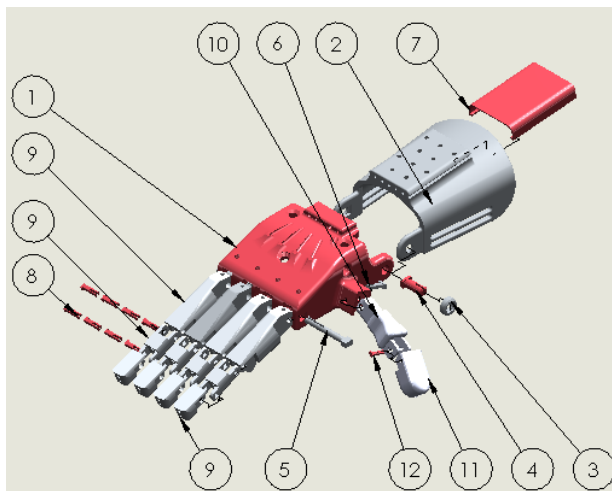


Figure 4: Prototype Hand (Three-Segment Finger)  
Exploded View

Table 6: Bill of Materials of Prototype Hand Assembly  
(Three-Segment Finger)

ITEM NO.	DESCRIPTION	QTY.
1	Hand Base	1
2	Gauntlet	1
3	wrist pin cap	2
4	wrist pin long	2
5	knuckle pin	2
6	Thumb To HandPin	1
7	Gauntlet_cover	1
8	Finger pin	8
9	Distal Finger	4
10	Middle Finger	4
11	Proximal Finger	4
12	Proximal Thumb	1
13	Distal Thumb	1
14	Thumb Pin	1

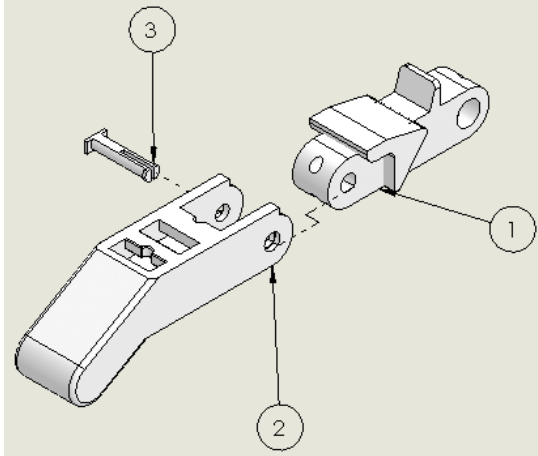


Figure 5: Two-Segment Finger Exploded View

Table 7: Bill of Materials of Two-Segment Finger

ITEM NO.	DESCRIPTION	QTY.
1	Proximal Finger	1
2	Distal Finger	1
3	Finger Pin	1

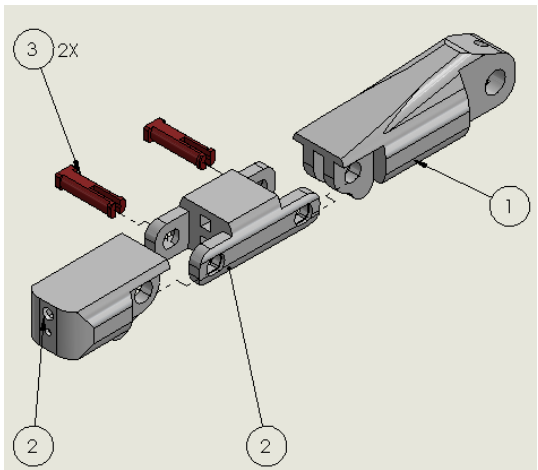


Figure 6: Three-Segment Finger Exploded View

Table 8: Bill of Materials of Three-Segment Finger

ITEM NO.	DESCRIPTION	QTY.
1	Proximal Finger	1
2	Middle Finger	1
3	Distal Finger	1
4	Finger Pin	2

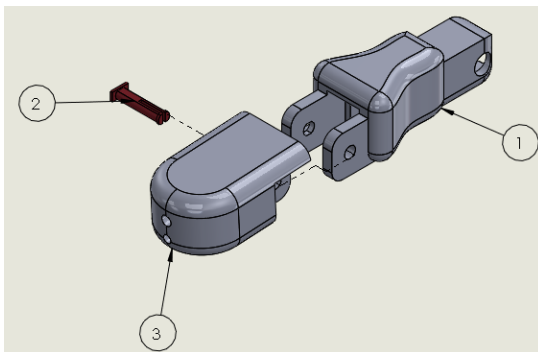


Figure 7: Thumb Exploded View

Table 9: Bill of Materials of Thumb Assembly

ITEM NO.	DESCRIPTION	QTY.
1	Proximal Thumb	1
2	Thumb Pin	1
3	Distal Thumb	1

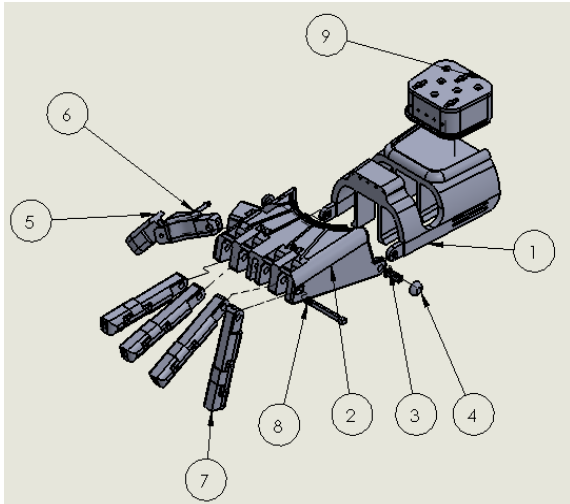


Figure 8: First Generation Hand Exploded View

Table 10: Bill of Materials of First Generation Hand Assembly

ITEM NO.	DESCRIPTION	QTY.
1	Gauntlet	1
2	Hand Base	1
3	Wrist Pin	2
4	Hinge Cap	2
5	Thumb	1
6	Thumb Pin Connection	1
7	Finger	4
8	snap pin for hand	1
9	Gauntlet Tension Mechanism	1

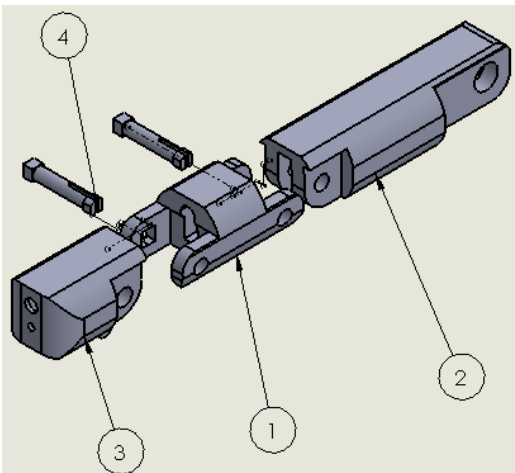


Figure 9: First Generation Finger Exploded View

Table 11: Bill of Materials of First Generation Finger Assembly

ITEM NO.	DESCRIPTION	QTY.
1	Middle Phalange	1
2	Proximal Phalange	1
3	Distal Phalange	1
4	Thumb Pin Connection	2

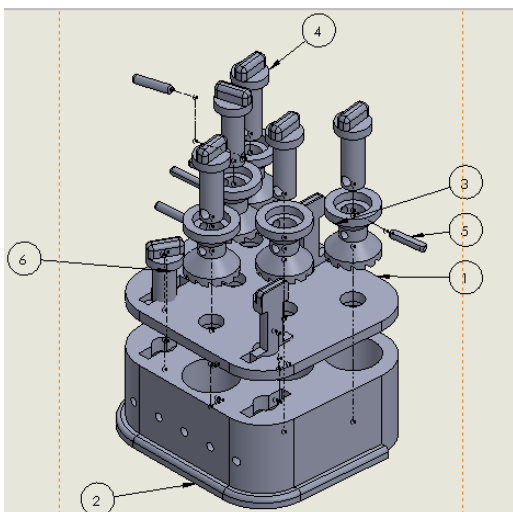


Figure 10: Ratcheting Tensioning Mechanism Exploded View

Table 12: Bill of Materials of Ratcheting Tension Mechanism Assembly

ITEM NO.	DESCRIPTION	QTY.
1	Gauntlet Tension Mechanism Top	1
2	Gauntlet Tension Mechanism Bottom	1
3	Gauntlet Tension Mechanism Spool	5
4	Tension mechanism shaft	5
5	Gauntlet Spool Shaft	5
6	Top "T Shape" Locking Device	3

## e-NABLE Group and Designs

e-NABLE is a non-profit group founded by Jon Schull, a professor and research scientist at the Rochester Institute of Technology. He started this community to build a better future and change the world, which the group hopes to do by helping provide affordable, 3D printed, prosthetic hands. The ever-growing group has more than 3000 volunteers, communicating through channels like Google+, that continue to develop better prosthetic hand designs, as well as help provide printed hands to those in need. They estimate that they have delivered over 1500 prosthetic hands to people in need around the world. Their main prosthetic designs do not use electronics, and are for anyone three years or older that has motion in their wrist, but are unable to use their fingers.

There are currently seven hands designs, which vary in difficulty to use and assemble, and provide different levels of functionality. They also have designs available for individual fingers, an arm that uses electronics, and an arm that does not use electronics<sup>xvii</sup>. All of these designs have available STL files to print, several designs such as the Raptor Hand have online sizing tools, and several designs such as the Raptor Reloaded have the source files available to directly edit the parts.

All of the hands available operate using wrist movement. The hands are operated by two types of cables, elastic and non-elastic cables, attached to each finger to offer mechanical movement to grip an object whenever the wrist is bent. The non-elastic cables are fed through the bottoms of the fingers, so that when they are tensioned it will pull them closed, as shown in Figure 14 later in the section. The elastic cables are strung through the top, and kept in constant tension. These elastics both provide some resistance when moving your wrist for a basic capacitive feedback, and return the fingers to their outright position when you let go. Guides and instructional videos on assembly are also available for most hand designs. Due to printing and scaling issues, however, assembly may be significantly more time consuming than shown. Some parts also have the potential to fit together incorrectly when scaled, so that pins will not



work or fingers will bend too far backwards. A more in depth description of several e-NABLE prosthetic hands are provided in Benchmarking section in Page 29.

## Previous MQPs

Although previous MQP's were completed in related fields such as hand orthosis and robotic hands, our goals and projected outcomes were not the same. However, valuable insight and information were used for reference in the design and analysis of the scalable prosthetic hand.

## Design of a Powered Hand Orthosis

Designing a “fully functional powered hand orthosis” and a purely mechanical prosthetic hand are quite different in terms of design strategy and the calculations used. On the other hand, the forces on the fingers are the same, so looking at the analysis performed by Elyssa et al. (2013) gives us insight on what analyses to perform, as well as how to set them up. Below, in Figure 11 an example of one of the analyses is shown.

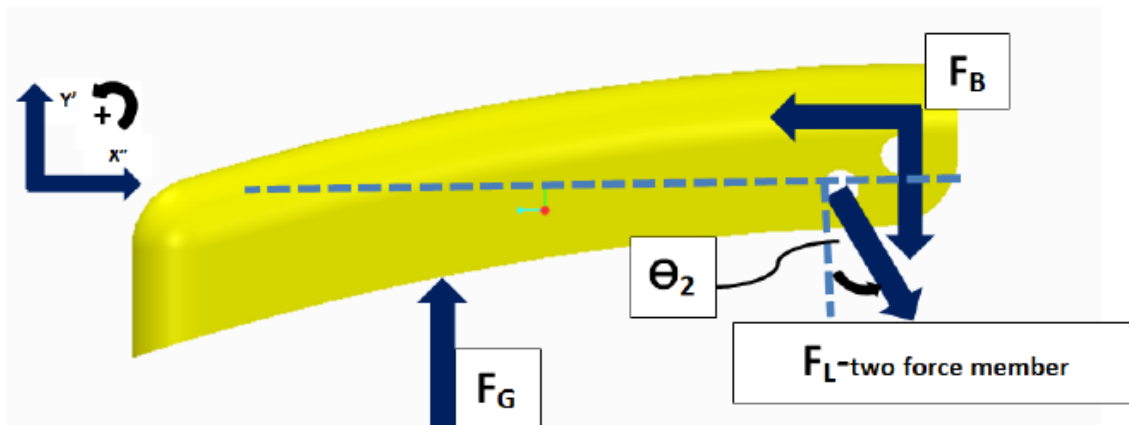


Figure 11: FBD Example from MQP

## Design of a Powered Hand Orthosis 2

In 2014, Ian Crowe, Reed Hebert, and Brittany Nichols set out to develop a powered hand orthosis for use as both rehabilitation and as a wearable assistive device. Similar to our design, the hand orthosis ‘uses cables to pull the fingers closed,’ and additionally uses gears and a

linear actuator to control the thumb. This device uses switches worn on a belt that are operated with the working hand. While the design of the mechanism was not fully relevant to our design, it was due to its use of electronics. The background and analysis provided helped formulate a plan for creating our own design.

## Intelligent Robotic Hand Design

This MQP from 2006 does not have significant relevance to our project, as it relies on linkages and electronics, whereas ours is cable driven. This robotic hand does use cables as well, however, and the analysis performed on the angle of cables with relation to force transmission shows the importance of limiting finger angles to increase force available.

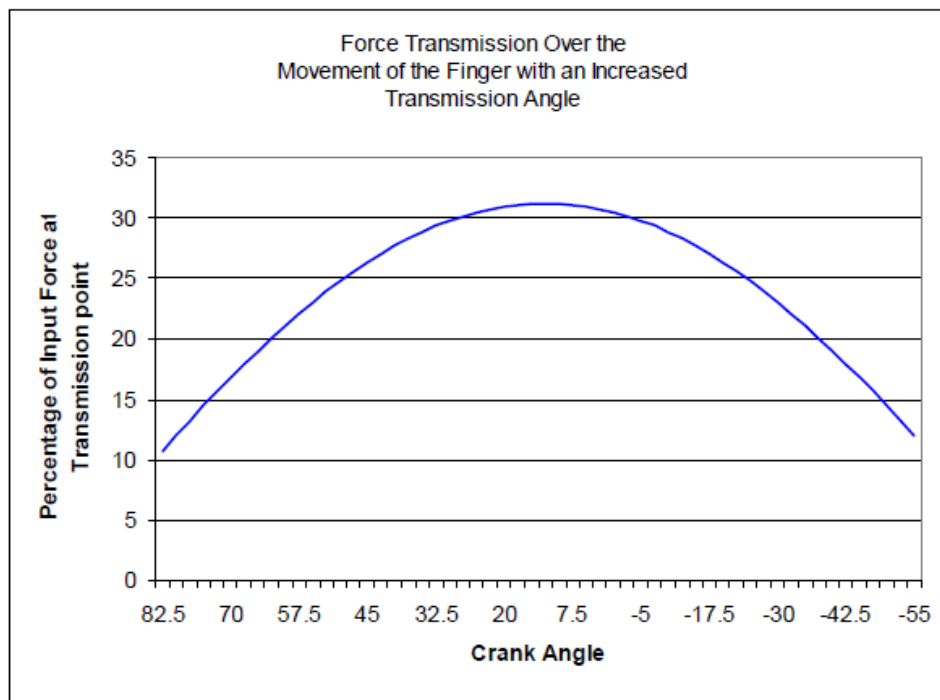
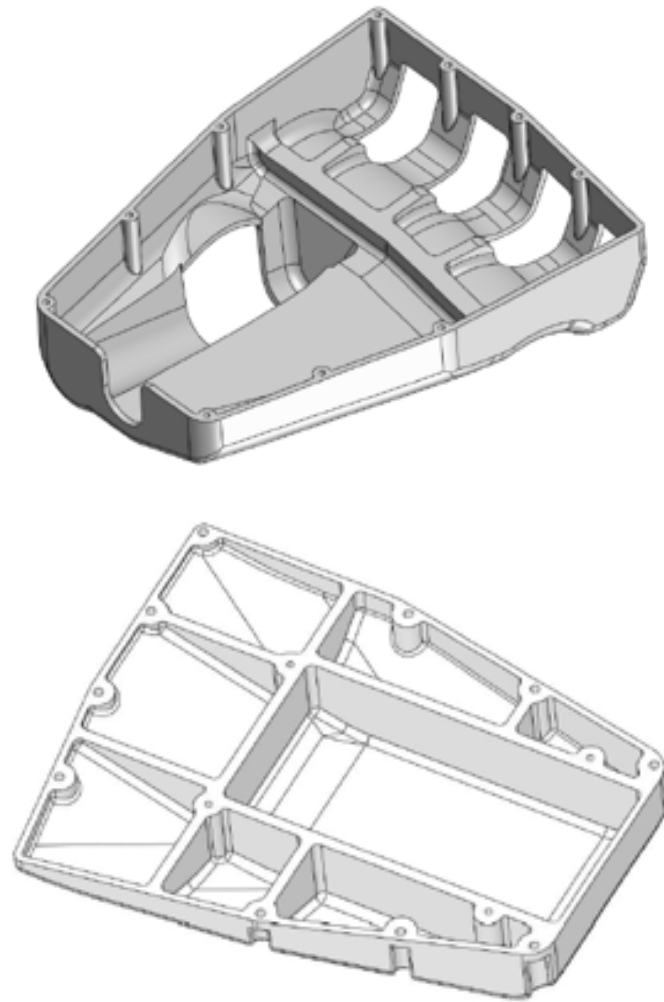


Figure 12: Force vs Cable Angle

## Design of a Human Hand Prosthesis

As with other robotic hand projects, there are differences in the designs and results compared with those of our mechanical prosthetic. Reading through this project, background information and analyses performed in the other MQPs were reinforced. This design did mention one

different idea: a cover. The palm cover in the Human Hand Prosthesis is designed to protect the internal components and provide a more aesthetic appearance. Having an attachable cover would protect the cables from catching or tearing, prevent dirt from entering any holes, and give more options to the appearance of the hand without changing functionality. This cover is not within the scope of the project, but is provided as a recommendation for future work.



*Figure 13: Hand Cover Designs*

## Design of a Prosthetic Robotic Hand

While the robotic hand designed by Elaine Kristant and Montira Satiempoch in 2004 was too dissimilar to our device to compare and learn from in terms of design, their report provided valuable background information. By keeping our device at a similar weight to that of a real hand makes sure that it is comfortable and feels more like an extension of the body than a separate entity. Knowingly that, on average, a “Male hand [weighs] 1.4lb, male lower arm [weighs] 3.3lb. Female hand [weighs] 1.1lb, female lower arm [weighs] 2.7lb,” we have targets to aim for in benchmarking<sup>xviii</sup>.

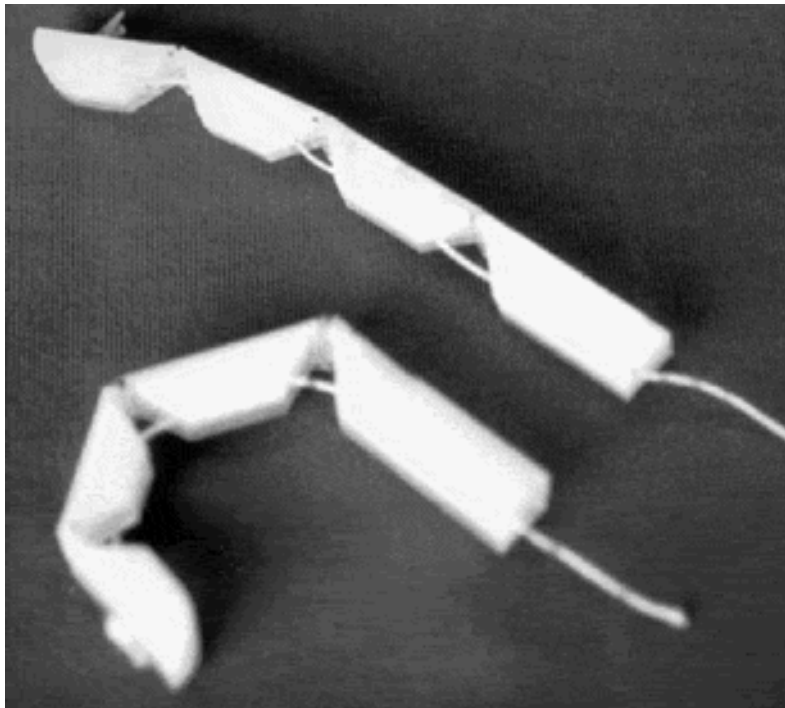


*Figure 14: Cable Tension Mechanism*

## Benchmarking

In order to develop a design, the team assessed the strengths and weakness of popular 3D printed prosthetic hands. Seven hands were selected and assessed in the following sections and tables. By assessing each category the team was able to determine common issues in the assembled product through user reviews, videos, and online forums that had potential for optimization. Conducting Standard Benchmarking would not be helpful as most categories would overlap and with models in varying sizes and scales, quantifiable data was both arbitrary and difficult to compare. To properly benchmark various designs, the team would need to print a large sample of various sizes for each hand model which is not feasible with the budget and time of this project.

## Cyborg Beast

The Cyborg Beast is one of the most popular 3D printed prosthetic hands. Developed at Creighton University, it has an appealing, organic appearance. There are only two-segment joints, which slightly reduces functionality in exchange for robustness. Like most 3D printed prosthetics, the thumb is fixed at an angle, which makes it much stronger while limiting variable grips. One main issue with this hand is that metal fasteners are used for all of the pins. While this increases the lifetime of the hand, it increases the cost, reduces the design's ability to scale, and the screws can loosen and fall off easily.



*Figure 15: Cyborg Beast*

## Talon Hand

The Talon Hand is fairly unique, using a cut leather gauntlet instead of a standard printed gauntlet. While this is more attractive and comfortable than a printed gauntlet, it is much more expensive and uses over 20 screws. The leather also takes some of the strain away from the plastic, increasing the lifetime of the prosthetic. The design includes options for both Chicago screws and snap pins, which allows users to have more choice in their prosthetic. Snap pins are a cheaper option less prone to falling out than the Chicago screws, but are less strong and more likely to wear out. The design uses much less plastic as well, as leather replaces a large portion of the volume<sup>xix</sup>.



*Figure 16: Talon Hand*

## Odysseus Hand

The Odysseus is a 'starter' version of the Talon hand. Having only two fingers, the force required to close the hand is greatly decreased, so this hand is recommended for the young and old, as well as those with weaker wrists. The downsides are that it is harder to pick up some objects and has a lower maximum load.

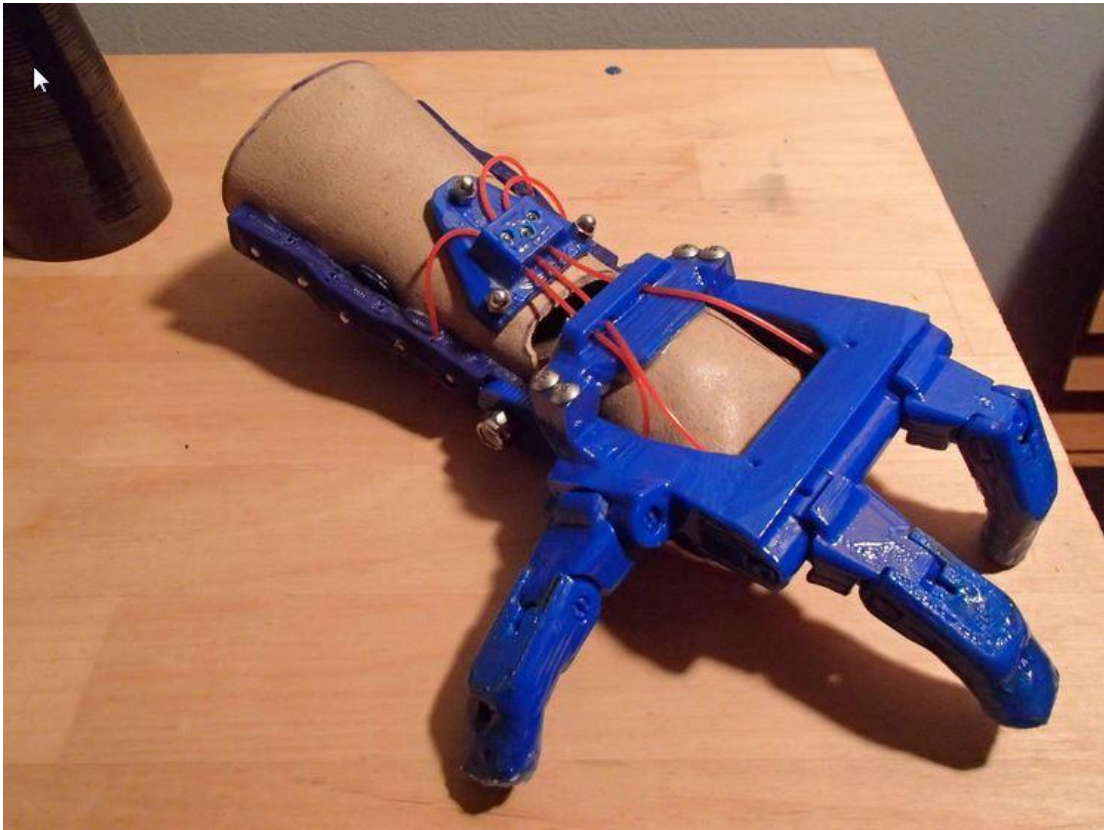


*Figure 16: Odysseus Hand*



## Flexy Hand

The Flexy Hand 1 is the most realistic looking 3D printed hand currently available. When a glove is put over it, it is almost indistinguishable from a regular hand, as shown below in Figure 17.

Utilizing Filaflex filament for the joints, no elastics are needed, as the joints are pre-stressed to return to its outward position when released from tension. The main disadvantages of using this filament are that it requires a second build plate, switching out the filament, and is more expensive than standard PLA or ABS. This design is meant for use with the Limbless Arm, meaning that elbow movement will close the hand instead of a wrist and allowing those without wrists can use it.



*Figure 17: Flexy Hand 1*

## Flexy Hand 2

The Flexy Hand 2 is nearly identical to the Flexy Hand 1, with the exception that it uses a gauntlet instead of an arm. One main issue with the gauntlet is that there is only bridge between the sides. While this reduces plastic, it also makes it more difficult to apply force, as the fulcrum is further back. This design also has the cables unprotected and directly against the wearer's arm, which could cause them to break or cause discomfort.



*Figure 18: Flexy Hand 2*

## Raptor Hand

The Raptor Hand is one of the most popular hand designs, and even has an online sizing tool available. While not the most cosmetically attractive, this design is one of the easiest to assemble, providing bars to tie off cables and fairly large parts. This comes at the expense of dirt-trapping holes, exposed cables, and a fairly bulky hand. It uses snap pins, meaning the only screws required are for the tensioning system and attaching the Velcro to the palm. The tensioning system works by having a sliding holder for several pins that the cables tie into, which can then be screwed in for additional tensioning.

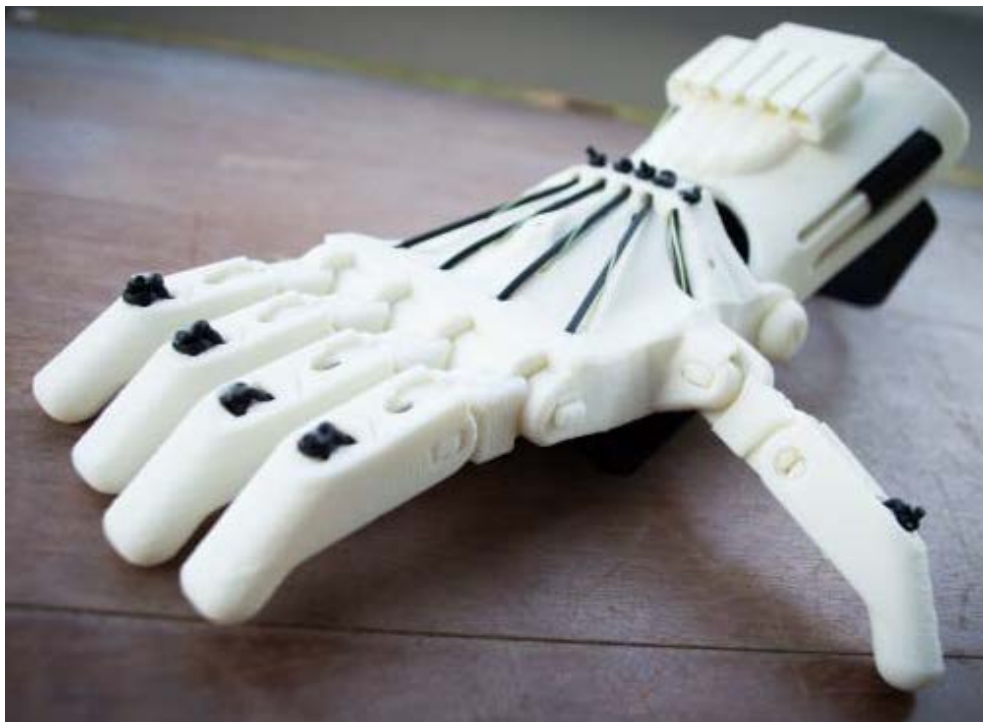


*Figure 19: Raptor Hand*

## Raptor-Reloaded Hand

The Raptor-Reloaded hand is largely the same as the Raptor hand, but was created in an open-source CAD program called Fusion 360 with improved cosmetics and printability. It also has more recessed channels, allowing the elastics and cables to go over the hand while still being protected. The hand is generally less bulky as well, which reduces print time and improves the appearance.



*Figure 20: Raptor-Reloaded Hand*

## Dextrus Hand

The Dextrus hand has many advantages as it has more degrees of freedom (DOF) than most hands available. This hand has distal joints on the phalanxes giving it a more anthropomorphic motion. The thumb is capable of rotation to enhance usability with gripping various objects. This hand however is controlled electronically and uses steel cables, metal bearings, and an internal pulley subassembly which increases the cost of the prosthetic<sup>xx</sup>.

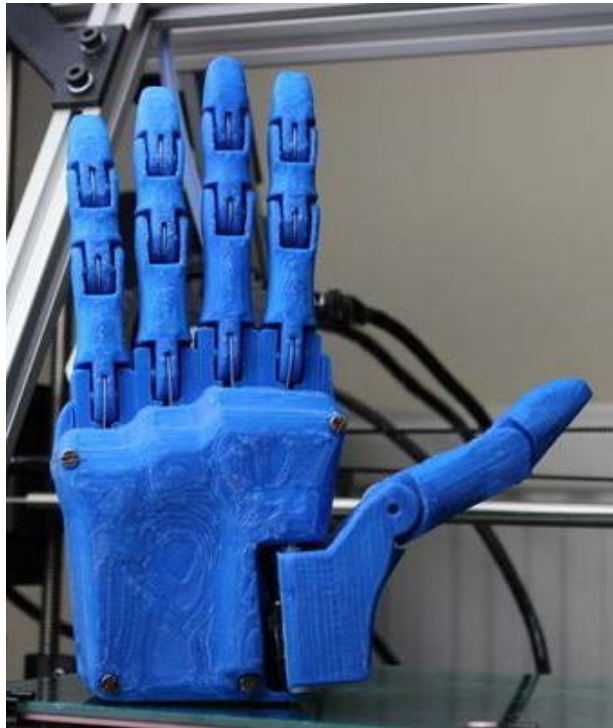


*Figure 21: Dextrus Hand*

## Osprey Hand

The Osprey Hand has one of the more unique tensioning mechanisms. Instead of tying the cable to a pin or around a spool, the cable is simply fed through the gauntlet and compressed by set screws. The cable is also melted into a ball at the end of the fingers instead of tying it, which makes assembly easier. In addition, there are no separate elastics, so only one set of cables needs to be tensioned. Downsides of this hand are the cost of leather, usage of many screws for securing the leather, and requiring a special cable that is not available in most hardware or craft stores, or even Amazon. In addition, inadequate instructions are provided, and the cable does not tend to retract well.



Figure 22: Osprey Hand<sup>xxi</sup>

## Phoenix Hand

The Phoenix Hand is a combination of the Raptor Reloaded and Falcon V1 hands. Instead of a traditional elastic cable, the Phoenix Hand uses small elastics that attach to tabs on the fingers. Another unique feature of this hand is the use of only three tensioning pins for the five fingers, allowing the tensioner to fit on a smaller gauntlet. The Phoenix Hand also provides a lengthy instruction document, as well as a shorter document for advanced consumers.

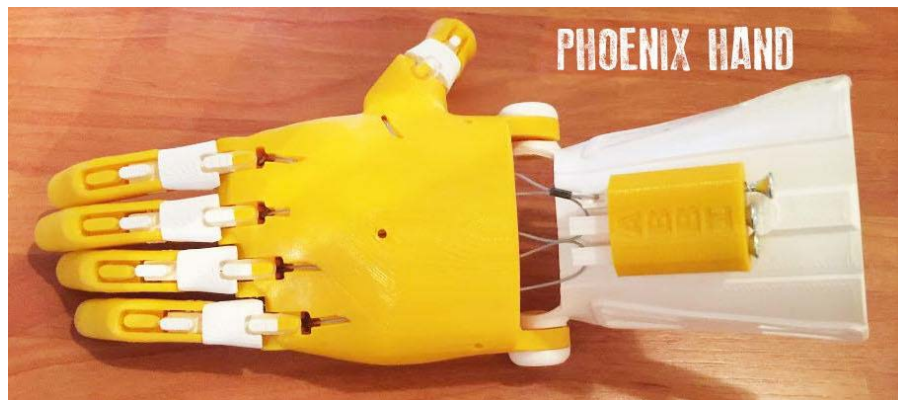


Figure 23: Phoenix Hand<sup>xxii</sup>

## K-1 Hand

While not necessarily realistic, the K-1 Hand has excellent aesthetics due to its organic shapes and recessed cables. The K-1 Hand is also one of the few prosthetics that uses three finger joints, so we were specifically interested in its cable routing. Another advantage of the K-1 Hand is that there is no hardware, so all you need is a 3D printer and cables to make it. One of the major downsides of the prosthetic is that there are no instructions currently unavailable, making it much harder for those assembling it<sup>xiii</sup>.



Figure 24: K-1 Hand



# Methods and Procedure

In this section, design specifications, the methods and procedures of mechanical design, rapid prototyping, material research and mechanical calculations and analysis are discussed.

## Design Specifications

Table 13: Design Specifications

Specification	Unit/Description	Information
Weight	$0.4 \pm 0.1\text{lb}$ ( $.18 \pm .05\text{kg}$ )	Weight of the assembled hand
Max load	$7 \pm 1\text{lb}$ ( $31 \pm 0.44\text{ N}$ )	Total allowed force on the fingers from carrying a weight
Range of Motion Wrist	$+20$ to $-20 \pm 10$ degrees	Angle 0 when wrist and arm are parallel. Positive angle indicates bending wrist upwards.
Range of Motion MCP	$0$ to $-90 \pm 5$ degrees	Joint and knuckle. Angle 0 at straight extension, curving inwards
Range of Motion PIP	$0$ to $-60 \pm 5$ degrees	Joint at end of proximal phalanx
Range of Motion DIP	$0$ to $-80 \pm 5$ degrees	Joint at end of Middle phalanx
Cost to Assemble	$\$50 \pm \$10$	Cost of all printed and non-printed parts, including wires, elastics, hardware etc.
Time to Assemble	$4 \pm 1$ hours	Cleaning/finishing parts and connecting finished pieces with the given tools by someone 16+
Time to Print	$30 \pm 5$ hours	Time for all parts to print
Life Expectancy	$1000 \pm 50$ grip cycles	Number of times the hand can open and close before reduction in performance

Table 14: Design Specifications; Continued

<b>Specification</b>	<b>Unit/Description</b>	<b>Information</b>
Scalable Range	Ages 7+	Based on average size of fingers and taking into account grip strength
Max Operating Temperature	140F (60C) ± 10F (5C)	At around 140F, the PLA will reach its glass transition temperature.
Min Operating Temperature	-10F (-23.3C) ± 10F (5C)	At around -10F, most rubbers will begin to reach their glass transition temperature. Significant performance degradation will occur at around 0F. <sup>xxiv</sup>
Material	PLA	biodegradable thermoplastic aliphatic polyester derived from corn starch

## Weighted Decision Matrix

Table 15: Weighted Decision Matrix

	Scaling weight	Material		Number of joints		Tensioning device		
		ABS	PLA	2	3	Ratchet System	Pin System	Screw System
Weight	7	5	5	N/A	N/A	5	7	7
Max Capable Load	9	5	5	7	6	7	5	4
Range of Motion	8	N/A	N/A	5	9	7	5	8
Cost	7	5	5	N/A	N/A	5	7	7
Time to Assemble	8	N/A	N/A	6	5	5	7	8
Durability	10	5	5	6	5	7	5	6
Operating Temperature	7	8	6	N/A	N/A	N/A	N/A	N/A
Time to Print	5	N/A	N/A	5	5	5	6	6
Scalability	8	N/A	N/A	5	5	9	6	9
Cosmetics	7	N/A	N/A	5	7	5	6	7
Safety	10	6	9	N/A	N/A	N/A	N/A	N/A
Serviceability	10	7	6	6	5	5	7	10
Sum		351	<b>357</b>	371	<b>380</b>	481	479	<b>573</b>

Table 16: Weighted Decision Matrix; Continued

		Printer Needed				Infill		
	Scaling Weight	XYZ da Vinci 1.0 AiO	Dimension SST 1200es	Makerbot Replicator 2	Sindoh	10%	30%	90%
Weight	7	N/A	N/A	N/A	N/A	9	6	3
Max Capable Load	9	N/A	N/A	N/A	N/A	5	7	9
Range of Motion	8	N/A	N/A	N/A	N/A	N/A	N/A	N/A
Cost	7	8	4	7	6	9	6	3
Time to Assemble	8	N/A	N/A	N/A	N/A	N/A	N/A	N/A
Durability	10	3	6	5	5	5	7	9
Operating Temperature	7	N/A	N/A	N/A	N/A	N/A	N/A	N/A
Time to Print	5	4	6	6	6	8	6	3
Scalability	8	N/A	N/A	N/A	N/A	N/A	N/A	N/A
Cosmetics	7	N/A	N/A	N/A	N/A	N/A	N/A	N/A
Safety	10	N/A	N/A	N/A	N/A	N/A	N/A	N/A
Serviceability	10	N/A	N/A	N/A	N/A	N/A	N/A	N/A
Sum		106	118	<b>129</b>	122	<b>261</b>	247	228

## Decision Matrix Scaling weights

### Weight

If the device is to be equipped by a child, the system will need to be very lightweight. Even for adults, keeping the system as light as a regular hand will help the device feel more natural and reduce discomfort.

### Max capable load

If the device cannot hold a weight or withstand a load, its functionality is greatly diminished.

### Range of motion

Limiting the range of motion of the fingers would reduce the functionality of the device. By allowing for a greater range of motion, smaller objects can be grasped, and larger objects can be grasped more tightly and in different ways.

### Cost

One of the main goals of this project is to provide a prosthetic hand to as many people as possible, so lowering the cost makes it more widely available.

### Time to assemble

Not everyone has a significant amount of time that they can devote to assembling a product. By reducing the time to assemble, parents can assemble their children a prosthetic hand after work instead of taking an entire day to work on it.

### Durability

Increasing durability means that the device can operate for a longer period of time without need for repair. This lowers the cost of replacement parts, and makes the prosthetic more of a convenience than a hassle.

## Operating temperature

By allowing for a wider range of temperatures means that the device can be used around the year and around the world.

## Time to print

In case something goes wrong or replacement parts need to be made, reducing the time to print allows for getting back to operation sooner.

## Scalability

Factors like age, weight, genetics, and sex will all influence the size of a person's hand and arm. Scalability allows for almost anyone to print out an appropriately sized hand without the need for a custom model.

## Cosmetics

While functionality is important, the cosmetics of a prosthetic are critical to the usage of the device. An ugly prosthetic will generally be used less than a more attractive option, regardless of the functionality.

## Safety

Safety is critical to the prosthetic, as the device is meant to help a person with a disability, rather than cause any harm.

## Serviceability

Because the device is made of plastic, parts are expected to break at one point or another. A device that is easy to repair or fine-tune is always a more preferable option than one less so.

## Determination of Decision Matrix Scores

### Material

We chose to decide between ABS and PLA because they are the most widely available materials for 3D printers, and have many favorable qualities in terms of their printed parts.

### ABS



*Figure 25: ABS*

An advantage of ABS over PLA is that ABS has a significantly higher glass transition temperature, at around 219.2F (104C) for ABS<sup>xxv</sup> vs 113F (45C) for PLA<sup>xxvi</sup>. One safety concern for the use of ABS is the production of ultrafine particles (UFPs). UFPs have been linked with causing health problems<sup>xxvii</sup>, though their concentrations in a well-ventilated area are generally negligible. Another advantage is that ABS is typically stronger and flexible than PLA, and is also machinable.

## PLA



Figure 26: PLA

One large advantage of PLA over ABS is their chemical compositions. PLA is biodegradable and created from renewable resources such as corn starch. This means that PLA has a minimal effect on the environment, and does not create toxic fumes when melted. It also means that PLA is typically non-toxic when accidentally consumed; meaning use around a small child is not a hazardous situation<sup>xxviii</sup>. PLA is also a widely used plastic, meaning that it will be fairly cheap to buy<sup>xxix</sup>. PLA typically results in less warping, and does not require a heated bed as well<sup>xxx</sup>.

## Number of Joints

Two



Figure 27: Two-Segment Finger

One slight advantage of having two joints is that having a single part for the middle and distal joints will allow for a higher load capability. A reduction in parts also means a slight increase in serviceability.



Three



*Figure 28: Three-Segment Finger*

Three joints allow for a larger range of motion than two joints. While limiting the rotation to prevent the distal joint from moving past its fulcrum will be necessary, additional rotation will still be possible. Another advantage of three joints is that it makes the fingers look more realistic in terms of general appearance and movement. While more parts to deal with is usually a negative, the extra joint makes it easier to feed wires through the fingers as well.

## Tensioning Device

Ratchet

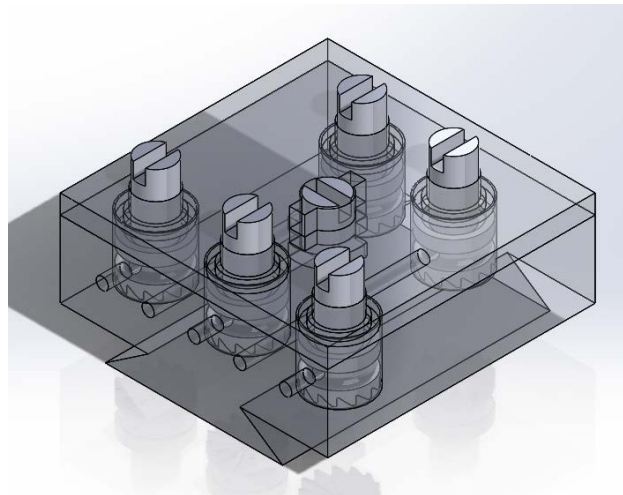


*Figure 29: Ratchet System*

One of the main advantages of the ratchet system is that it can be adjusted on the fly without tooling. While the assembly may be more complicated to initially assemble and replace parts,

the tool less adjustment makes up for it. The system also does not need to scale as the cables remain the same size. The down side of this device is that it does have a lot of parts, more so than all of the current systems available, some of which are pretty small. These parts being small can lead to print failure. Assembly of the tensioning system would also be somewhat difficult for individuals without engineering knowledge.

## Pin

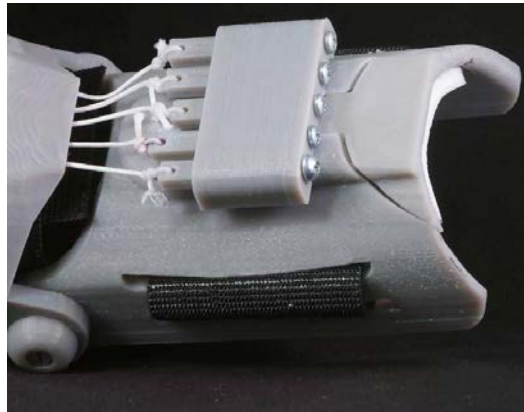


*Figure 30: Pin System*

The pin system is inherently lighter due to its small size. It also has very few parts, which makes it fairly serviceable and scalable.

## Screw

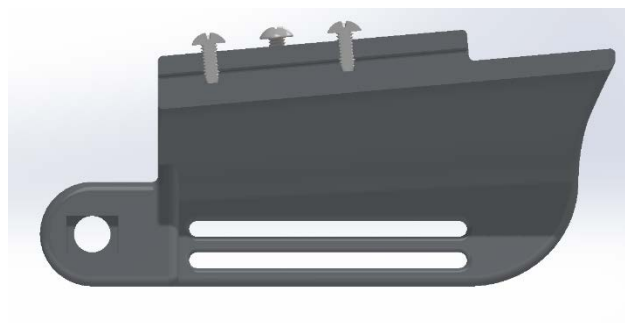


*Figure 31: Screw System*

The screw system is a simple system utilized for tensioning. It requires screws to be inserted into holes to tension the prosthetic. Using #8-32-1/2 machine screws the tension cables are secured into place to offer a proper grip and usability.



## Printer Information

### XYZ da Vinci 1.0 AiO

By designing parts that can be printed for a lower end 3D printer like the XYZ, more people can print their parts with their own printer, rather than getting their parts printed through a printing service. This will reduce the cost of printing dramatically, as consumers will only be paying for filament and electricity, rather than the additional wages of the operator.



Figure 32: XYZ da Vinci 1.0 AiO<sup>xxx</sup>

### Dimension SST 1200es

Using a higher end printer like the Dimension would allow for tighter tolerances that would increase durability and functionality. Higher end printers typically allow for faster printing as well.



Figure 33: Dimension SST 1200es<sup>xxxii</sup>

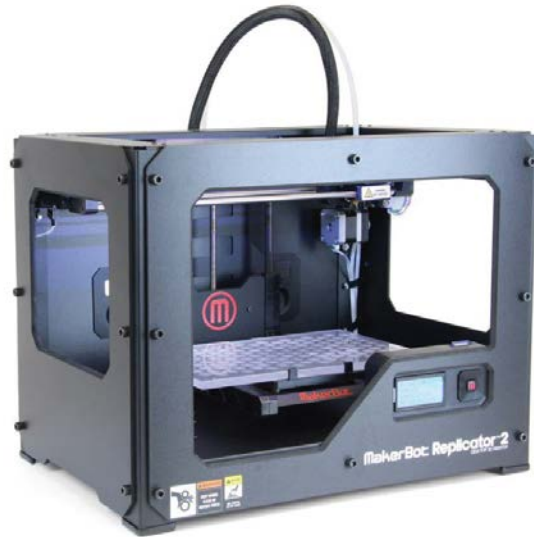


Figure 34: MakerBot Replicator 2<sup>xxxiii</sup>

### Makerbot Replicator 2

The Makerbot Replicator 2 is a mid-range consumer 3D printer. More people can print components with their 3D printers than outsourcing to a printing service.

### Sindoh Printer

The Sindoh 3DWOX is a recently released 3D printer from South Korea that is available to consumers in a price range similar to the MakerBot Replicator 2 and similar models. It features an enclosed system with assisted leveling systems and auto-loading filament option.



Figure 35: Sindoh 3DWOX<sup>xxxiv</sup>

## Infill

Infill is the percentage of the internal structure that is printed in a 3D printing operation.

Depending on the forces applied and need for a low cost part; infill can be adjusted to more accurately meet the property needs.

10 %

Using a low infill will reduce print time and cost, while having a minimal reduction on strength and durability of the printed part.

30 %

A medium infill will balance the amount of force the parts can withstand with the costs and print times.

90 %

At high infill rates, the printed parts can withstand considerably greater forces, but take significantly longer to print and use much more material.

# Design Methodology

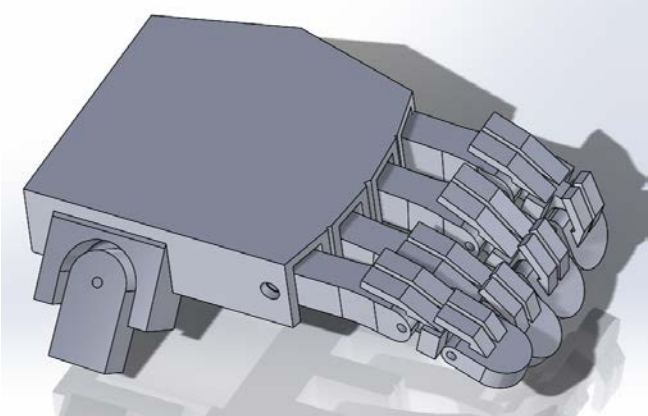


Figure 36: Hand Assembly 1

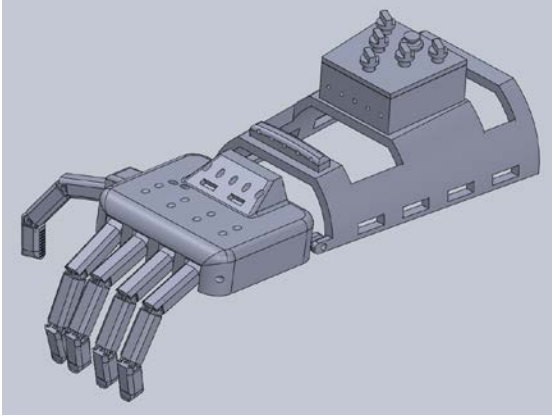


Figure 37: Hand Assembly 2

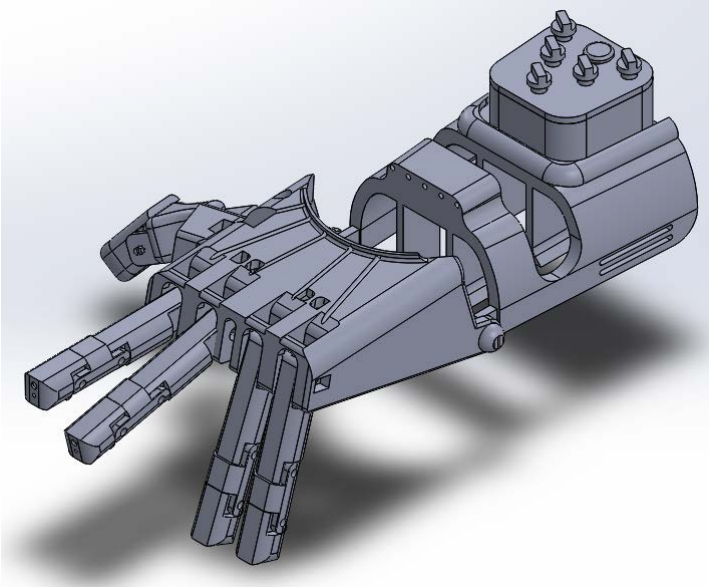
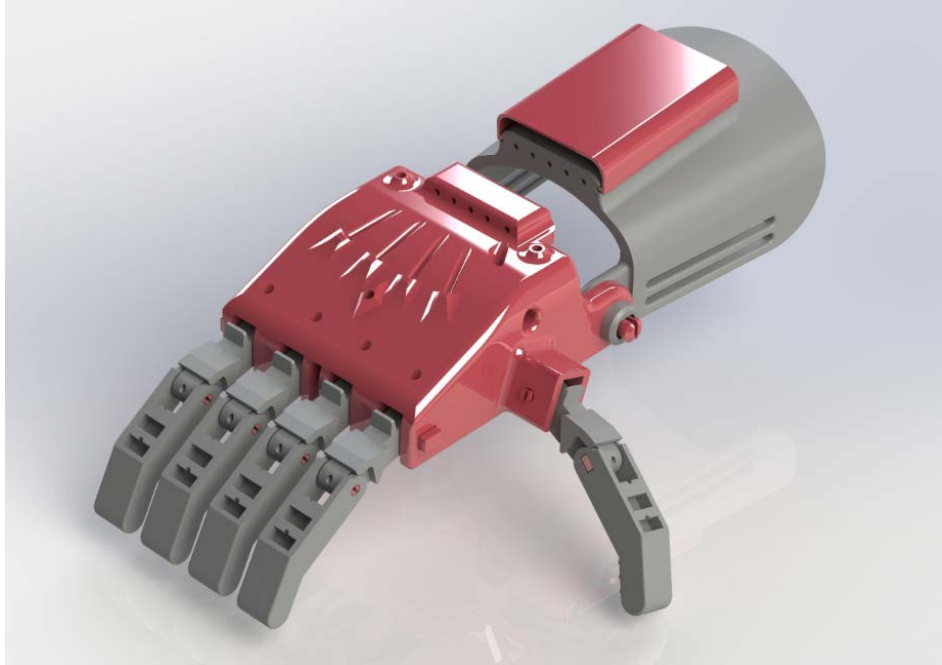
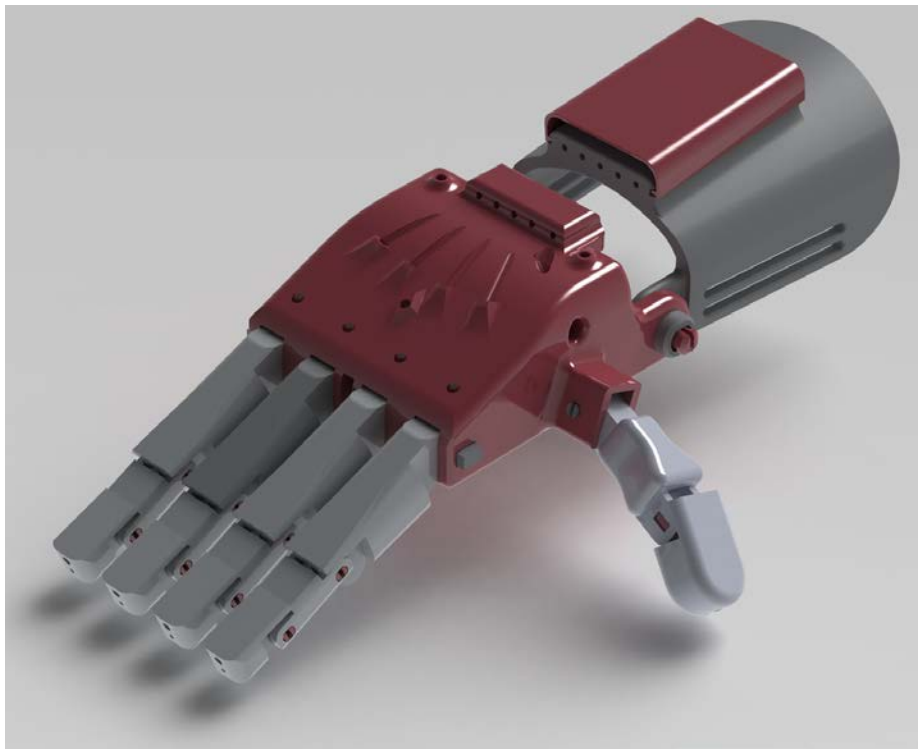


Figure 38: Hand Assembly 3



*Figure 39: Hand Assembly 4*



*Figure 40: Hand Assembly 5*



## Hand base

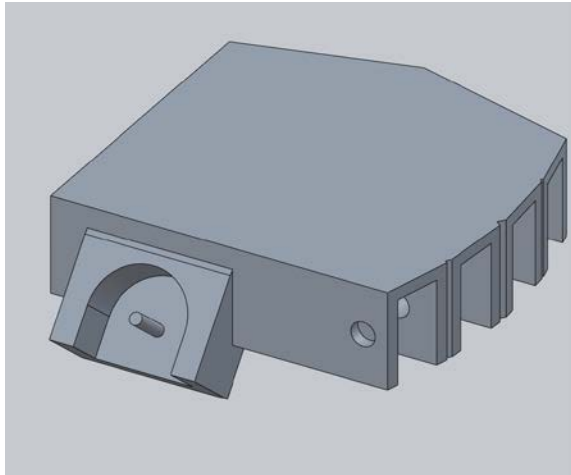


Figure 41: Concept Hand Base with Adjustable Thumb

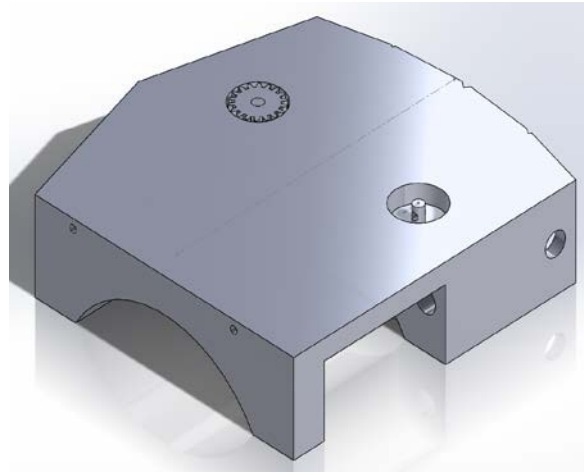


Figure 42: Concept Hand Base with Two Ratchet Systems

After benchmarking products that are currently available on the market from user reviews, the team developed a simple conceptual hand base design, which is shown in Figure 41. One design idea was the use of a rotatable thumb, which would allow the wearer to change the thumb's position depending on the task.

Subsequently, the ratchet system was taken into account as a part of our design. Two ratchets were mounted into the hand base, shown in Figure 42, to allow for larger ratchet gears.

Theoretically, a pair of fingers will be connected to each system, allowing manual adjustment and facilitation of the tensioning in fingers when necessary. Eventually it was decided to set aside this conceptual design, as the team felt that working on a simpler design that could scale more effectively was more important, and the idea of inserting the system into the hand base would cause other mechanical complications.

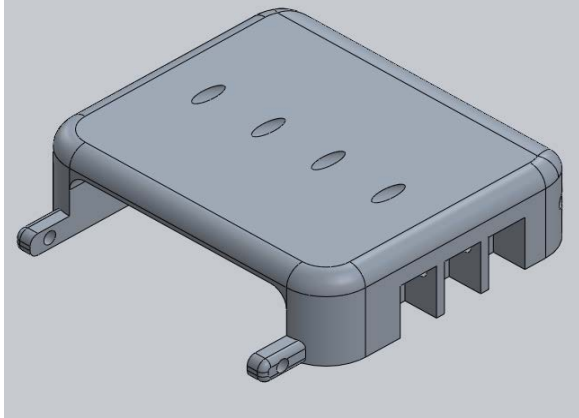


Figure 43: Gen 1 Hand Base; Isometric View

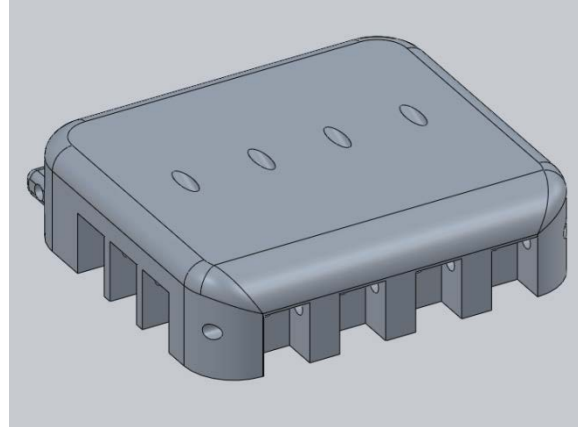


Figure 44: Gen 1 Hand Base; Alternate View

The first generation hand base, shown in Figure 44 and Figure 45, was designed keeping simplicity in mind so that it would be able to scale and the area where the thumb attaches was recessed to create a smaller device.

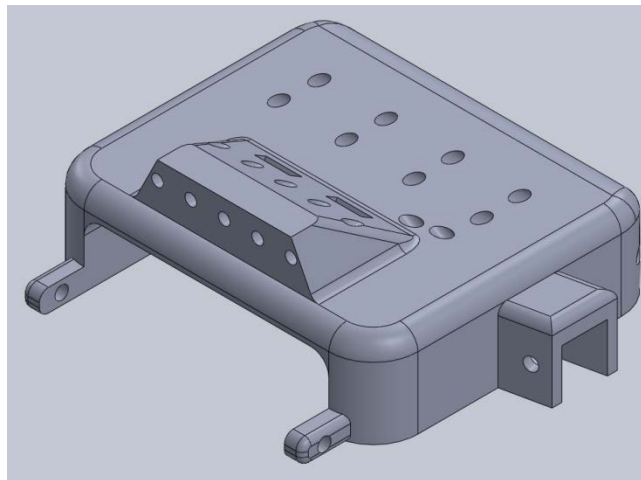


Figure 45: Gen 1.1 Hand Base

The design was slightly improved in Generation 1.1, as displayed in Figure 46, by having a cable bridge on top of the hand base. This allows for cables to easily align with the gauntlet, as well as provide more support to the cables, reduce contact with sharp corners, and provide a smoother bending angle. More holes were created to feed both types of cables, elastic and non-elastic, in the front of the hand base. Additionally, the thumb housing was added for improved cosmetics and a better angle of orientation to facilitate gripping.

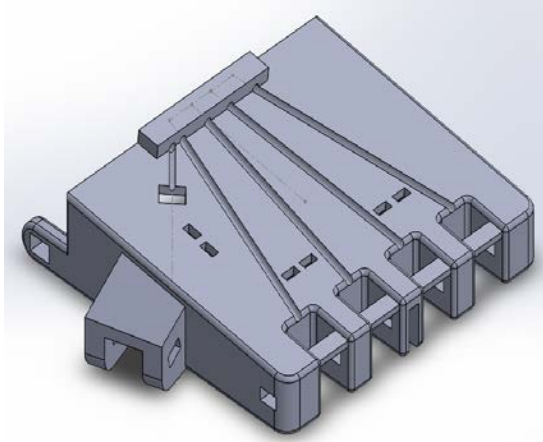


Figure 46: Gen 2 Hand Base; Isometric View

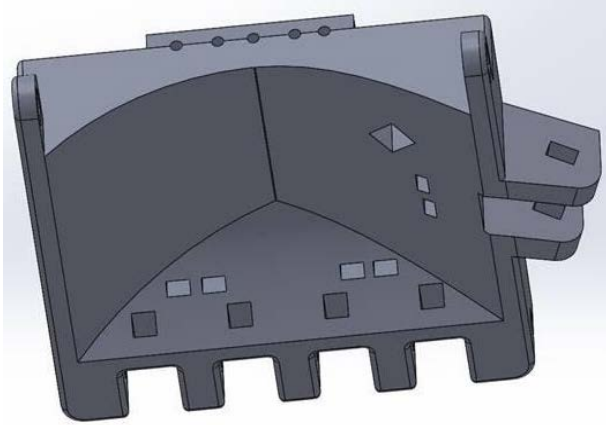


Figure 47: Gen 2 Hand Base; Bottom View

The team's generation 2 design, or Gen 2, shown in Figure 46, uses a style of cable channeling on the hand base rather than feeding cables through a hole. The idea was inspired by the Raptor Reloaded and Cyborg Beast hands and was intended to eliminate the hassle of cable feeding. Cable channels were also aligned to the center of each finger gap to prevent the cables getting jammed. In order to limit the rotation of fingers, hard stops were created between the finger gaps. The bottom of the hand was also designed to have a shallow curvature, allowing for increased printability without supports.

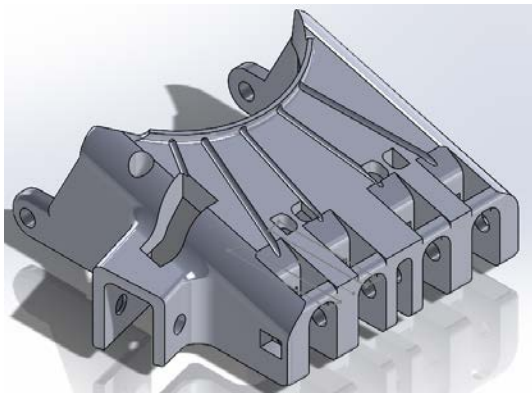


Figure 48: Gen 3 Hand Base; Isometric View

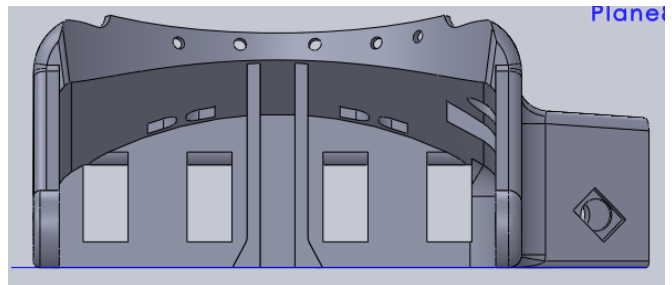
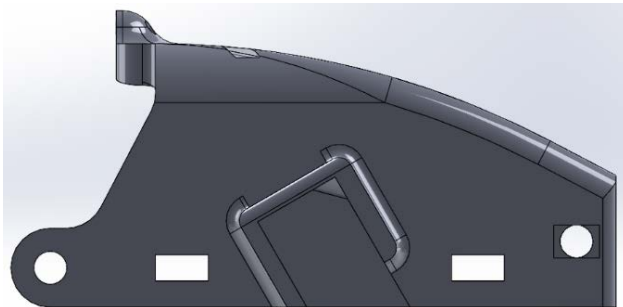


Figure 49: Gen 3 Hand Base; Back View

After reviewing all the modifications of Gen 2, the team decided to alter the design in Gen 3, shown in Figure 49, to improve manufacturing costs by removing unnecessary material, as well

as to improve aesthetics. Two supports were added to the middle to allow for a deeper hand base and reduce the amount of support material that would have been used by the 3D printing software, saving time and money. For better cable channeling to the thumb, the top section of the housing was removed as well.

One of the primary concerns with this design was the cable bridge that feeds into the gauntlet. Due to its small size, the team was worried that the bridge would wear off after continuous rubbing with the cables. After assembling the prototype with the gauntlet and cables, the wide open space became a safety concern as objects could get caught there, or the thin cables could dig into the wearer's arm. Subsequently, the bridge for cable to gauntlet was reintroduced back to solve the initial concern of previous version. Moreover, the housing of the thumb was rotated in order to support better gripping. The surfaces of the house were made sure flatten equally to the base of hand so it will not cause a failure in printing.



*Figure 50: Gen 4 Hand Base; Side View*

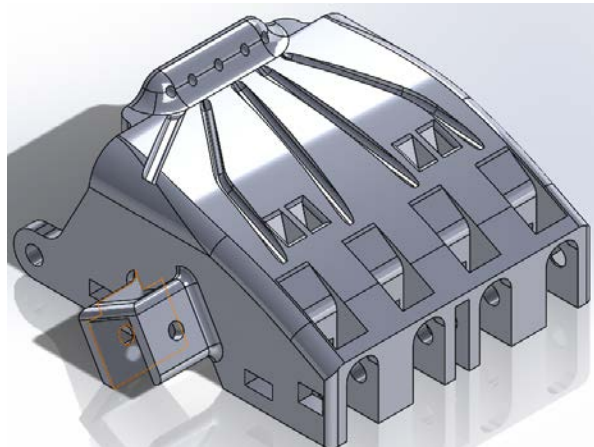


*Figure 51: Gen 4 Hand Base; Isometric View*

The team tried to address all of the concerns with previous versions. Cosmetically, the hand was made to resemble a more natural appearance, which also reduced the amount of material used. Subsequently, the bridge for cable to gauntlet was reintroduced back to solve the initial concern of previous version. Moreover, the housing of the thumb was rotated in order to support

better gripping. The surface of the house was made sure flatten equally to the base of hand so it will not cause a failure in printing.

The team tried to address areas of concern with previous hand base generations. This generation of the hand base has a more aesthetic appearance. This model also protects the prosthetic from exposure from dust and dirt from entering the routing channels for the cables. Internal channeling was added to protect the cables from dirt, dust, and potential snagging. The thumb connection was moved to the right side of the hand base to demonstrate the device compared with our dominant hands. As shown in Figure 53, the fifth generation design of the hand base was designed to be more robust and appealing to users. The simplification of this iteration made a more simple and effective design for adding equations.

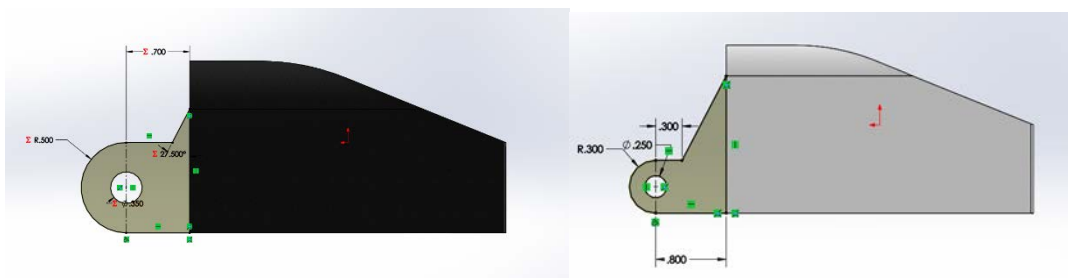


Figure 52: Gen 5.1 Hand Base; Isometric View

The improved model, generation 5.1, corrected remaining areas of concern from the generation 5 model. These designs are shown in Figure 52. Due to the shear stress force on the wrist pin, it was determined that the pin joint and pin should be stronger in order to withstand the expected force. To enhance the strength from the previous model the wrist joint was edited to increase the surface area and material around the pin connection. This design allowed for smoother movement of wrist joint.

The Figure 54 shows the improvement of Velcro attachment section. For safety purposes and ease of inserting the screws into the part, the holes were revised and designed to have countersunk surfaces for both sides so binding screws could be attached for easier maneuverability.

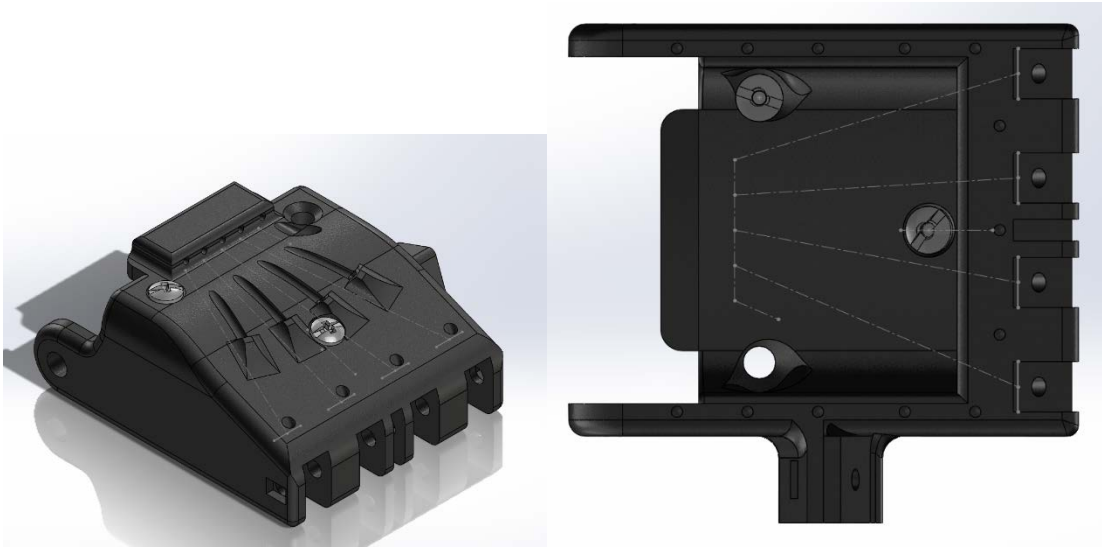


Figure 53: Gen 5.1 Hand Base with Velcro Attachment Screws

## Fingers, Thumb, and Pins

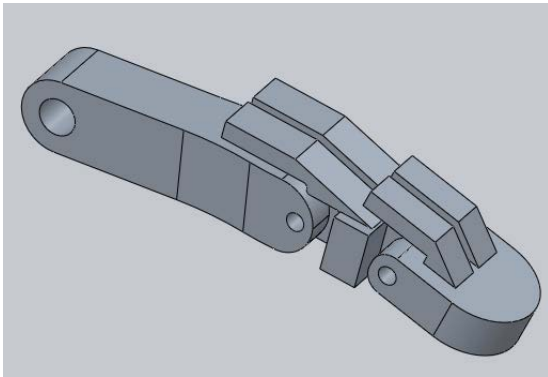


Figure 54: Concept Finger

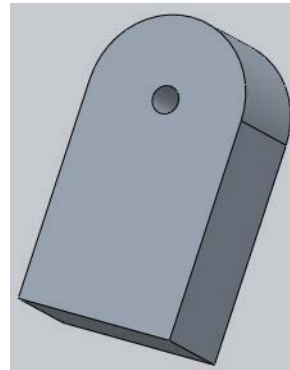


Figure 55: Concept Thumb

The concept finger was designed keeping in mind the need for rotational stops. As the part scaled down, however, issues arose with the stop being weakly supported, as shown in Figure

55. Having a center hole in the concept thumb, shown in Figure 56, allowed for rotation in the concept hand base system.

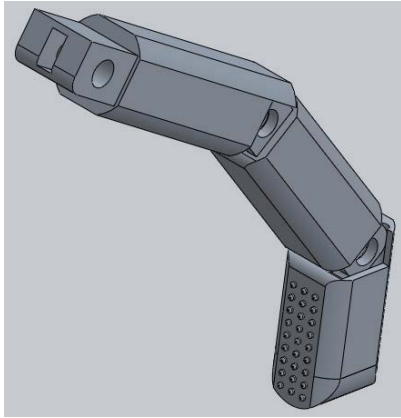


Figure 56: Gen 1 Finger; Assembly

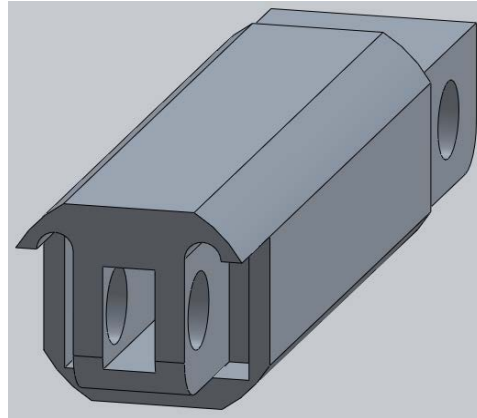


Figure 57: Gen 1 Finger; Proximal Phalange

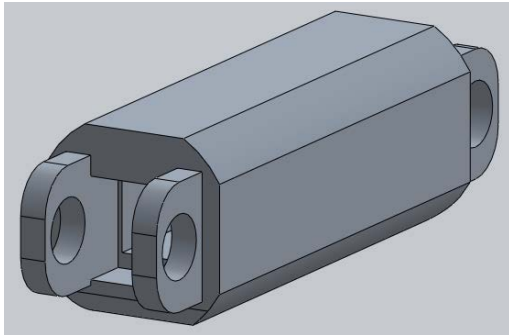


Figure 58: Gen 1 Finger; Middle Phalange

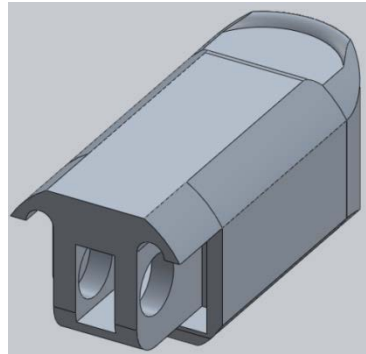


Figure 59: Gen 1 Finger; Distal Phalange

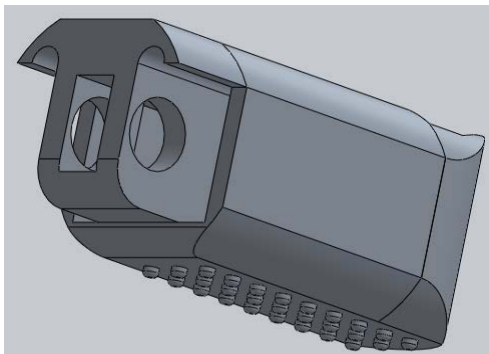


Figure 60: Gen 1 Finger; Distal Phalange; Isometric View

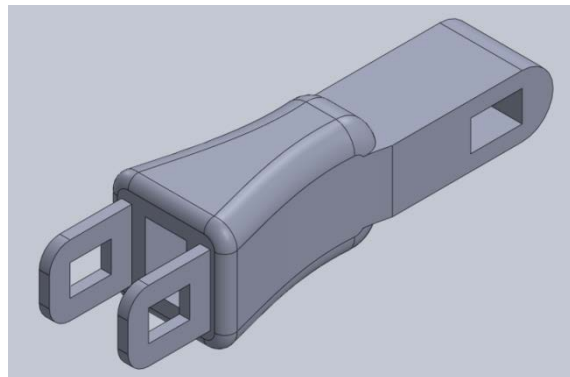


Figure 61: Gen 1 Thumb; Proximal Phalange

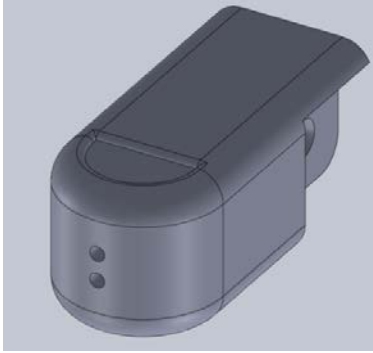


Figure 62: Gen 1 Thumb; Distal Phalange; Alternate View

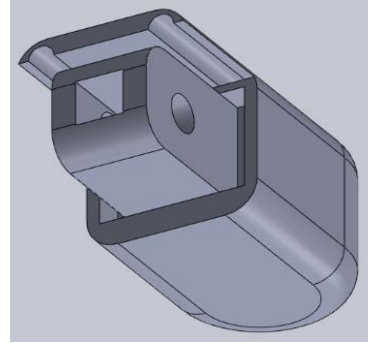


Figure 63: Gen 1 Thumb; Distal Phalange; Bottom View

The generation 1, or Gen 1, finger designs corrected many of the problems arising from the conceptual design. These designs are shown in Figure 56 to Figure 63. To make stronger stops, the top was flattened and the entire finger was made thicker, which allowed for a much larger part of the finger to prevent motion. This updated design also made the potential for scaling easier, as it was a continuation of the finger pieces, rather than separate extrusions from the top. It was determined that the pins would need to be larger in order to withstand the expected forces, so the hole sizes were increased. By making the end of the proximal joint thinner, a stronger overall finger that still fit into a smaller hand base was achieved. A set of cuts and flanges were made at the end of each finger in order to prevent lateral motion. Internally, a main channel allows for cables to easily fall through during assembly. The distal joint included a cosmetic fingertip, as well as nubs for improved gripping. Two holes are located on the front face of the fingers to allow for cables to pass through, and then be tied into knots so that they can't go back. These holes are identical to those in the thumb design, as shown in Figure 62.

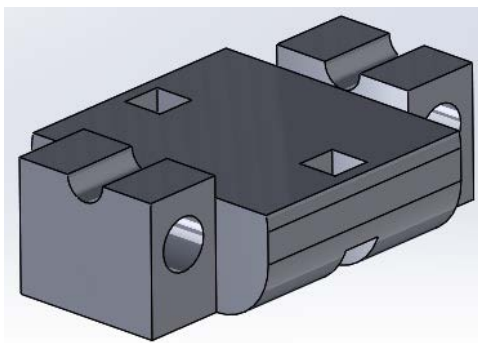


Figure 64: Gen 2 Finger; Middle Phalange Bottom

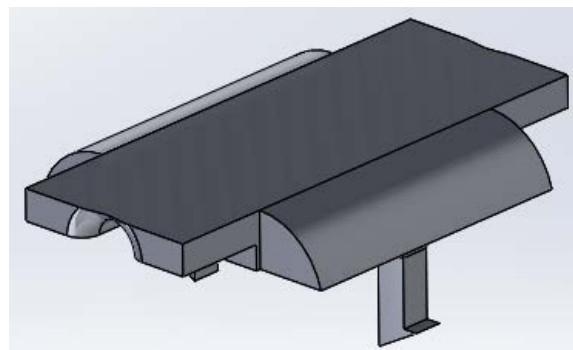


Figure 65: Gen 2 Finger; Middle Phalange Top



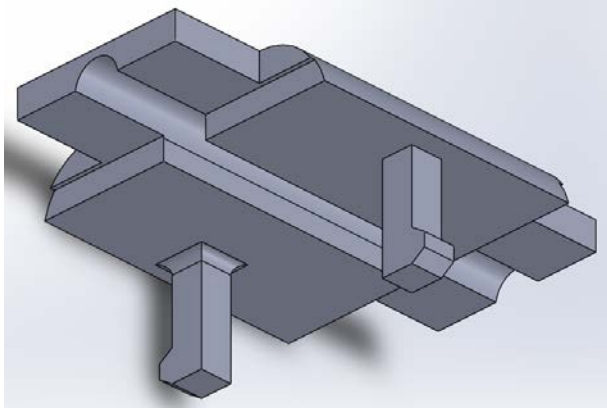


Figure 66: Gen 2 Finger; Middle Phalange Top Design 2

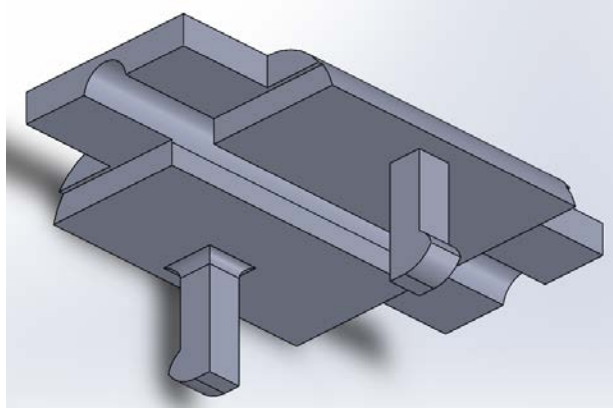


Figure 67: Gen 2 Finger; Middle Phalange Top Design 3

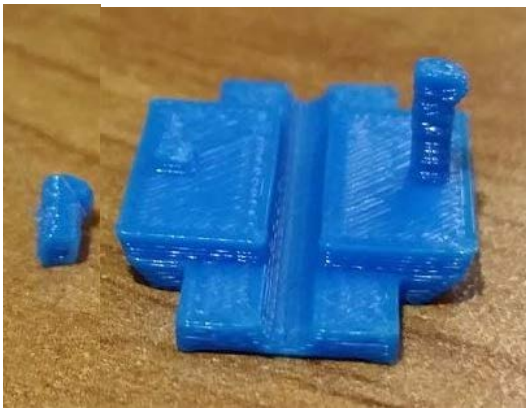


Figure 68: Gen 2 Finger; Top Design Print Failure



Figure 69: Gen 2 Finger; Snap Pin Failed Tolerance

While the appearance of the Gen 1 thumb may seem different than that of the fingers, it was designed keeping the same principles in mind. To ensure maximum strength and grip capabilities, it was made wider than the other fingers. The pin used to attach the thumb to the hand base and is also larger than those of the fingers, and there is a gap by the stop at the top, shown in Figure 64, to allow a larger range of motion.

At the same time as Gen 1 was being designed, a second idea was considered in Gen 2, which is shown in Figure 64 through Figure 69 and uses snap-fit pins to put together the fingers. This would not only make initially assembly faster, as the hassle of feeding cables is avoided, but would also make replacing the cables a quicker process. Slight modifications such as a rounded entry hole in Figure 66, flanges around the pins, and different ends for the pins, shown in Figure and Figure 67 were printed and tested in terms of force required to insert them. The design in

Figure 67 worked the best, but could be easily separated and often failed to print correctly.

Figure 68 and Figure 69 show the main issues with this design: easily broken pins and prints not meeting the required tolerance, causing the center to buckle.

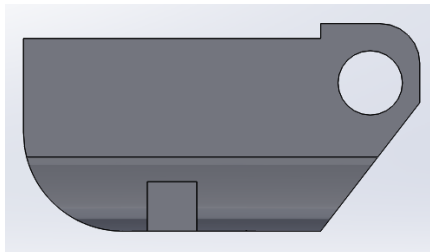


Figure 70: Gen 2 Finger; Distal Phalange; Side View

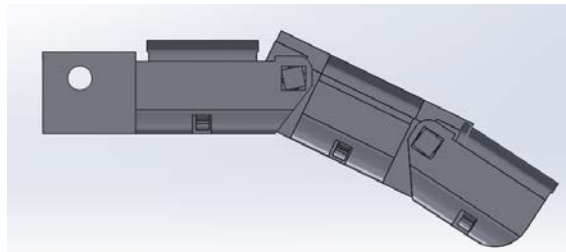


Figure 71: Gen 2 Finger; Assembly; Side View

The snap-fit pin design was continued to the other finger components to see if there was any advantage of this design to the Gen 1 design. The holes and pins were made slightly larger to make the parts stronger and reduce the failure rate of printed parts.

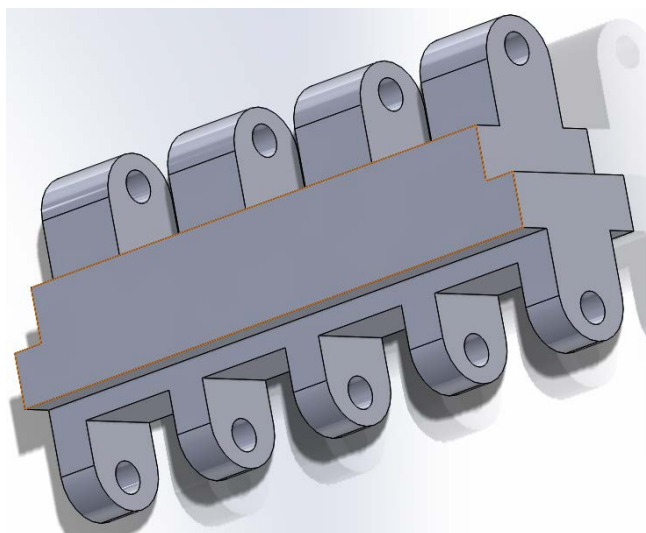


Figure 72: Single Piece Proximal Fingers

Figure 72 shows a potential design for a more robust set of proximal fingers. At the suggestion of Nathan Ramsey, who is a nurse at a rehabilitation clinic from the e-NABLE Google+ community, a basic CAD model of a design to reduce strain on the fingers was developed. This design would replace the first set of joints, allowing for reduced forces on individual components

and a potentially longer lifespan. The main concern with the design, and eventually the reason for not using it is that it would reduce flexibility and lessen the effective gripping functionality.

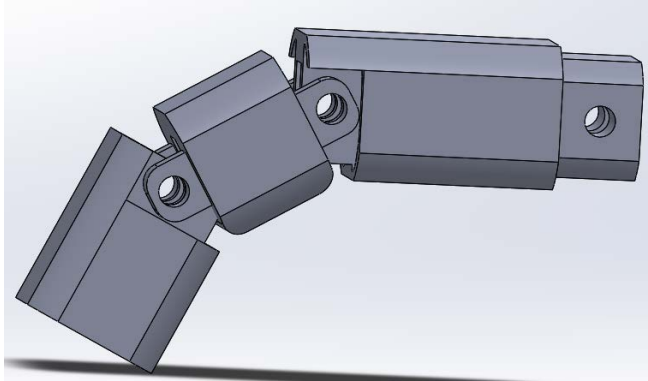


Figure 73: Gen 3 Finger Assembly

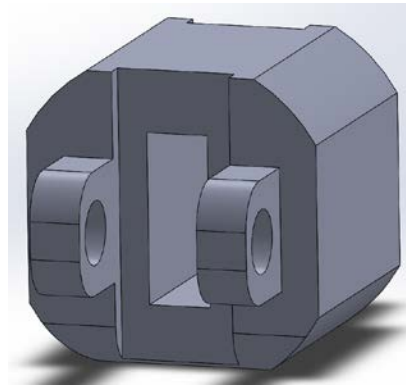


Figure 74: Gen 3 Finger; Middle Phalange; End View

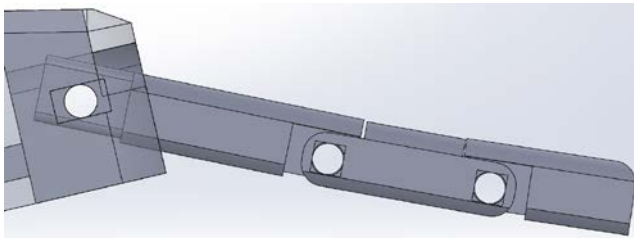


Figure 75: Gen 3.1 Finger Assembly

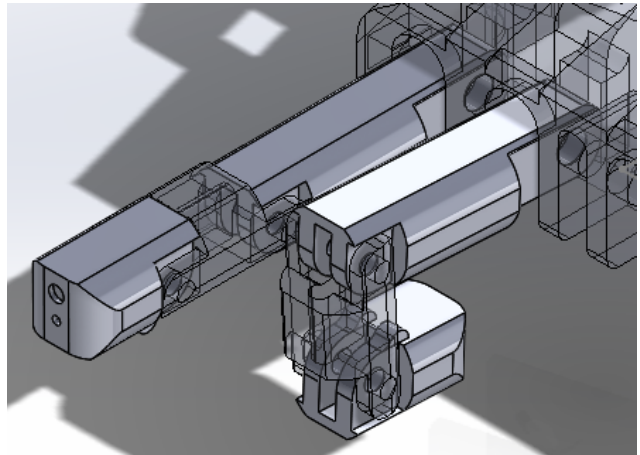


Figure 76: Gen 3.2 Finger; Assembly; Isometric View

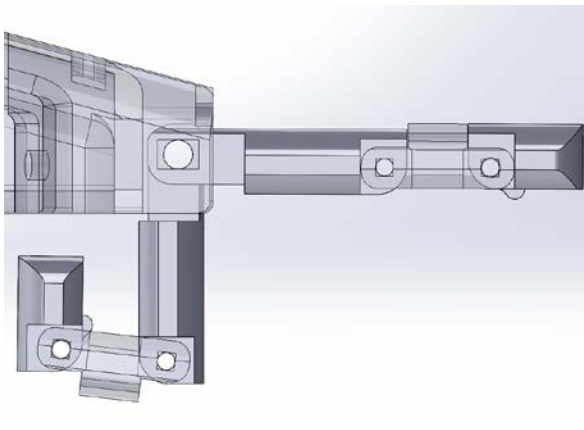


Figure 77: Gen 3.2 Finger; Assembly; Side View

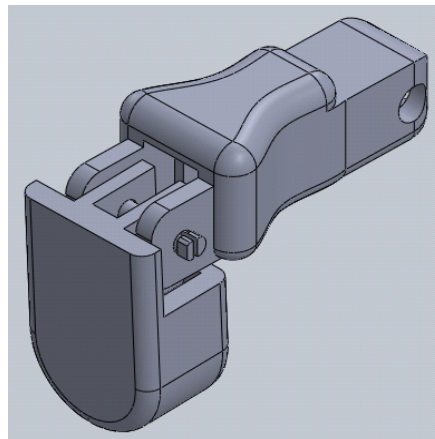


Figure 78: Gen 2 Thumb; Assembly

The design iterations of the third generation of fingers are shown in Figure 73 to Figure 78. While very similar in appearance to the Gen1 designs, these fingers have scaling capability through the use of equations. To accomplish that, the designs were slightly simplified in areas, such as removing the cosmetic fingernail and grip nubs. The grip nubs were determined nonessential because rubber covers will cover the fingertips.

Gen 3.1 fingers are slightly longer to match human finger proportions more accurately, and were rounded for cosmetic reasons and to remove sharp edges. The middle joint was also altered so that it would have a large, flat surface to print on. Holes on one side of each phalange were made square for the improved pin design as well.

The current design, generation 3.2, has added bumps on the distal joint to reduce the maximum rotation, as the finger was closing past the fulcrum and not returning to its original position. The space between the pin holes and the ends of the fingers was also increased for extra strength and durability. The top front hole was made larger to accommodate larger elastic, and the internal cavity was made larger to avoid the pinching of cables during rotation of the finger. The width of the fingers was also decreased, as there were some interference issues between fingers.

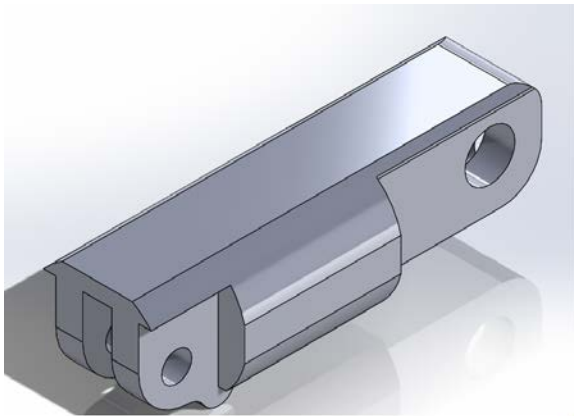


Figure 79: Generation 3.3 Finger, Proximal; Isometric View

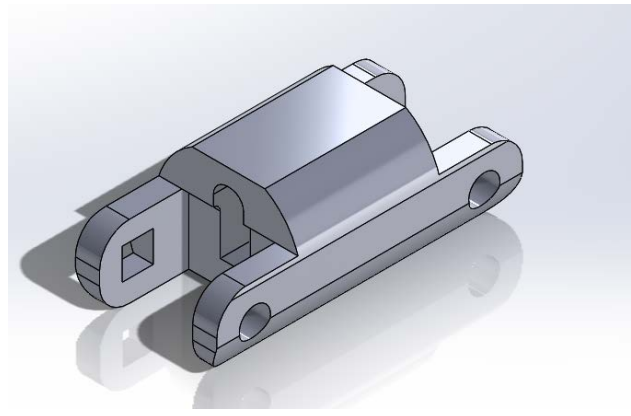


Figure 80: Generation 3.3 Finger, Middle; Isometric View

After printing and testing generation 3.2, slight modifications were made. Mechanical stops were needed in the proximal segment, as well as the distal segment, to further restrict the range

of motion. Without these stops, the fingers would bend past the fulcrum and stick in position. The middle part of finger was updated to fit better with the other parts and hold the pins in better. To reduce friction, the gaps between fingers were made larger.

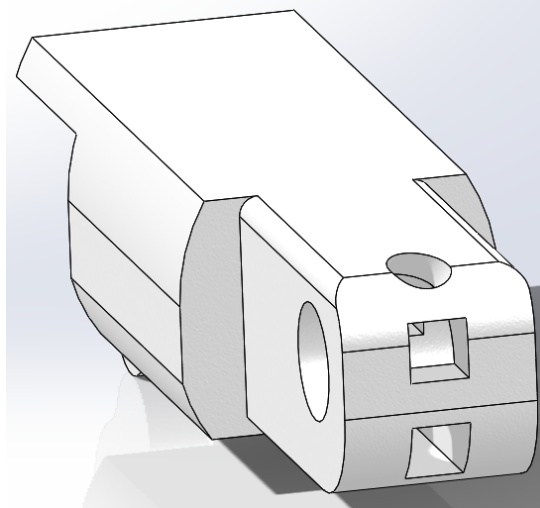


Figure 81: Generation 3.4 Finger, Proximal; End View

It was noticed that the knuckle pin and elastic cable fit together too tightly, so a hole was added to the top to allow for the cable to be fed past it. An alternative consideration was increasing the size of the internal channel and knuckle hole, but this was decided against due to the risks of weakening the part.

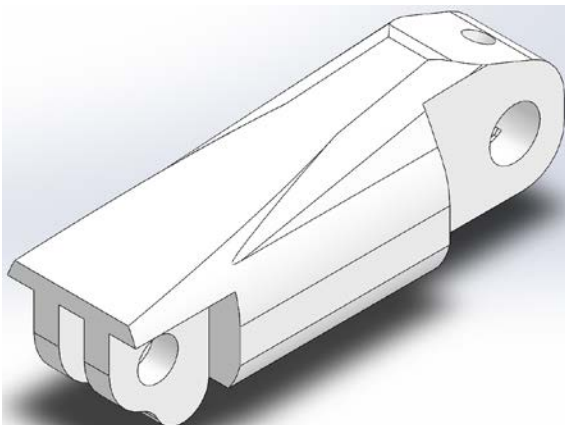


Figure 82: Generation 3.5 Finger, Proximal; Isometric View

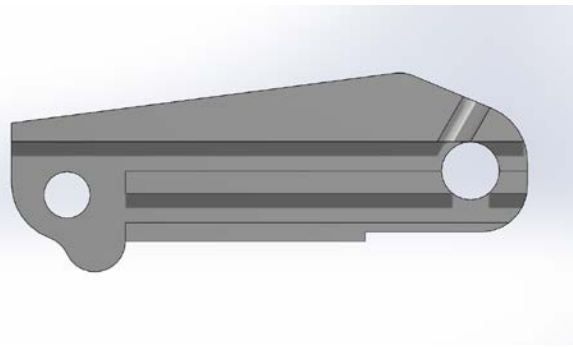


Figure 83: Generation 3.5 Finger, Proximal; Side Cross-Sectional View

During assembly with the most recent hand base design, the proximal finger would hyperextend, meaning that it would rotate past where it should. This not only looked strange, but was increased the force required to close the hand and the strain on the elastics. The team decided to pursue the different designs of fingers which are compatible with the hand base design. Users would be able to choose the option of having two or three joint fingers based on their preference. An assembly version with the hand base is seen in Figure 84.

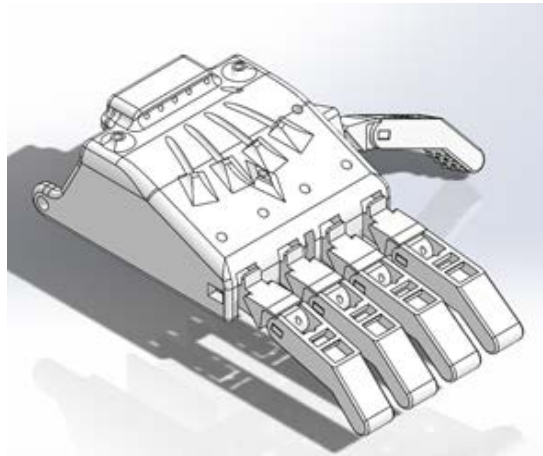


Figure 84: Two-Joint Finger; Assembly

This design has two parts of fingers which are the distal and proximal segments. The proximal finger was set to have an angle of 30 degree in the clockwise direction to provide better grip. The distal region has channeling regions to feed the cables through. The proximal regions have bars to tie the cable around as well as grooves for proper alignment and eliminate cable sliding.

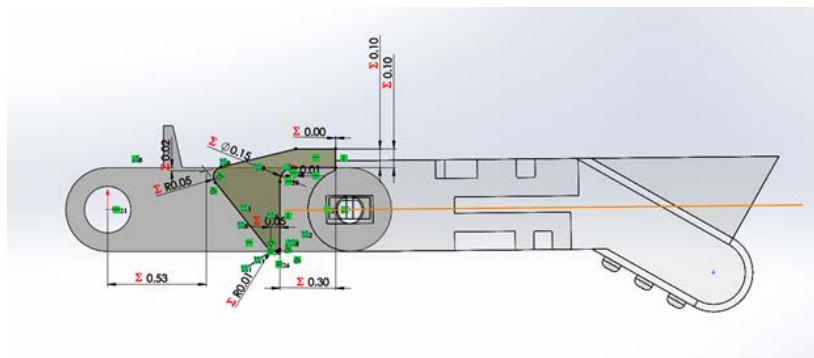


Figure 85: Two-Joint Finger; Sub-Assembly

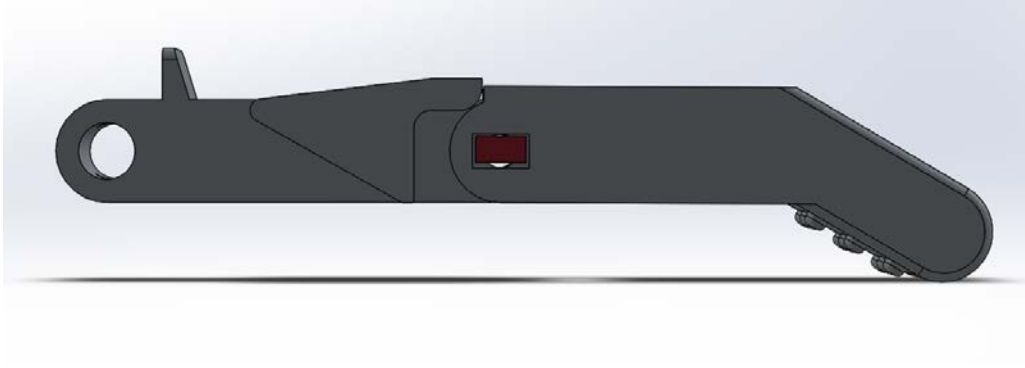


Figure 86: Two-Joint Finger; Sub-Assembly; Front View

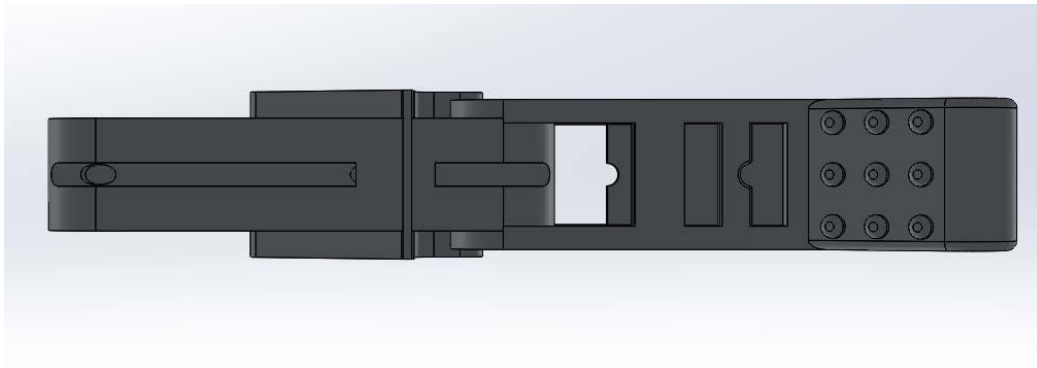


Figure 87: Two-Segment Finger; Sub-Assembly; Bottom View

After a few fabrications and testing, the mechanical stops on the top of proximal fingers tended to fail due to height and distance to the distal part. They were updated to be large enough to stop the distal finger when retracted to its original resting position. Moreover the global variables and equations were added to the fingers for scalability.

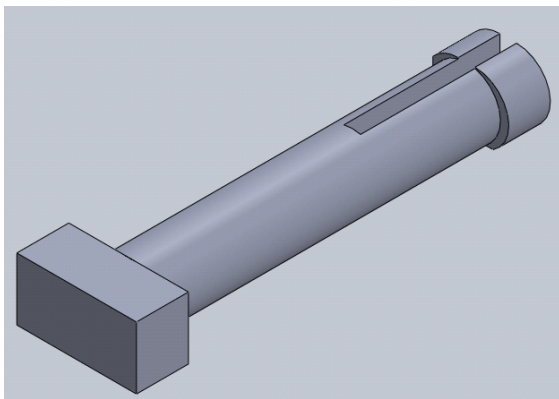


Figure 88: Finger Pin Gen 1

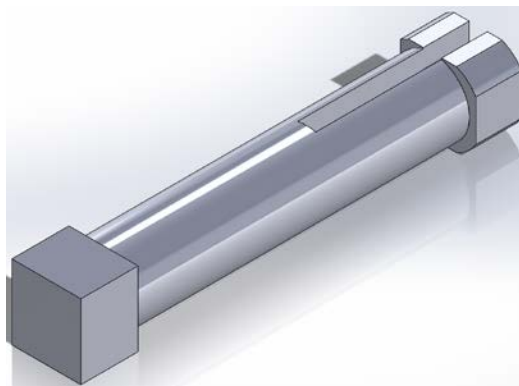


Figure 89: Finger Pin Gen 2

In order to keep the finger sections together, while allowing free rotation, pins were necessary. Movement would cause wear, which would both weaken and loosen the pin over time, so one end was made as a rectangle to prevent rotation. Generation 1, shown in Figure 88, had a very wide rectangle to provide a large resistance to rotation. The other end was slightly larger than the whole that it fit into, but had a slot in the middle so that it could bend inwards and fit through the hole, and then spring back to its larger diameter once it passes.

In the next design iteration, shown in Figure 89, the rectangular end of the pin was made squarer, as it would still prevent rotation while keeping the pin hole smaller and farther from edges. The first pin was having issues fitting through the holes, so the sides of the circular end were cut. While this slightly reduces the force the pin can withstand pushing against it, the majority of loads on the fingers will not affect it.

## Gauntlet

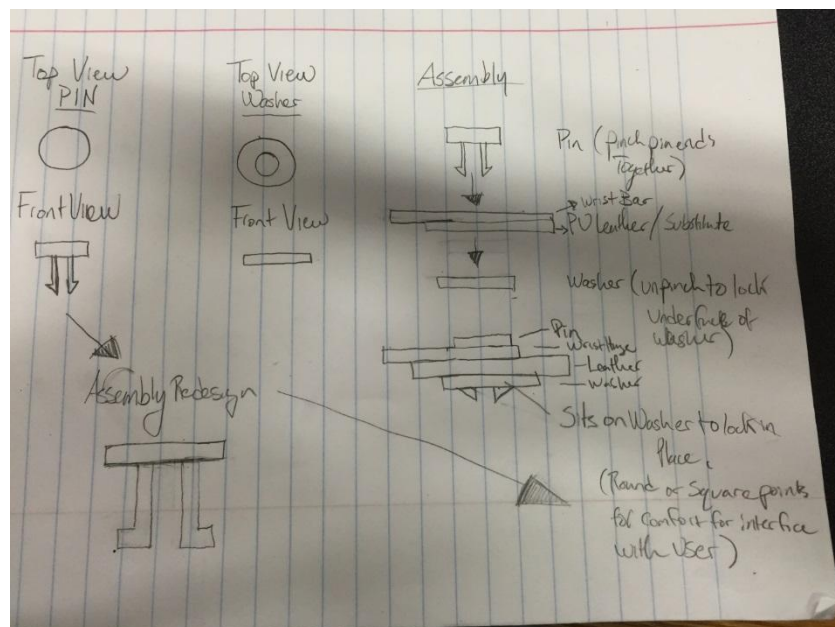
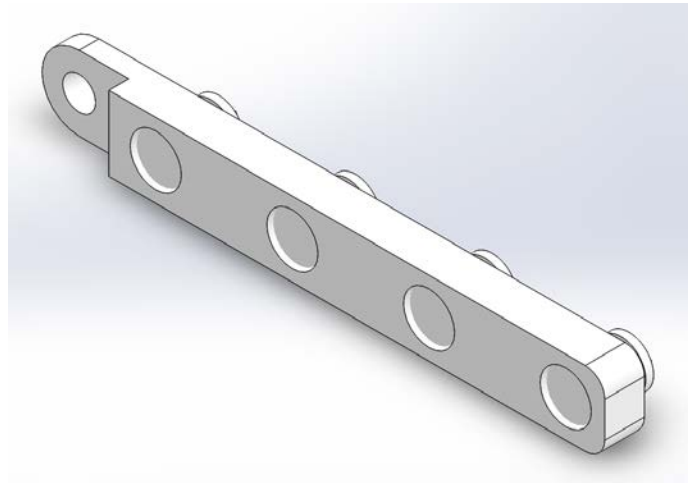


Figure 90: Leather Gauntlet Attachment Concept Sketch

During the initial research and design stages, the team considered pursuing a leather or synthetic polyurethane gauntlet to avoid potential impact stresses associated with 3D printed



gauntlets. This sketch would incorporate a leather gauntlet that is attached to a 3D printed rectangular bar that attaches through the use of snap pins and washers.



*Figure 91: Leather Gauntlet Attachment Concept Assembly*

After further consideration, the team decided to not pursue this gauntlet design. The synthetic polyurethane leather lacked the rigid structure and thickness needed as well as the time, tools, and methods needed to cut, shape, and assemble the finished gauntlet. This gauntlet would be more expensive to produce as it relies on special tools and materials.

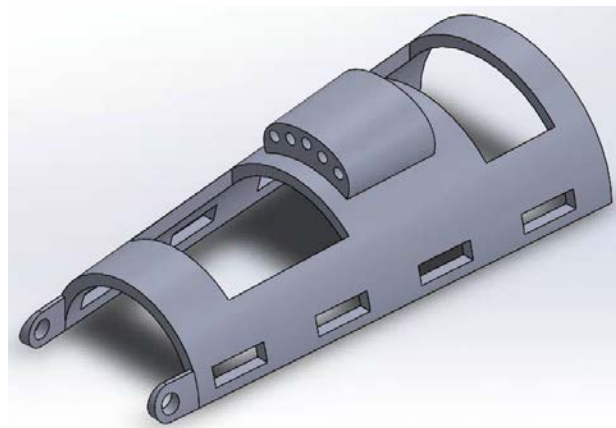


*Figure 92: Gen 1 Gauntlet with Holes for Tensioning Pins*

In the first generation gauntlet, the gauntlet was designed to have an increasing internal diameter to allow for increasing circumference from the wrist to a section of the forearm. Rectangular sections were cut on the top of the component to eliminate material as well as

make the device breathable for the user. Four rectangular sections were cut through the sides of the gauntlet for Velcro straps to be added to fasten around the user's forearm. The bottom of the device was flat for ease of printing.

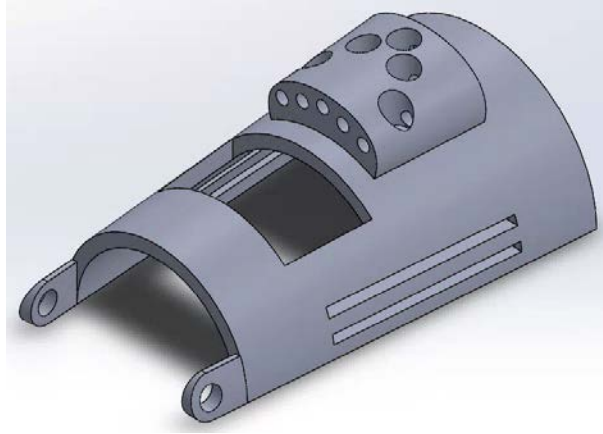


*Figure 93: Gen 2 Gauntlet with Holes for Ratchet Tensioning Mechanism*

After the team decided to investigate and pursue a ratchet tensioning mechanism that was housed on the gauntlet, holes were extruded on the top of the tensioning mechanism for ratchet tensioning system to be developed. The rectangular sections on the side for the Velcro straps were redesigned to allow the user to only need one strap to fasten instead of multiple in the first generation gauntlet.

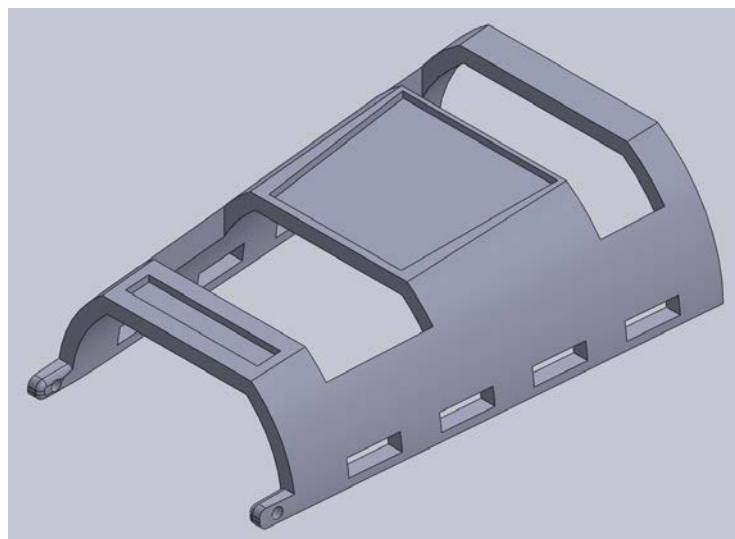


*Figure 94: Gen 3 Gauntlet with Mounting Space for Tensioning System*

After printing the second generation gauntlet, the team decided to redesign the component to have a flat or planar face on the top to reduce the amount of improperly melted polymer strands. The team decided to remove the tensioning mechanism from the gauntlet to improve the serviceability of the completed device. If one part of the mechanism were to fail, break, or wear down; only one part would need to be replaced. This gauntlet design was not as aesthetically pleasing as previous generation models or models publicly available. The tensioning mechanism and bridge for the cables would be separate components to address serviceability.

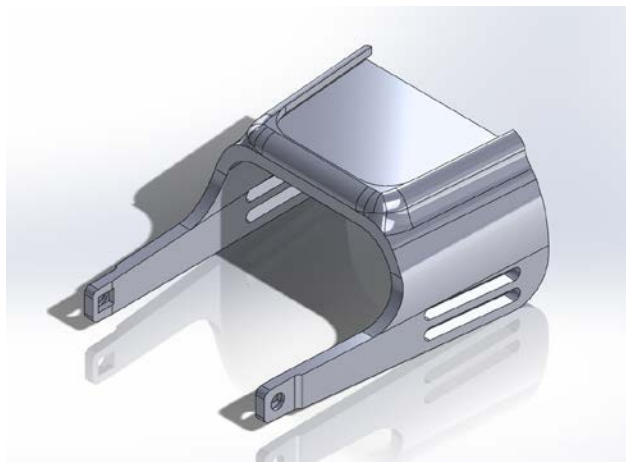


*Figure 95: Gen 4 Gauntlet with Sliding Mechanism*

In the fourth generation gauntlet design, a sliding mechanism was featured to house the ratchet tensioning mechanism. The tensioning mechanism would slide into the device and cables would be fed through the hand and into the fingers. This generation addresses the aesthetic appearance concerns from the third generation model while still incorporating a flat or planar face to reduce the amount of improperly melted polymer strands. Supports were modeled on the inner diameter (suppressed in Figure 95) to reduce print time, material, and need for program generated support material. The rectangular pin holes were added as well to fit the pins that were designed for the base hand to gauntlet connection.

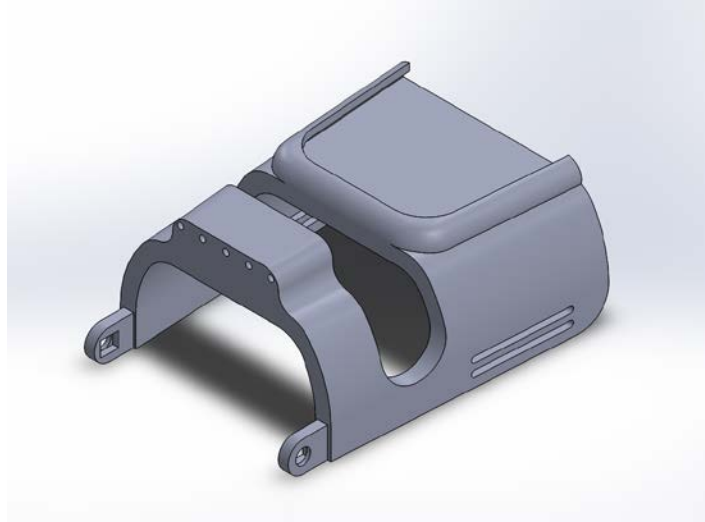


*Figure 96: Gen 5 Gauntlet with Sliding Mechanism and Cable Bridge*

After tensioning and testing gripping of the prosthetic, it was determined by the team that the addition of a cable bridge was needed. Without the cable bridge the cables were loose, lost tension easily, and affected the angle of rotation. The thickness of the gauntlet was also increased to increase the strength of the device.

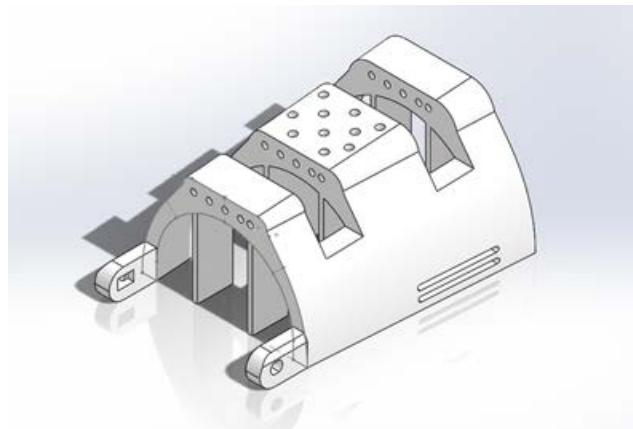


*Figure 97: Gen 6 Gauntlet with Cable Bridge*

After researching additional gauntlet designs, the fifth generation gauntlet design was inspired from Osprey tensioning device. After researching additional gauntlet designs, the fifth generation gauntlet design was inspired from Osprey tensioning device. This generation had a tensioning mechanism imbedded into the gauntlet incorporating machine screws. It allowed the

ease of tensioning just by cabling the tensioning cable into the channels and tensioning with screws.

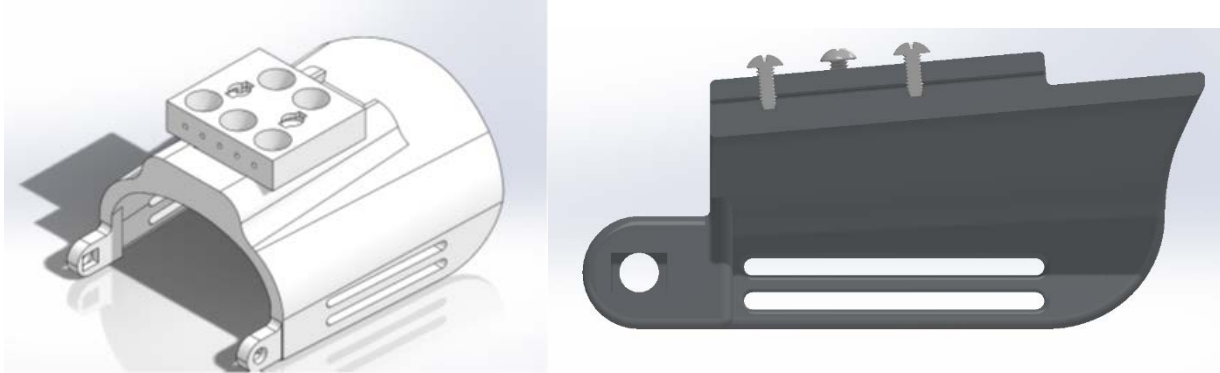


*Figure 98: Gen 7 Gauntlet with Sliding Mechanism and Cable Bridge*

The Figure 98 shows the two alternative designs using different tensioning methods of new generation of gauntlet. The volume was reduced by creating a curved gauntlet, thinning out the wall and body, and eliminating the last section of the bridge as seen in generation 6. After rapid prototyping several gauntlets, slight modifications were made to optimize the design. As shown in Figure 98, the wrist joints of gauntlet were adjusted to the same size of hand base to fit the larger pin and withstand large stresses and torques. In addition, the sliding cover was added to gauntlet for the cover in order to protect the users from injury and contact from the tensioning screws.

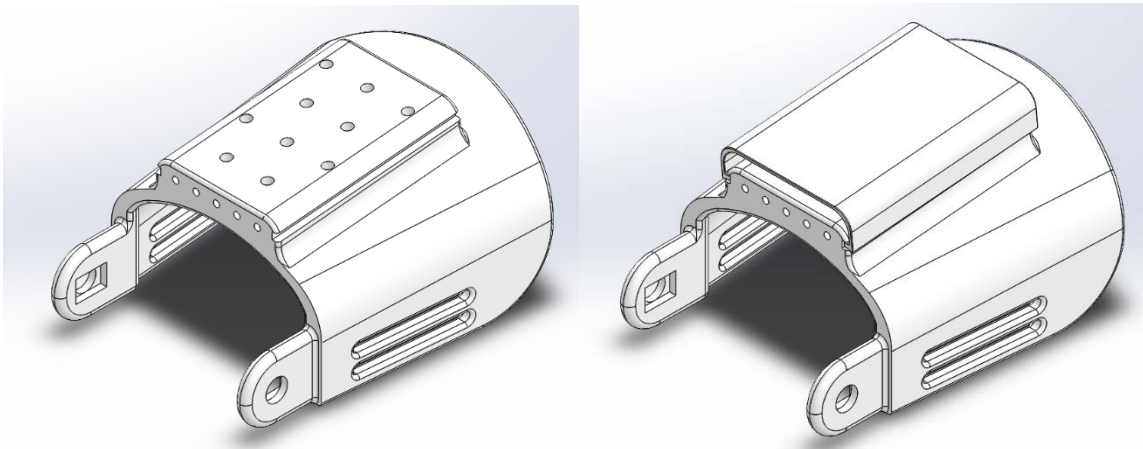


*Figure 99: Gen 7.1 Gauntlet with Sliding Cover*

## Tensioning Device

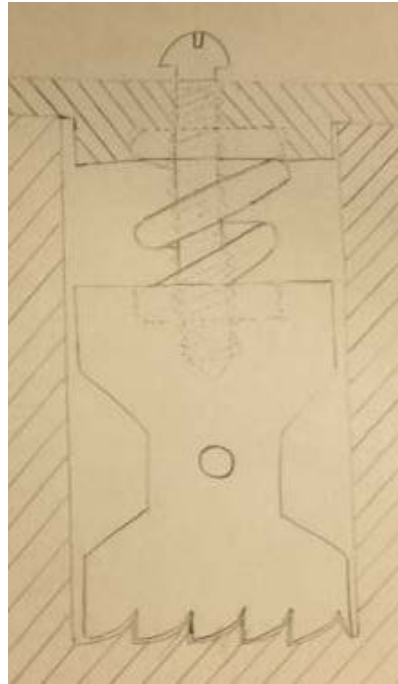


*Figure 100: Sketch of Early Concept Ratchet Tensioning Device*

After the team decided that a ratchet system on the hand base was not feasible, it was decided that a gauntlet based ratcheting system would be more realistic. A ratchet system would eliminate the need for the commonly used tensioning pins, which requires tools for tensioning. Figure 100 shows an early sketch of a simple ratchet device consisting of a spool, a spring, and a screw or shaft attached to the spool enclosed inside a cylinder.

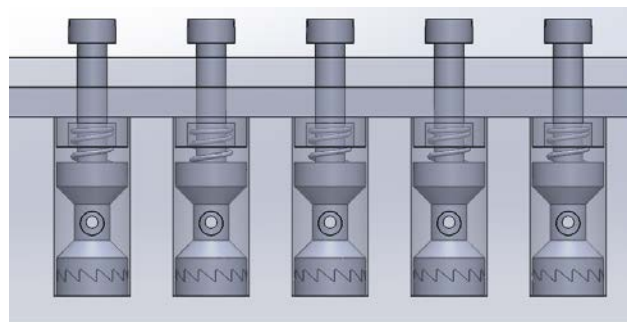


*Figure 101: Gen 1 Tensioning Mechanism; Front View*



Figure 102: Gen 1 Tensioning Mechanism; Exploded View

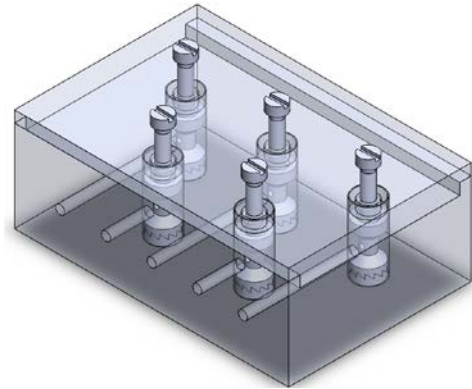


Figure 103: Gen 1 Tensioning Mechanism; Isometric View

Figure 102 shows the internal components of the Gen 1 tensioning device. At this point in the design process the tensioning device was purely conceptual. One design intention was to have all of the parts manufactured by 3D printing, with the exception of the spring. With the use of SolidWorks it could be determined that all of the other components for the device could be printed within the printer's resolution. Figure 102 and Figure 103 show the internal components as part of the Gen 1 tensioning device assembly.

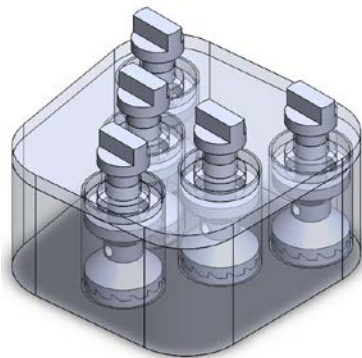
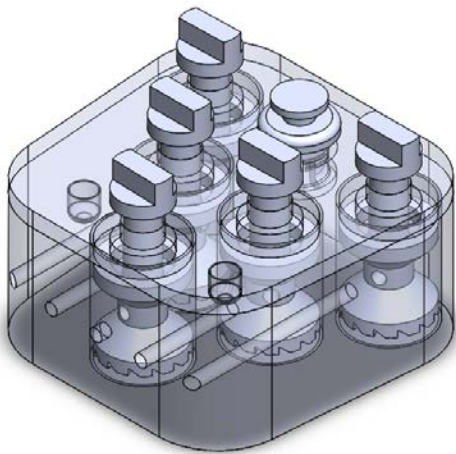


Figure 104: Gen 1.1 Gauntlet Tensioning Mechanism; Isometric View

For the Gen 1 Gauntlet tensioning device, the geometry had to be altered in order to fit on the gauntlet itself. Additionally, the internal components had to be arranged in a manner where they would fit closely together, but not interfere with each other, meaning that the cables could run parallel into the spools. Figure 104 shows the updated version of the Gen 1.1 tension device. In

this iteration, the tension mechanism was greatly reduced in size so that it would fit the gauntlet. Also, the internal components were arranged in a V-shape. The V-shaped arrangement proved to be the optimal choice for the device, as it allowed for the device to be greatly reduced in size without sacrificing strength. Reducing the size allowed for the parts to be printed more quickly and with less material. In addition, the shafts connected to the spools were modified with features that would allow the user to tension the spools without the need of a tool.



*Figure 105: Gen 1.2 Gauntlet Tensioning Mechanism; Isometric View*

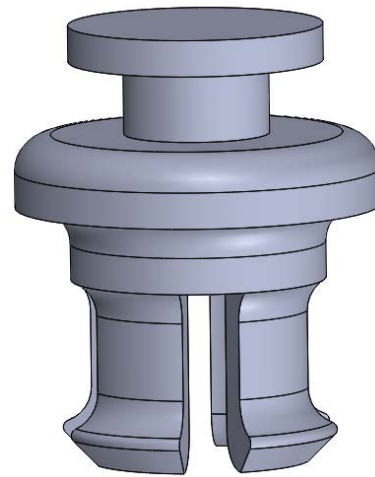


*Figure 106: Snap Pin; Front View*

One of the concerns that arose with the Gen 1.1 tensioning mechanism was creating a mechanism to close the lid, which was necessary for the springs to stay compressed. One method to keep the components compressed within the device was to design a snap pin, as shown in Figure 106, which could be used to lock the top and bottom components. Additionally, several pin features were added to the top and bottom components to aid in, as shown in Figure 105.



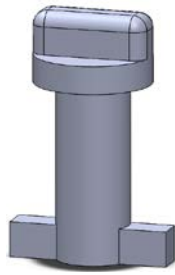


Figure 107: Top "T Shape" Locking Device - Isometric View

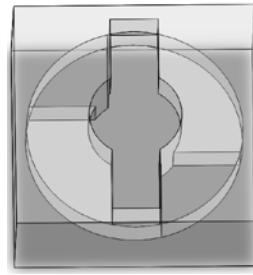


Figure 108: Locking Device Test piece - Isometric View

Through testing, it was found that the snap pin was not strong enough to compress the top and bottom components together. The force exerted upward by the springs was too great for the snap pin to overcome, so a new locking device was created to solve this problem. This device used a simple upside down "T" shaft Figure 108 that was inserted into a locking mechanism and rotated 90 degrees. The square features at the bottom of the shaft once rotated 90 degrees prevent the shaft from coming out of the locking mechanism. A locking device piece Figure 108 was made to test the T shaft to ensure that the device would work correctly. Once the device was tested and proven to be a successful solution, it was incorporated into the Gen 2 gauntlet tensioning device, Figure 110.

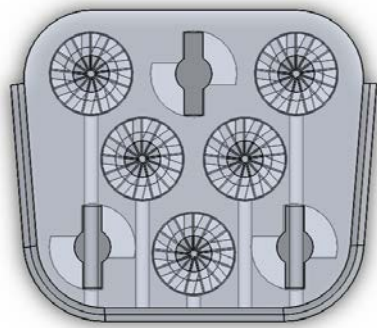


Figure 109: Gen 2 Gauntlet Tensioning Mechanism; Top View

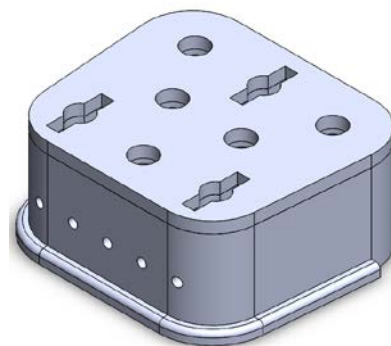


Figure 110: Gen 2 Gauntlet Tensioning Mechanism; Isometric View

For the Gen 2 gauntlet tensioning device, a few modifications were incorporated. The device was widened half an inch to accommodate the new locking device features. A sweep was added to the bottom of the tensioning device to allow it to slide into the current gauntlet for serviceability if the component breaks, and the new locking mechanism was added.

## Global Variables

Global variables are a key feature of our design that allows for independent scaling of specific features and components. Global variables exist at both the assembly and component levels and are stored in a text file independent of SolidWorks. These variables can be numbers or equations, depending on their application, as shown in Figure 111. Each critical feature of our design is referenced by one or more of these variables, which currently scale off of one master variable. Certain features need to be limited in their range of sizes, and benefit the most from variables. Those features can either be kept at a constant size or be sized differently from the other features, ensuring their maximum functionality at all sizes within the specified range. Traditionally, a design can only be scaled as a whole, meaning that each part will scale equally in the x, y, and z directions, which can cause tolerance and assembly issues, as well as kinematic failures. The use of global variables and equations allows our design to scale while taking into account areas of concern.

Name	Value / Equation
"q2"	= 45deg
"h2"	= .25
"d2"	= .1
"h3"	= .8
"angle3"	= 30deg
"d3"	= .15deg
"angle4"	= 17deg
"d4"	= .325
"d5"	= .3
"draftangle"	= 12deg
"angle5"	= 140deg
"d6"	= .18
"padding3"	= .4
"draftangle2"	= 3deg
"padding4"	= .3
"padding5"	= .15
"fillet"	= .05
"fillet1"	= .1

Figure 111: Global Variables and Equations

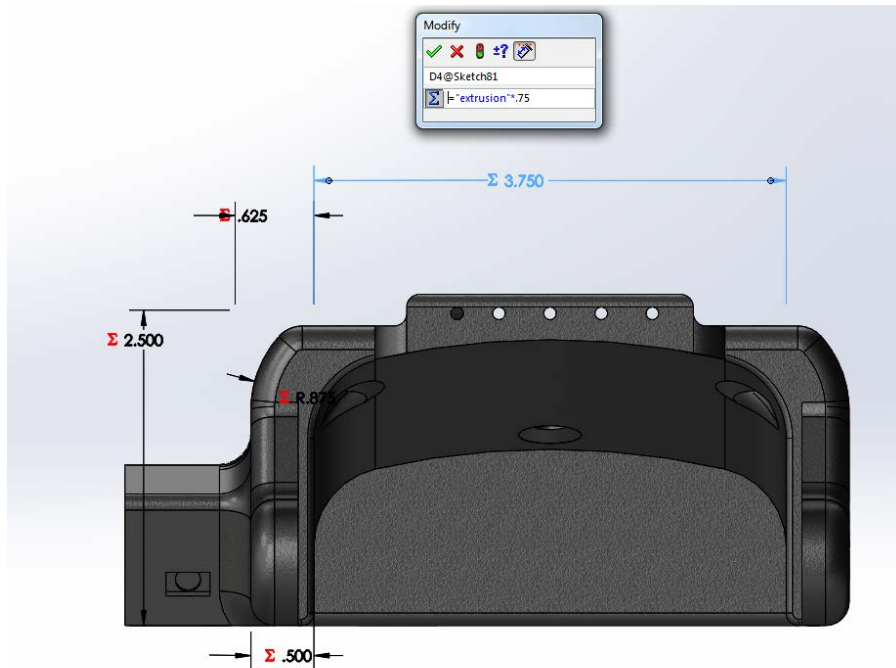


Figure 112: Each dimension is inserted into global variable or equation

The master variable is currently measured from the width of the human hand, which is represented by the highlighted dimension in Figure 112. In the future, the prosthetic would ideally scale from additional master variables, such as the length of the hand and width of the wrist. By defining master variables from measurements of the user, a proper scale is much more achievable. Individual features can be modified to scale at a different rate, or not at all, ensuring better fits and a higher rate of successfully printed parts as well. A higher success rate reduces printing and assembly time, as well as cost of the prosthetic.

For our design, we kept all of the holes the same time. Keeping cable channels and holes at a constant size allows for using the same size cables with every sized hand. Changing the size of holes for hardware may cause the need for expensive custom parts, so keeping the holes at the same size avoids that issue. If the printed pins scale too small, they will not print. If they become too large, they may not bend enough to properly snap into the holes. Scaling the length of the pins as the width of the fingers changes while keeping the hole diameter constant allows for proper tolerancing.

## Testing Procedure

In order to test our design iterations, our team devised a detailed procedure to test the components of our prosthetic hand. Using this testing procedure, we tested each of our components and iterations and analyzed the results. From our testing results we were able to compare each component and either redesign or eliminate components. Below is each stage of testing in order of how components were tested:

After test pieces were printed and proven to function at their dimensions and scales, we used SolidWorks Simulation Package to test various theoretical values of:

1. Strength (In respect to an applied force)
2. Von Mises Stress

SolidWorks does not offer PLA as a material choice in its package and any values achieved would not be an accurate reflection of the material. ABS was chosen for the simulation testing of the components. The simulation testing is utilized for analyzing critical sections of components with respect to potential failure and critical stresses.

Once the pieces have met our design requirements and theoretical values from simulation testing in SolidWorks, the pieces were printed and assembled into their subassemblies. The main sub assembly in the prosthetic hand we developed is the components of the fingers that connect to the base of the hand component. The testing of the finger and thumb subassembly included:

1. Strength: applying a force of approximately 7lb (31 N)
2. Kinematics: measuring the range of motion (angle of joints measured with a protractor)
3. Tensile, Cyclic, and Compressive Testing (Instron 5544 Uniaxial Tensile Testing Machine)

After the subassemblies have passed initial testing and met our design requirements, testing of a fully assembled prosthetic hand was conducted.

1. Strength: Force needed to fully close hand
2. Kinematics: Angle or range of motion needed to fully close hand
3. Functionality:
  - a. Gripping water bottles of various size
  - b. Carrying grocery bags (weights used)
  - c. Holding a phone or cell phone
  - d. Opening doors

The assembled prosthetic device will also be tested against our design requirements and other hands on the market from e-NABLE for benchmarking. Tests conducted against our design requirements are:

1. Assembly time
2. Assemble as a team
3. Ease of Assembly
  - a. Does it require tools to assemble the components
  - b. Does it need additional finishing after the print

# Kinematic Analysis

## Mobility

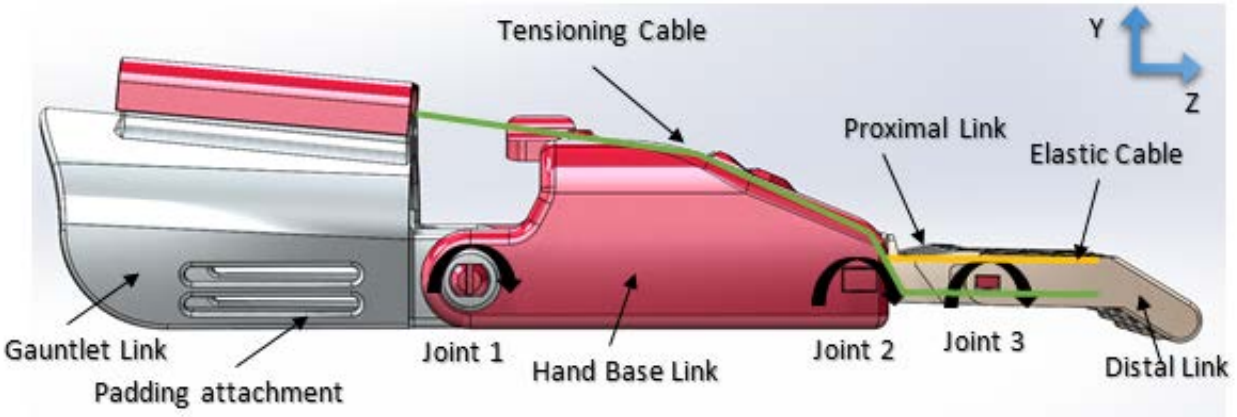


Figure 113: Mobility of Two-Segment Finger-Hand Design

As all 5 fingers functions the same approach, all the fingers will be lumped into one sub-finger in this calculation. Moreover gauntlet is assumed to be grounded because padding attachment to a human's arm as Figure 113 is shown. This whole system includes 6 pin joints and 6 links (with ground link accounted). The first pin joint is at where the wrist joint is and two links which are the hand base and gauntlet. As gauntlet is a ground link for this sub-assembly, the pin joint will facilitate the mobility of the hand base rotating around x-axis which is away from paper. The same approach is implied on two other pin joints (2 and 3) which facilitate the connected links around x-axis. The 3 places where cables will be attached counted as 3 joints and cables will be accounted as 2 links. This design provides 3 degree of freedoms. Those degrees of freedoms are independent on its axis. The formula below illustrates the degree of freedom of Figure 1.

Number of links ( $n$ ) = 6, Number of Joints ( $j$ ) = 6, Degree of Freedom of each pin joint ( $f$ ) = 1

$$M=3(n-1)-2j$$

$$M=3(6-1)-2(6)$$

$$M=3$$

Where  $M$  = mobility,  $n$  = number of links,  $j$  = number of joints with DOF

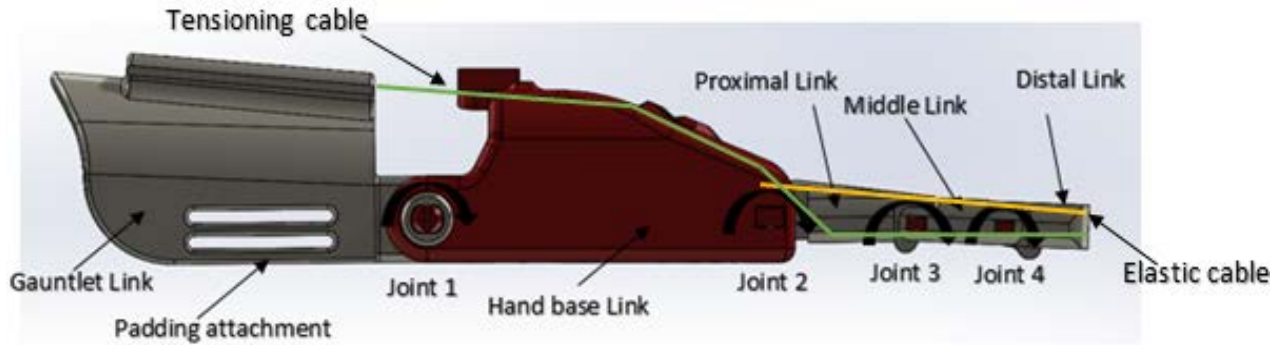


Figure 114: Mobility of Three-Segment Finger-Hand Design

All 5 fingers are lumped onto one finger as it is assumed, they function the same way. Moreover by means of gauntlet is fixed with padding attachment to a human's arm, it is counted as a ground link. For this design, we will have 7 joints and 7 links including the ground. This design will have 4 degree of freedoms in total. However this total degree of freedom implies that each joint has 1 degree of freedom in its own axis which is x-axis. As it will be also limited by the tensioning cables, these will work as together and will have 1 degree of freedom overall. The following formula illustrates the degree of freedom of Figure 114.

Number of links (n) = 7

Number of Joints (j) = 7

Degree of Freedom of each pin joint (f) = 1

Kutzbach equation

$$M=3(n-1)-2j$$

$$M=3(7-1)-2(7)$$

$$M=4$$

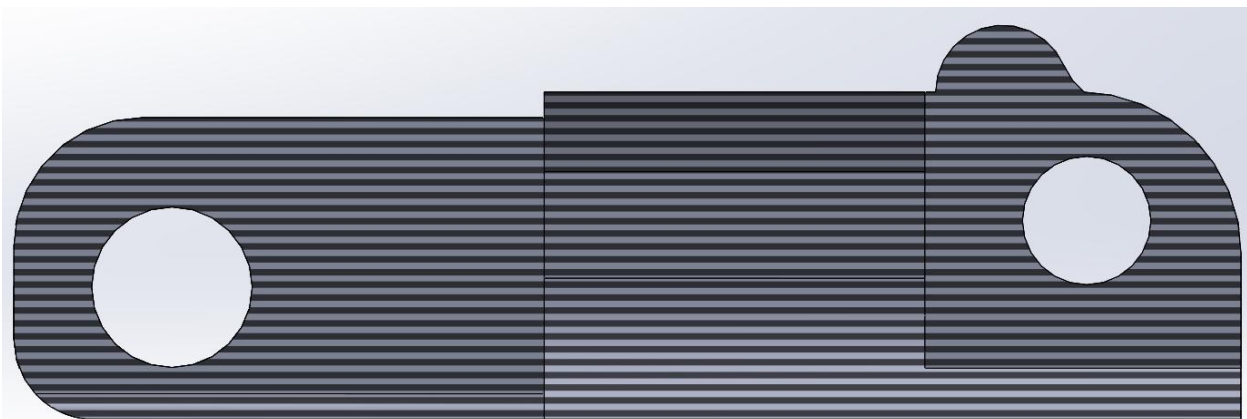
Where M = mobility, n = number of links, j = number of joints with DOF

# Design Analysis

In addition to design changes for improved cosmetics, printability, and use of equations, design changes for improved strength were necessary for a functional prosthetic hand. The parts used are all plastic, so withstanding large forces is not to be expected; however, everyday loads should not cause significant stress or deformation to the parts. One way to objectively look at the impact of design changes is to use force analysis through the use of simulations.

These analyses are very basic and make broad assumptions, so their exact values, especially displacement, are mainly used for design purposes. One of the main considerations is that 3D printed parts are significantly stronger along the plane of printing than normal to that plane.

While the plastic prints each layer, hot plastic comes into contact with hot plastic, and melts together fully. As the next layer is printed, the previous layer has begun cooling, reducing the 'weld' between the printed filament. Any shear force between these layers is therefore much more effective. A representation of these layers with respect to the plane the part is being printed on is shown in Figure 115.



## Plane of Printing

*Figure 115: Representation of Print Layers*

What these analyses do show very well, however, are areas of stress concentrations and concerns or deformation. While the exact stresses and displacements will not be completely accurate, using the max load to estimate the real results was an effective method for



determining any weak points in the design. The first set of analyses performed depicts a force of 15 pounds-force on the middle joint of the finger in the form of reaction forces from the pin. For simulation parameters, the forces are assumed to be the main force broken into x and y components.

$$F_x = F_y = 15 \text{ lbf} * \frac{\sqrt{2}}{2} = 10.62 \text{ lbf}$$

The reaction torque is calculated as:

$$T = 15 \text{ lbf} * 0.54 \text{ in} = 8.1 \text{ lbf} - \text{in}$$

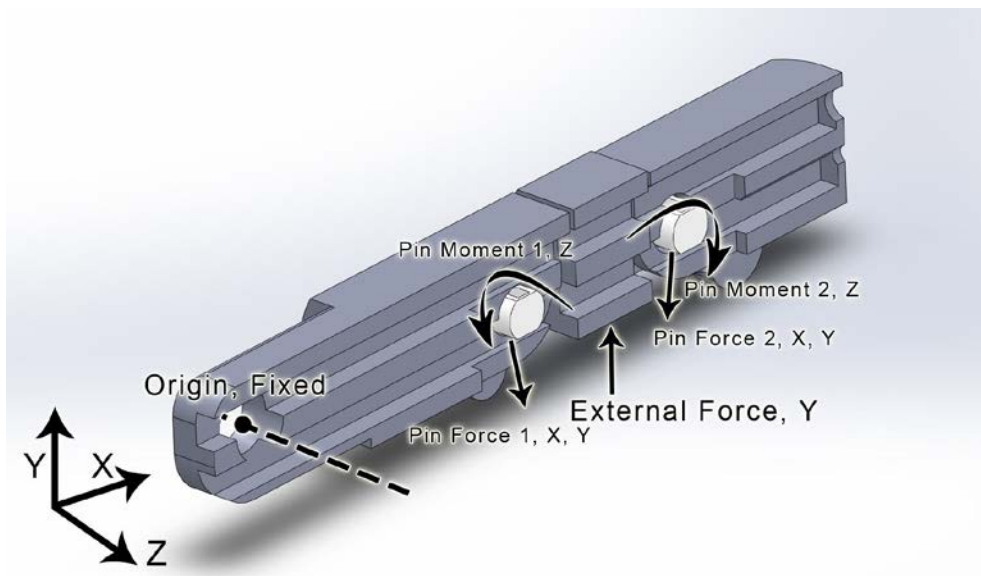


Figure 116: Cross Section View of the Finger Assembly

Finite element analysis (FEA) was performed on several parts to look for excessive forces and deformations. For the finger parts, the above forces and torques were applied at the locations shown in Figure 116. For the distal segment, the part was fixtured along its flat end, shown in Figure 117. Forces were applied in x and y components to the pin holes, where forces would act on the parts. For the proximal and middle segments, one hole was fixtured while forces were applied to the other hole.

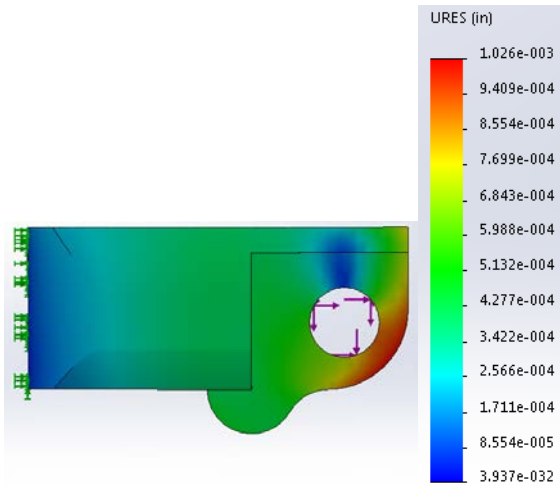


Figure 117: Distal Phalange Displacement Analysis

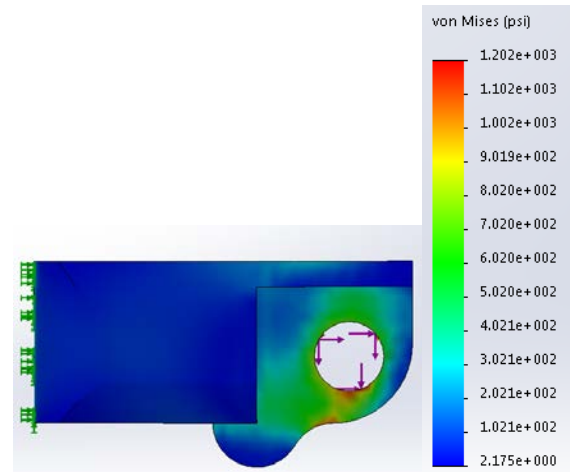


Figure 118: Distal Phalange Von Mises Stress Analysis

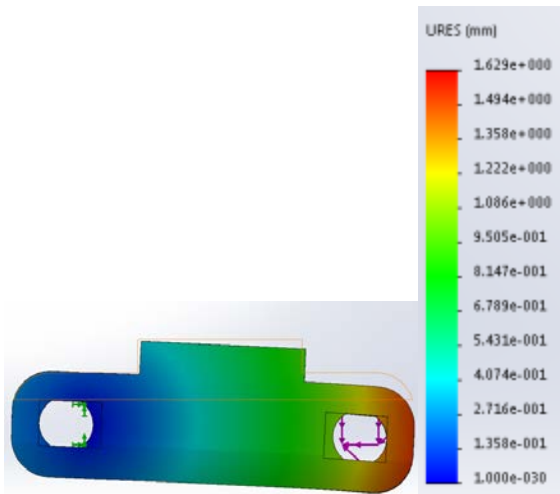


Figure 119: Middle Phalange Displacement Analysis

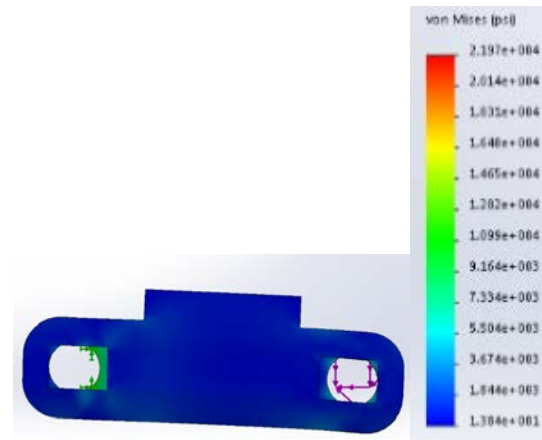


Figure 120: Middle Phalange Von Mises Stress Analysis

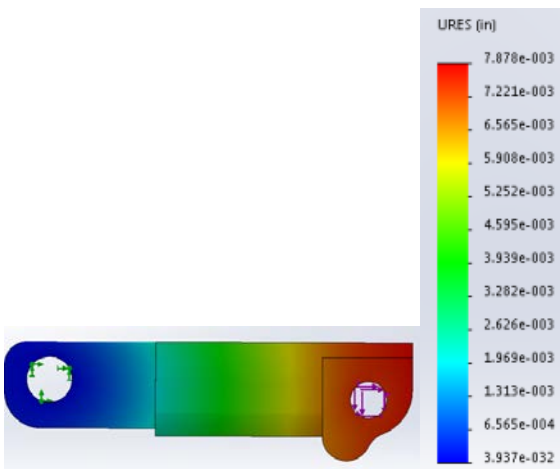


Figure 121: Proximal Phalange Displacement Analysis

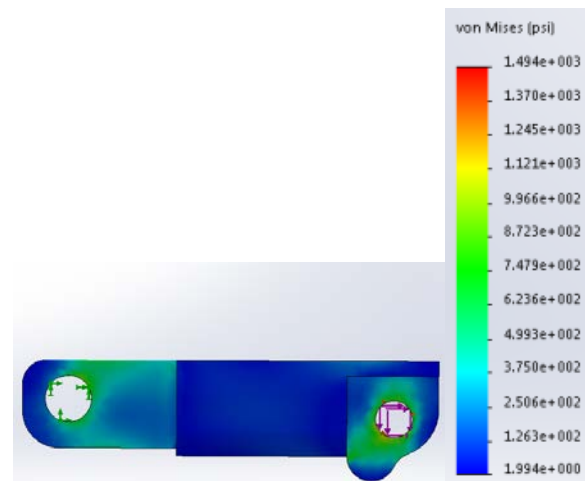


Figure 122: Proximal Phalange Von Mises Stress Analysis

While untested, there was concern that the previous pin hole design was too weak. Analysis was performed and, as predicted, there was significant deformation, as shown in Figure 123. The design was revised, and analysis, shown in Figure 124 was performed again with significantly less deformation. While the level of deformation is still not ideal, this test was performed with the maximum load being on only one end.

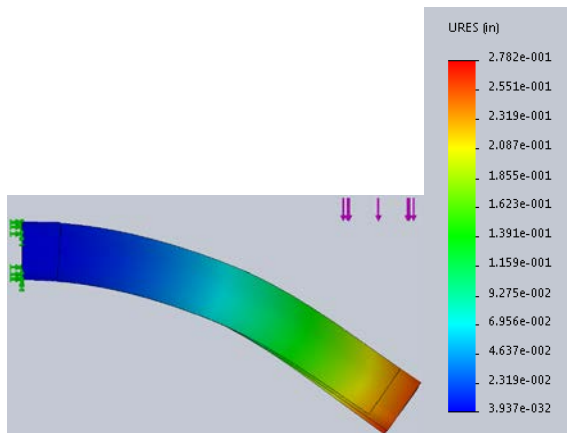


Figure 123: Old Pin Design

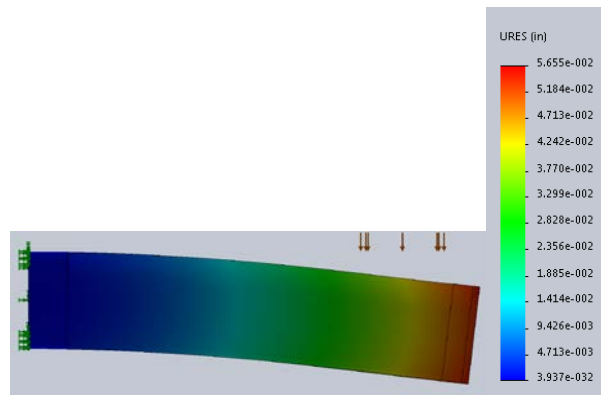


Figure 124: New Pin Design

To fit the new pin design, the middle joint needed to be modified to hold the new ends. In addition, because the new pin was larger, the hole size needed to be increased. However, the rounded corners and uniform hole shape distributed the forces more evenly than the smaller holes, which results in less deformation. The changes in hole shape and size, and their resulting deformations are shown in Figure 125 and Figure 126.

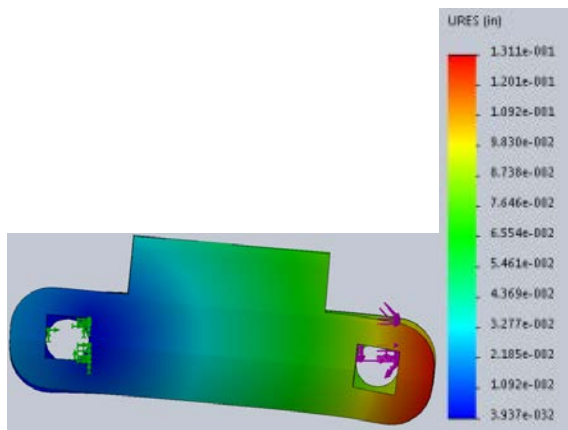


Figure 125: Previous Design

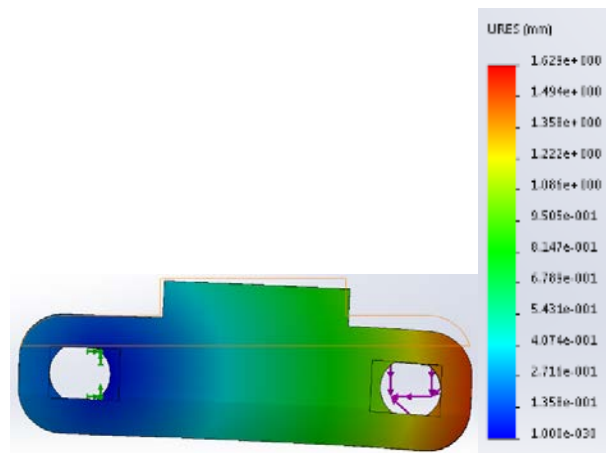


Figure 126: Improved Design

Despite the limitation of the analysis, the simulation run in detail could give reasonable results, which could give insightful information regarding the design conditions. As most of the parts in this product model have complex shapes, the use of curvature mesh instead of standard ones could produce more accurate results. The analysis was performed on depict of forces acting on gauntlet. With the assumption of the weight of an object (which is around 15lb) carried by the hand is vertically downward as shown in Figure 127, the reaction forces on gauntlet are vertical along y-axis in the opposite direction.

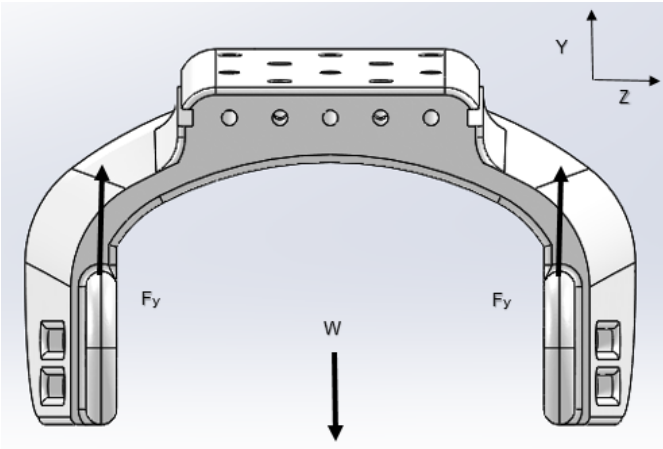


Figure 127: Free Body Diagram of Gauntlet

$$F_y = W * \frac{1}{2} = 15 \text{ lbf} * \frac{1}{2} = 7.5 \text{ lbf}$$

\*The reaction force,  $F_y$ , will be on each side of gauntlet.

Before the analysis, there were also concerns whether the wrist pin of gauntlet would be able to withstand the shear stress and deformation because the reaction forces at the joint, resulting from the applied load, produced shear stresses at the pin on its cross section so it was important to determine the amount of maximum shear stress at the pin. The analysis was performed by fixing the pin at the side surface and applying linear axial load by applying 7.5lbf which is the maximum load. By looking at the corner where pin and its base are connected as in Figure 128, it can be observed that the deformation of the pin was very low but there was high concentration of maximum stress around the area of pin. This explained that maximum forces

were acting around the pin and there would be high value of shear stress on the pin. The formula below illustrates the uniform shear stress over the cross-sectional surface area on a pin.

$$\tau = \frac{F}{A} = \frac{7.50\text{ lbf}}{.07\text{ in}^2} = 107.14 \text{ psi}$$

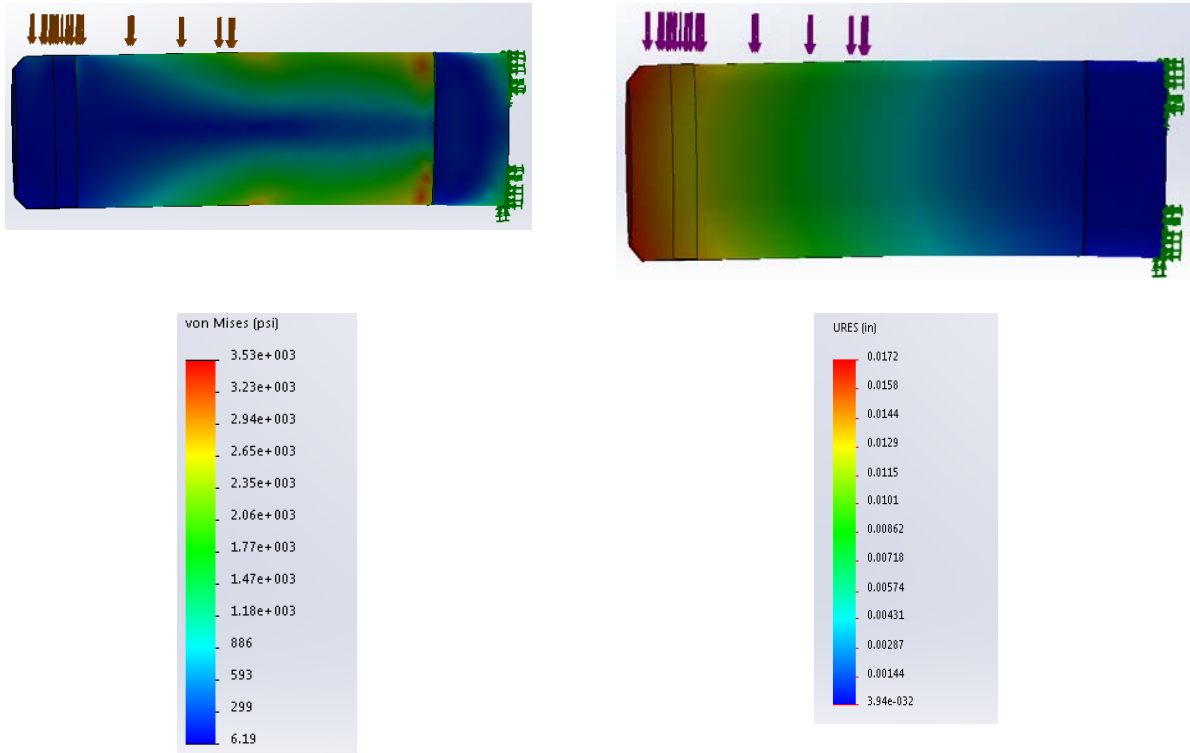


Figure 128: Old Wrist Pin Von Mises Analysis (left) and Deformation Analysis (right)

However, shear stress on the pin could be reduced by increasing the surface area of pin. By adjusting the diameter of a pin size, the cross-sectional surface area was increased which in turn, reduced the shear stress at the pin. It can also be observed that the area of stress concentration at the corner was reduced. As shown in Figure 128 and Figure 129, the maximum stress is reduced from 3.53e+3 to 3.25e+3 psi. The formula below illustrates the reduced uniform shear stress.

$$\tau = \frac{F}{A} = \frac{7.50\text{ lbf}}{.10\text{ in}^2} = 75 \text{ psi}$$

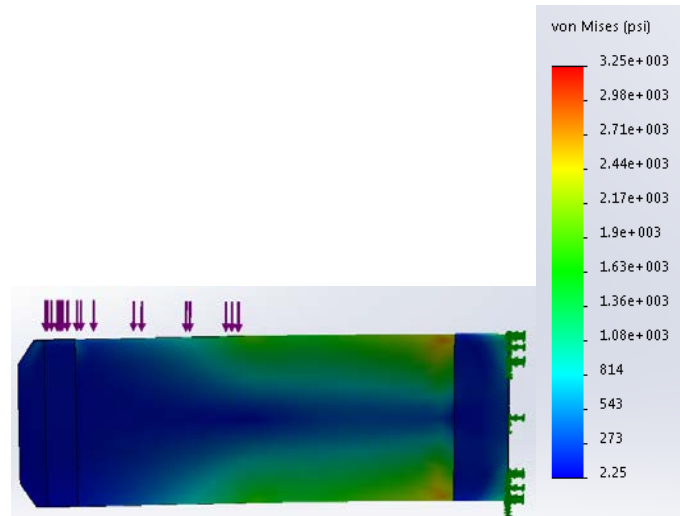


Figure 129: New Wrist Pin Von Mises Analysis

This analysis above, did not consider the orientation of how a product is actually fabricated in 3D printers. Most of the 3D printed parts are significantly stronger along the plane of printing than normal to the plane of printing. The pins could resist more shear stress if they were printed along the normal plane than printed vertically which is normal to plane of printing.

As the size of pins was revised, the gauntlet wrist joints acquired updates on wrist joints in order to fit the updated wrist pins. By increasing the size of pinhole and wrist joint, the forces acting vertically on joint would be more evenly distributed as potentially reduce the deformation. As shown in Figure 130, the vertical forces were applied while top surface is fixed as the gauntlet would be attached to the arm. The maximum displacements due to the loads on the wrist were significantly reduced.

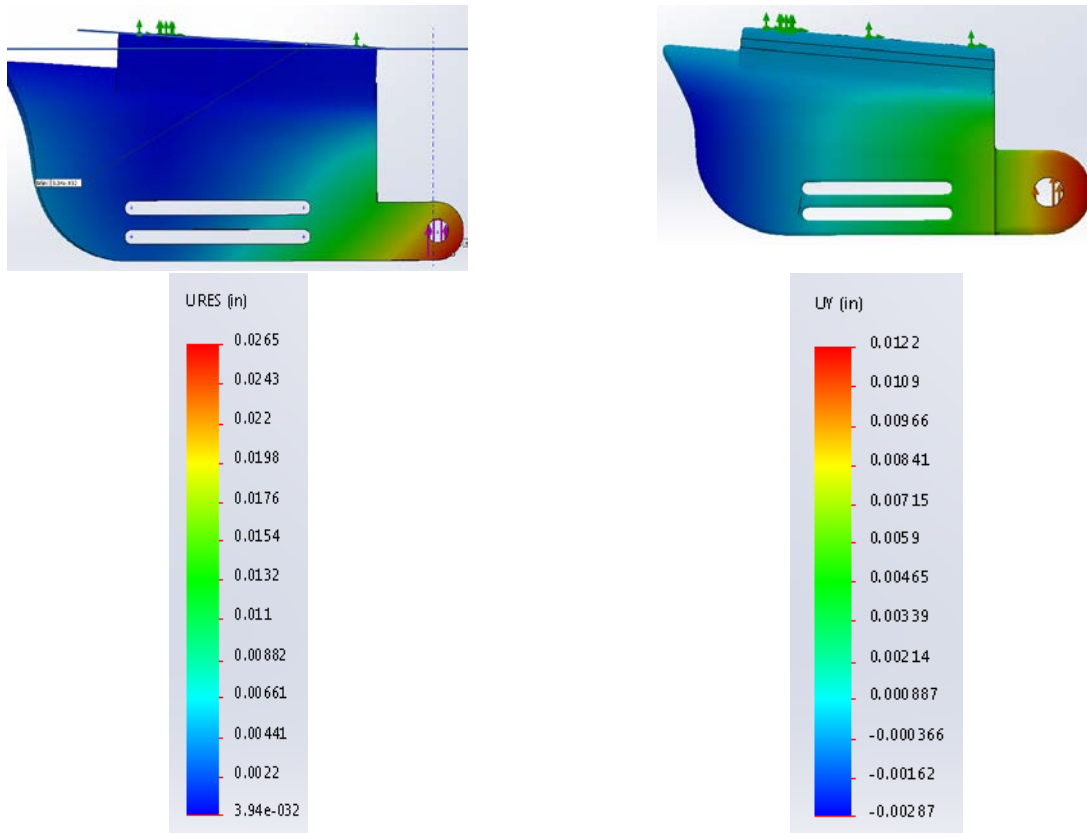


Figure 130: Old Wrist Joint (left) and Updated Wrist Joint (right) of a Gauntlet

In general for 3D printed products, compression loads are not effective for products that are bulky. However for a prosthetic gauntlet, its geometry and material could influence the strength of a product. To find out whether the load from the sides have an adverse effect on the strength of the product in its current shape, the model was simulated again with the fixed top flat part and the two external axial forces applied from the sides as shown in Figure 131.

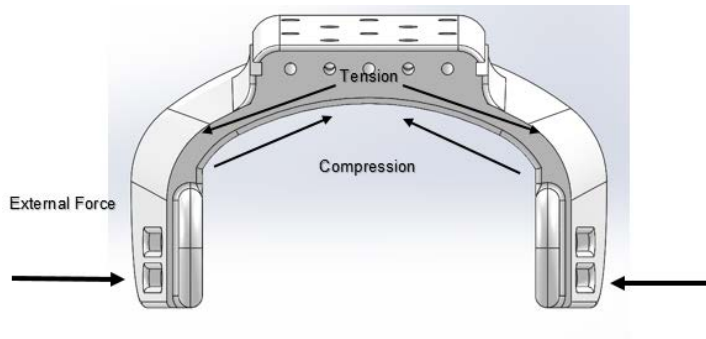


Figure 131: Free Body Diagram of a Gauntlet

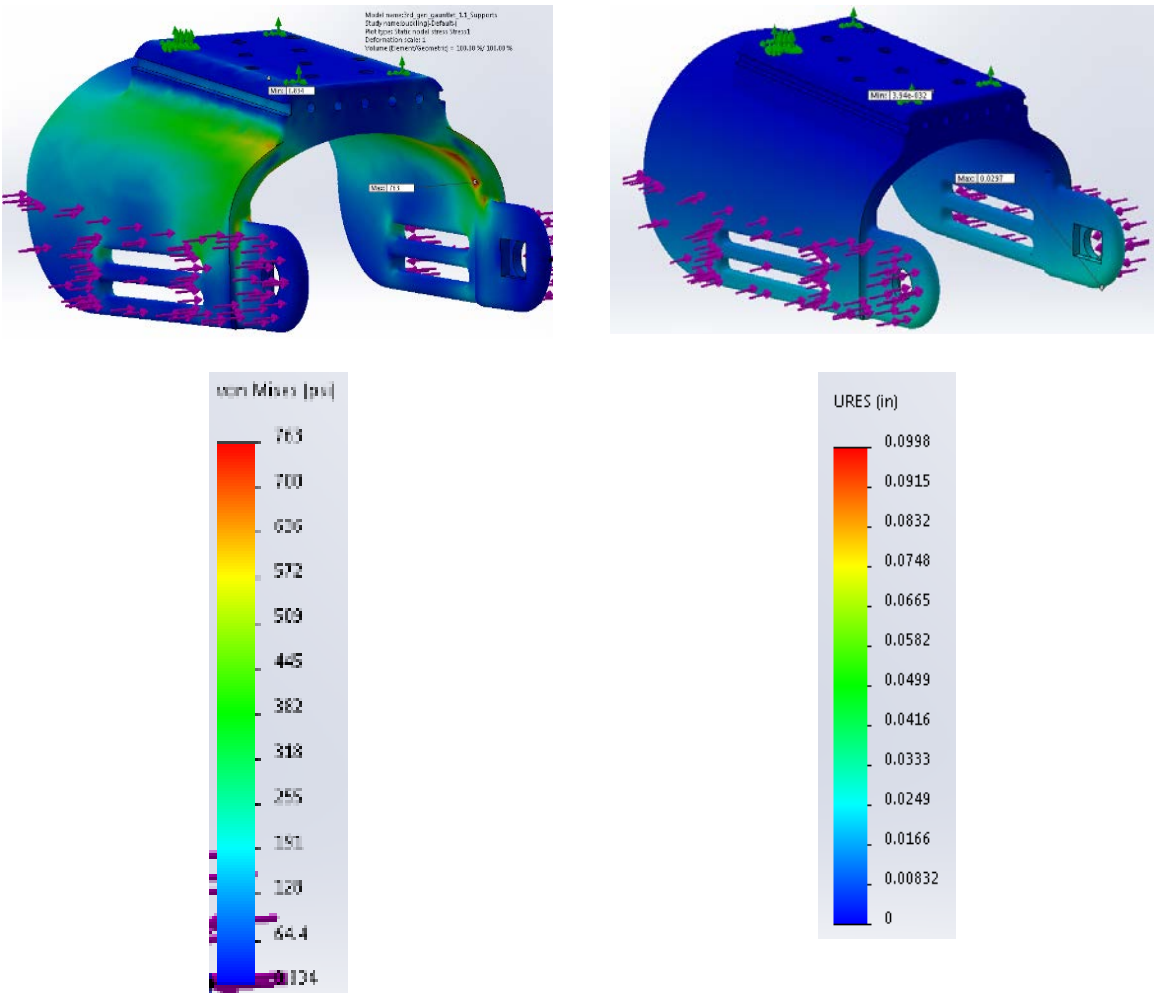


Figure 132: Gauntlet Von Mises Analysis (left) & Deformation Analysis (right)

Figure 132 shows that the highest stress area was around the corner and the maximum deformation occurred at the bottom part of gauntlet. This shows the potential failure location of the design where breaking or cracking might occur. Due to the two external axial buckling loads, the product experienced compressive stresses on its interior side and tensile stresses on its exterior side. The products would fail if the external load produced the stress more than yield strength or critical buckling stress, whichever was lower. To avoid this kind of failures, the thickness of the wall and curvature can be increased, as these could reduce the stresses caused by the axial loads and prevent the product from snapping and cracking at the edges where the stresses were concentrated.



# Experiences with Additive Manufacturing

Since the team's design required the manufacture of a 3D printed prosthetic hand, the only available sources for rapid prototyping were through the Worcester Polytechnic Institute Rapid Prototype Lab (RP Lab), or our advisor's 3D's printers. Due to the predicted volume of 3D printed parts needed over the course of the MQP, the RP Lab was not a cost effective approach to accomplish our goals. The RP Lab was also being utilized by many of the other MQP teams, as well as courses requiring students to 3D print parts for prototypes. This greatly increased the volume of parts needed, which would cause turnaround times to be approximately 3-5 business days at a minimum. Our advisor's printer was significantly faster and more available, but could not be relied upon for use at night or over weekends, preventing continuous work.

In order to increase the team's productivity, a few members of the team decided to purchase two 3D printers. We saw this as an opportunity for the team to have the ability to model parts and print without having to outsource. Based on low cost, marketed ease-of-use, and large print bed volume, the team decided to purchase a pair of XYZ Da Vinci 1.0 all-in-one 3D Printers. The reason for the purchase of these particular printers was mainly due to the product specifications being very similar to that of the MakerBot Replicator 2 3D printer models which were utilized in earlier prototyping.

Rapid Prototyping being the main method of manufacturing, it is essential to understand how to operate the printer efficiently which effectively reduces printing time, operating cost, and material consumption, one of project's objectives. While many low cost printers claim that they are easy to operate, the reality is they are not, most manufacturers do not mention any of the issues that arise due to repeated use. These include print failures due low extruder temperature settings, ambient temperatures and excessive moisture in the air causing de-lamination, calibration and re-calibration after each print, poor material adhesion to print surface, clogging of extruder nozzle causing catastrophic failure, ruined prints due to the inability to exchange

cartridges during printing, failure due to poor material quality, uneven layering due to unlevelled print surface, uncommon power failures, issues with data cable connecting to computer, and common software issues. Proper maintenance can reduce the risk of failures, but it is not guaranteed.

An important lesson that the team learned while using a low-cost printer was that the design of parts was limited to the ability of the printer to print parts with requiring supports. Meaning, complex geometries proved to be difficult to print without having to waste excessive material on support structures automatically placed by the slicing software. Since, one of the team's goals was to reduce cost; this was an important thing to consider while designing the hand. The way that the team was able to reduce the amount of material used for the printing was to include supports in the CAD files that could then be removed after printing.

As a team we learned a lot about the capabilities and limitations of non-commercial low cost home 3D printers. The team experienced a fair amount of failures, from these failures we were able to learn different ways to reduce the amount of times they occurred. We learned that 3D printing is not an exact science, failures will occur, sometimes when you least expect them. Not all low cost 3D printers are the same either, each and every one is unique, and although they perform essentially the same thing not all failures occur the same way, and not all failures occur on all printers.

Printing parts and learning from mistakes was a valuable learning experience when creating and editing SolidWorks models for printability. By printing and analyzing resulting failures and errors the team was able to recognize design flaws before conducting a print. As shown in Figure 134 and Figure 135, the gauntlet on the left did not have user designed support features and require program generated support in order to complete the print without failure. Printing this component required close to eight hours of printing and produced large quantities of wasted material. In Figure 134, the gauntlet was designed with two extrusions to create supports reduce print time and material waste while still ensuring a quality print.

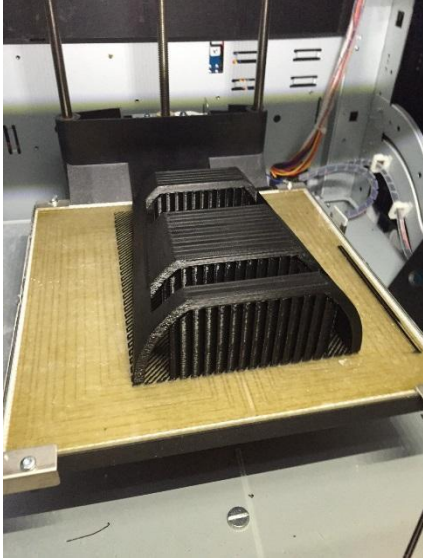


*Figure 133: Program Generated Supports*

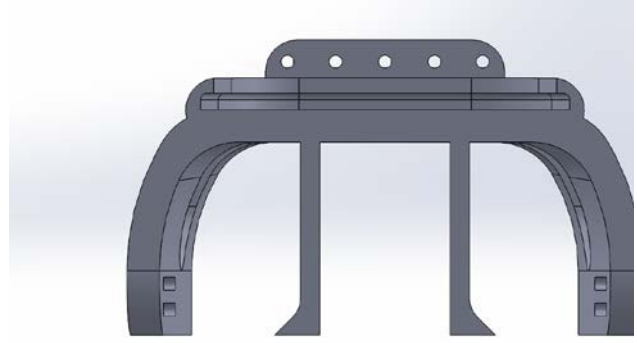


*Figure 134: Added Supports in Gauntlet Design*

One of the initial problems the team encountered was designing within the resolution range of the 3D printer. The printers that the team utilized have 100 micron resolution; however, in reality, the resolution is less than advertised when printing at its minimum capable resolution. As observed in Figure 135 and Figure 136, the hole in the distal phalange and teeth in the spool were at the minimum resolution and were not successful prints. To avoid failed prints, parts need to be designed slightly larger than the minimum resolution. Another example would be making sure one side or surface of a part is flat to avoid needing support material and further finishing.



*Figure 135: Failed Distal Phalange with Ratchet System*



*Figure 136: Failed Ratchet Mechanism System Spool*



*Figure 137: Failed Ratchet Mechanism System Shaft*

It is also important to know how to utilize the print bed efficiently. As shown in Figure 138 below, the parts were aligned and printed on a same bed at the same time to save setup and printing time. 3D printers will often need to recalibrate due to repeated motions and changes in temperature, and will need time for the nozzle to heat back up again. In addition, the job can be left to print a large quantity of parts while the user is busy with other tasks. These advantages come with added risk, as if one part fails in the printing process, the whole build could potentially fail.

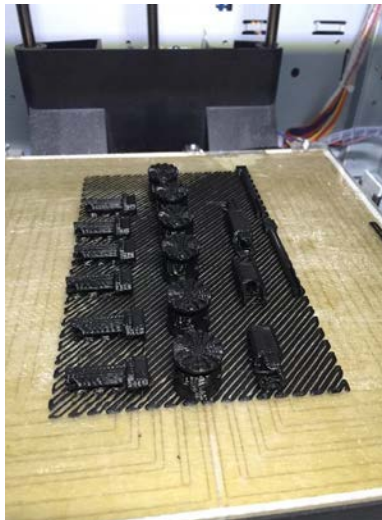


*Figure 138: Printing Multiple Components*

As mentioned, some of the failures that were associated with these types of printers were caused by ambient temperatures and moisture in the environment surrounding the printer. A

way that these issues were combated were by confining the printers in rooms without windows and placing a dehumidifier in the room to remove the moisture in the air, a huge contributor of Z layer separation or simply, delamination. Delamination is a condition that occurs one or more layers in the z axis not sticking correctly to the layers beneath it as can be seen on Figure 139 below.

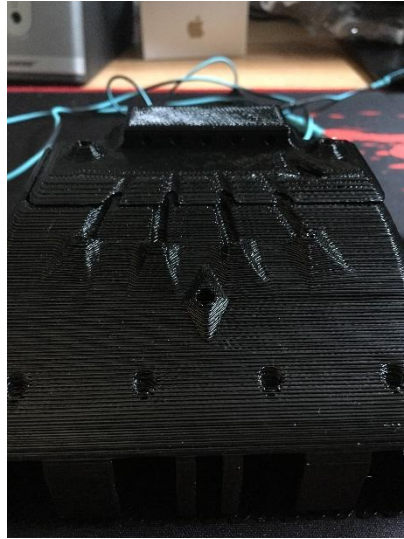


*Figure 139: Example of De-Lamination*

# Instron Testing

Instron testing was completed to test the finger subassemblies. These fingers and their joints are areas of critical concern with respect to failure and stresses. Tensile, cyclic, and compression testing were completed on the finger subassemblies to determine the force (lbf) necessary to cause failure or fracture of the assembly. These results were then analyzed in Mathcad to determine their respective safety factors.

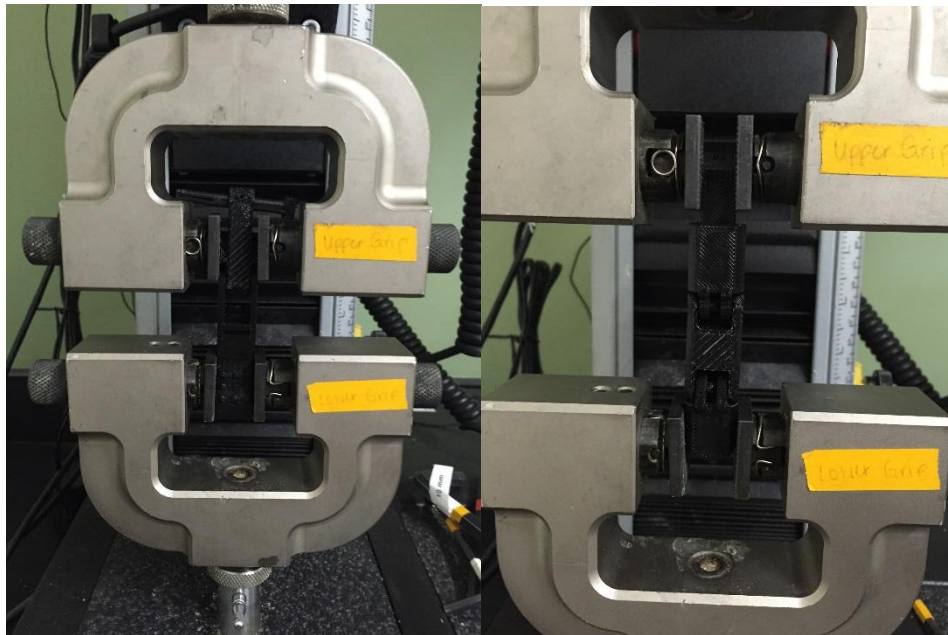


*Figure 140: Instron Testing Setup*

The two and three joint fingers were secured to both sections of the Instron machine while leaving the joints exposed. This setup remained consistent for all testing procedures for tensile, cyclic, and compression. A load of approximately 10lbf was applied to fine adjust the set up before beginning the testing procedure.

From the Instron results, the following graphs and data were generated for each of the tests. The first set of data is broken down into four samples of the three joint fingers for the tensile test.

Specimen 1 to 4

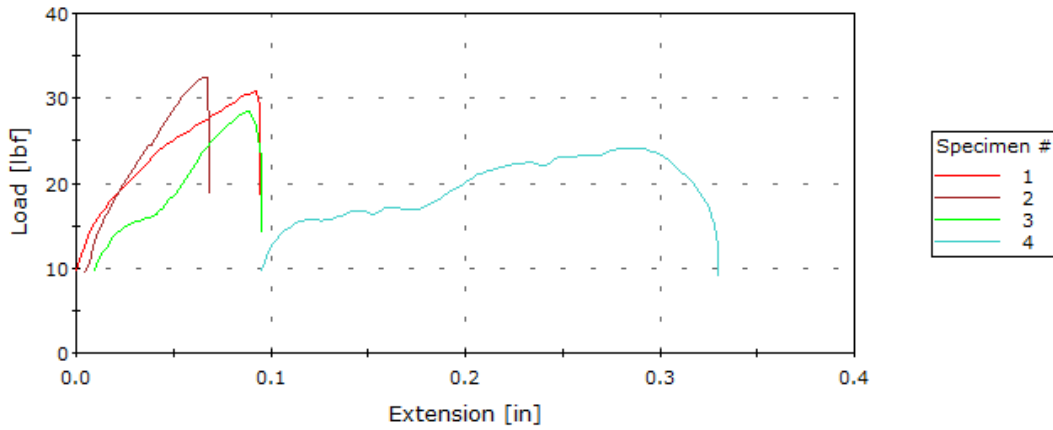


Figure 141: Instron Testing Results for 4 Samples in Tensile for Three-Segment Fingers

Table 17: Instron Testing Results for 4 Samples in Tensile for Three-Segment Fingers

	<i>Data point at Break (Standard)</i>	<i>Extension at Break (Standard)</i>	<i>Load at Break (Standard)</i>	<i>Tensile strain (Extension) at Break (Standard)</i>
		<i>[in]</i>	<i>[lbf]</i>	<i>[in/in]</i>
1	58	0.09405	29.17256	0.02542
2	39	0.06271	32.46377	0.01695
3	53	0.08451	24.31022	0.02284
4	141	0.31412	15.03853	0.08490
	<i>Tensile stress at Break (Standard)</i>	<i>Modulus (Automatic Young's)</i>	<i>Tensile strain (Extension) at Yield (Zero slope)</i>	<i>Tensile stress at Yield (Zero slope)</i>
	<i>[psi]</i>	<i>[psi]</i>	<i>[in/in]</i>	<i>[psi]</i>
1	75.80337	6637.12871	-----	-----
2	84.35540	6706.85390	-----	-----
3	63.16884	3449.78943	-----	-----
4	39.07682	5426.65350	0.03944	44.55652

The graph in Figure 141 depicts four samples for the two-segment fingers for tensile testing.

### Specimen 1 to 4

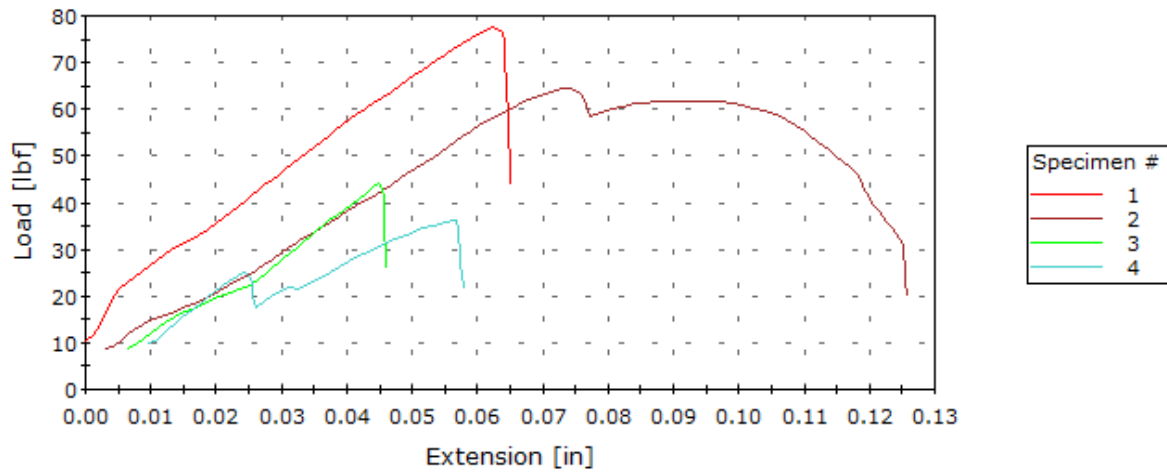


Figure 142: Instron Testing Results for 4 Samples in Tensile for Two-Segment Fingers

Table 18: Instron Testing Results for 4 Samples in Tensile for Two-Segment Fingers

	<i>Tensile stress at Break (Standard)</i> [psi]	<i>Modulus (Automatic Young's)</i> [psi]	<i>Tensile strain (Extension) at Yield (Zero slope)</i> [in/in]	<i>Tensile stress at Yield (Zero slope)</i> [psi]
1	258.47976	28630.56137	-----	-----
2	111.62736	11658.07230	0.01925	215.28437
3	146.82880	14593.31126	-----	-----
4	120.09722	14199.18083	-----	-----
5	202.30430	12164.37832	-----	-----
	<i>Data point at Break (Standard)</i> [in]	<i>Extension at Break (Standard)</i> [in]	<i>Load at Break (Standard)</i> [lbf]	<i>Tensile strain (Extension) at Break (Standard)</i> [in/in]
1	58	0.06236	77.54393	0.01685
2	97	0.12083	33.48821	0.03266
3	33	0.03834	44.04864	0.01036
4	41	0.04692	36.02917	0.01268
5	71	0.09195	60.69129	0.02485



Table 19: Testing Results for 4 Samples in Tensile for Two-Segment Fingers; Continued

	<i>Data point at Break (Standard)</i>	<i>Extension at Break (Standard)</i> [in]	<i>Load at Break (Standard)</i> [lbf]	<i>Tensile strain (Extension) at Break (Standard)</i> [in/in]
1	84	0.08509	23.42418	0.02300
2	86	0.11073	70.66397	0.02993
3	96	0.13439	57.35184	0.03632
4	52	0.07769	41.14728	0.02100
5	30	0.03602	12.09616	0.00974
6	39	0.05078	47.66749	0.01372
7	114	0.13655	37.44975	0.03691
8	59	0.07753	68.64727	0.02095
9	83	0.10121	54.47172	0.02735
10	58	0.07188	67.41324	0.01943
11	267	0.42559	8.70474	0.11502
12	74	0.10180	50.29330	0.02751
13	78	0.09619	39.09857	0.02600
14	364	0.58335	-0.04663	0.15766
15	64	0.08457	50.87061	0.02286
16	62	0.07329	50.14013	0.01981
17	121	0.15677	37.36342	0.04237
18	60	0.06823	71.32731	0.01844

Table 20: Testing Results for 4 Samples in Tensile for Two-Segment Fingers; Continued

	<i>Tensile stress at Break (Standard)</i> [psi]	<i>Modulus (Automatic Young's)</i> [psi]	<i>Tensile strain (Extension) at Yield (Zero slope)</i> [in/in]	<i>Tensile stress at Yield (Zero slope)</i> [psi]
1	70.38516	10970.08196	-----	-----
2	212.33165	11949.56803	-----	-----
3	172.33125	11518.08826	0.02333	229.62130
4	123.63967	9223.59414	-----	-----
5	36.34663	23025.34381	-----	-----
6	143.23165	11146.64734	-----	-----
7	112.52930	13537.30230	0.01595	181.95474
8	206.27185	12736.07820	-----	-----
9	163.67704	12349.04453	-----	-----
10	202.56382	14726.80658	-----	-----
11	26.15607	13087.87174	0.01322	91.77312
12	151.12168	10847.69604	-----	-----
13	117.48368	13807.34224	-----	-----
14	-0.14010	8495.35667	0.01420	117.39588
15	152.85642	11738.03284	-----	-----
16	150.66145	11565.66707	-----	-----
17	112.26990	11737.50331	0.02288	209.03366
18	214.32486	15445.11814	-----	-----

The graph in Figure 142 portrays the results from the compression testing from four samples of the two-segment fingers.

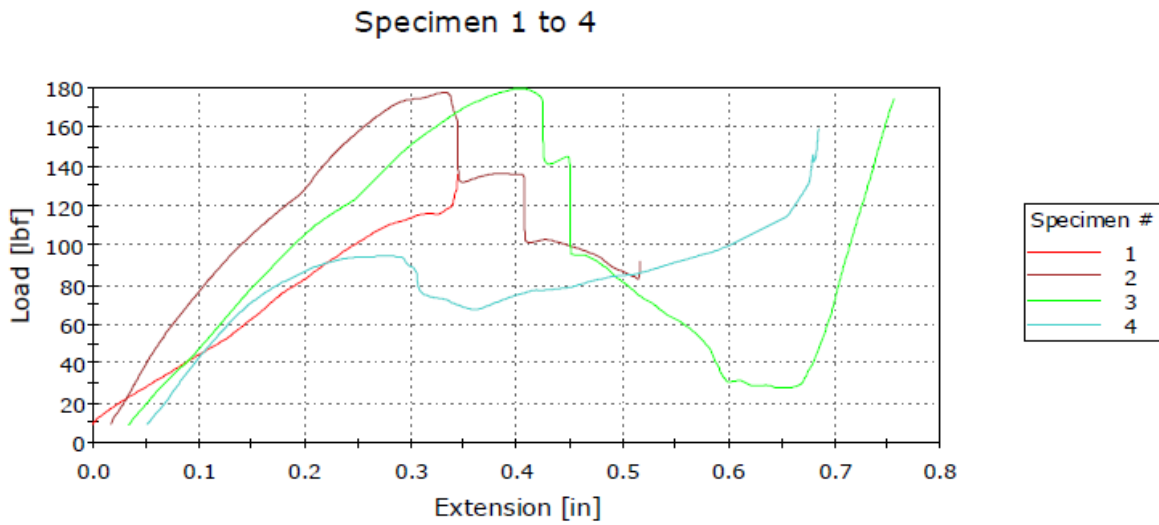


Figure 143: Testing Results for 4 Samples in Compression for Two-Segment Fingers

In the graph in Figure 143, four samples underwent cyclic testing and were compressed for ten cycles at a load of 15lbf before being pulled to failure or fracture.

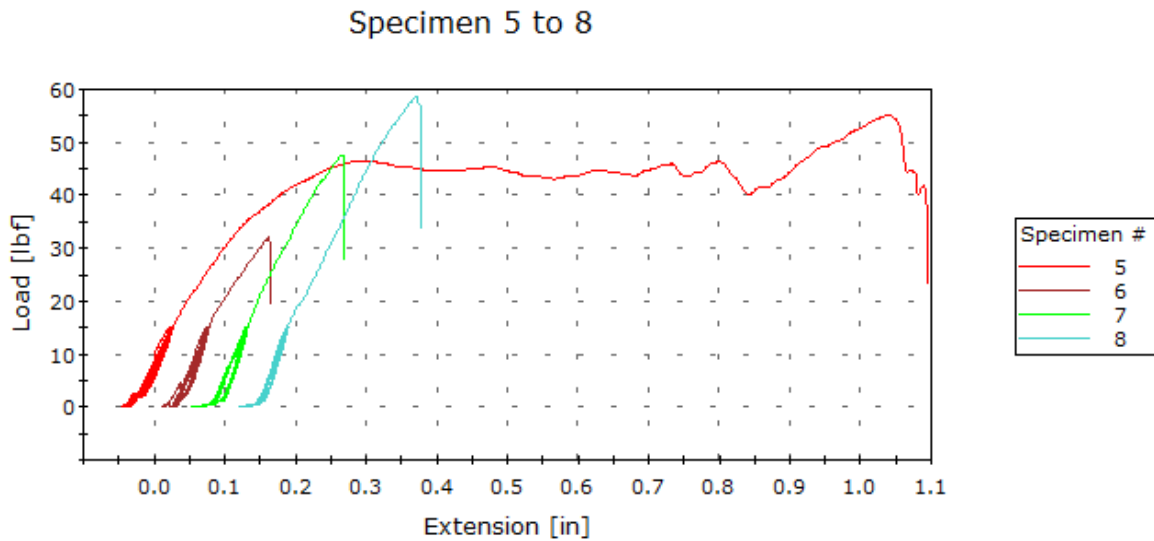


Figure 144: Instron Testing Results for 4 Samples in Cyclic for Two-Segment Fingers

Table 21: Testing Results for 4 Samples in Cyclic for Two-Segment Fingers

	Data point at Break (Standard)	Extension at Break (Standard) [in]	Load at Break (Standard) [lbf]	Tensile strain (Extension) at Break (Standard) [in/in]
1	-----	-----	-----	-----
2	1973	0.76532	17.49858	0.20684
3	1682	0.83793	27.96492	0.22647
4	2500	1.49501	5.70497	0.40406
5	2230	1.09280	39.99246	0.29535
6	1308	0.10700	30.77332	0.02892
7	1954	0.15489	47.48729	0.04186
8	1727	0.20770	54.55284	0.05614
9	1367	0.08483	37.26089	0.02293
10	1585	0.25185	73.49201	0.06807
11	1569	0.16402	57.23729	0.04433
12	1482	0.22691	79.02110	0.06133
13	1558	0.21958	59.39479	0.05935
14	1780	0.14806	60.53239	0.04002

Table 22: Results for 4 Samples in Cyclic for Two-Segment Fingers; Continued

	Tensile stress at Break (Standard) [psi]	Modulus (Automatic Young's) [psi]	Tensile strain (Extension) at Yield (Zero slope) [in/in]	Tensile stress at Yield (Zero slope) [psi]
1	-----	-----	-----	-----
2	52.57988	3049.75522	0.03837	74.91800
3	84.02920	4437.35133	0.11733	121.74099
4	17.14234	3538.00983	0.08562	88.46972
5	120.16966	3495.29718	0.08290	139.57508
6	92.46790	4397.41019	-----	-----
7	142.69019	4011.65513	0.04141	142.95722
8	163.92081	4166.89503	0.05443	176.56344
9	111.96180	4765.18668	-----	-----
10	220.82937	4461.65929	0.06807	220.82937
11	171.98706	4689.20625	0.04433	171.98706
12	237.44321	4957.88590	-----	-----
13	178.46992	5414.88833	0.05555	230.28129
14	181.88819	5636.10241	0.03416	175.26890

From these results, safety factors were calculated for each test and finger type in Mathcad. The safety factors in Figure 145 portray the average safety factor calculated as well as the standard deviation to acquire the distribution of the results. Each of the tests were individually calculated as well and can be seen in Mathcad calculations.

Tensile: Safety Factors

$$\text{mean}(\text{BreakingStrength}) = 50.957\text{-lb}$$

$$\text{mean} := 50.957\text{lb}$$

$$FS_{21} := \frac{\text{mean}}{\text{NormalWorkingLoad}} = 7.28$$

$$\text{Stdev}(\text{BreakingStrength}) = 14.853\text{-lb}$$

$$\text{Stdev} = 14.853\text{lb}$$

$$FS_{22} := \frac{\text{Stdev}}{\text{NormalWorkingLoad}} = 2.122$$

$$SEM := \frac{\text{Stdev}}{\sqrt{20}} = 3.321\text{-lb}$$

Distribution (Mean+/-Stdev):  
Factor of Safety: 7.3 +/- 2.1

Figure 145: Safety Factor Calculation for Two-Segment Fingers in Tensile

Cyclic Testing: Safety Factors

$$\text{mean}(\text{BreakingStrength2}) := 48.767323331\text{lb}$$

$$\text{meanCyclic} := 48.767323331\text{lb}$$

$$FS_{35} := \frac{\text{meanCyclic}}{\text{NormalWorkingLoad}} = 6.967$$

$$\text{stdev}(\text{BreakingStrength2}) := 18.65589521\text{lb}$$

$$\text{stdevCyclic} := 18.65589521\text{lb}$$

$$FS_{36} := \frac{\text{stdevCyclic}}{\text{NormalWorkingLoad}} = 2.665$$

$$SEM2 := \frac{\text{stdevCyclic}}{\sqrt{12}} = 5.385\text{-lb}$$

**Distribution (Mean+/-Stdev):  
Factor of Safety: 6.9 +/- 2.7**

Figure 146: Safety Factor Calculation for Two-Segment Fingers in Cyclic

Compression Testing: Safety Factors

$$\text{mean}(\text{CompressionBreaking}) := 125\text{lb}$$

$$FS_{42} := \frac{\text{mean}(\text{CompressionBreaking})}{\text{NormalWorkingLoad}} = 17.857$$

$$\text{stdev}(\text{CompressionBreaking}) := 53.735463151\text{lb}$$

$$FS_{43} := \frac{\text{stdev}(\text{CompressionBreaking})}{\text{NormalWorkingLoad}} = 7.676$$

$$SEM3 := \frac{\text{stdev}(\text{CompressionBreaking})}{\sqrt{5}} = 24.031\text{-lb}$$

**Distribution (Mean+/-Stdev):  
Factor of Safety: 17.9 +/- 7.7**

Figure 147: Safety Factor Calculation for Two-Segment Fingers in Compression

Tensile: Safety Factors (3 Joint Fingers)

$$\text{mean}(TensileBreakingStrength) := 25.246271b$$

---

$$FS_{48} := \frac{\text{mean}(TensileBreakingStrength)}{NormalWorkingLoad} = 3.607$$

$$\text{stdev}(TensileBreakingStrength) := 7.584682041b$$

$$FS_{49} := \frac{\text{stdev}(TensileBreakingStrength)}{NormalWorkingLoad} = 1.084$$

$$SEM4 := \frac{\text{stdev}(TensileBreakingStrength)}{\sqrt{4}} = 3.792\text{-}1b$$

**Distribution (Mean+/-Stdev):**  
**Factor of Safety: 3.6 +/- 1.1**

Figure 148: Safety Factor Calculation for Three-Segment Fingers in Tensile



The team tested the prosthetic hands force necessary to close using another instron. A platform and some alteration to the setup were needed to secure the gauntlet and expose the hand to be applied to apply a force necessary to close the hand. A screw was attached as well to eliminate slipping on the plastic hand base when in contact with the Instron. The testing set up can be seen in Figure 149.

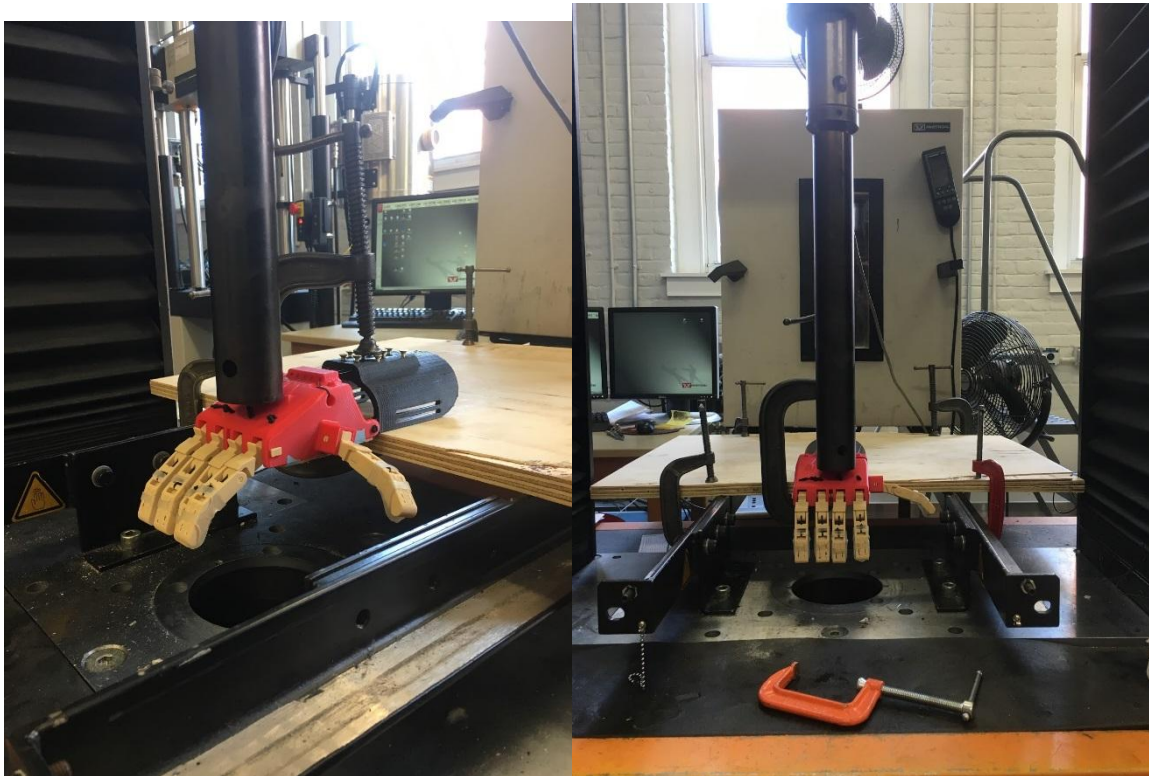
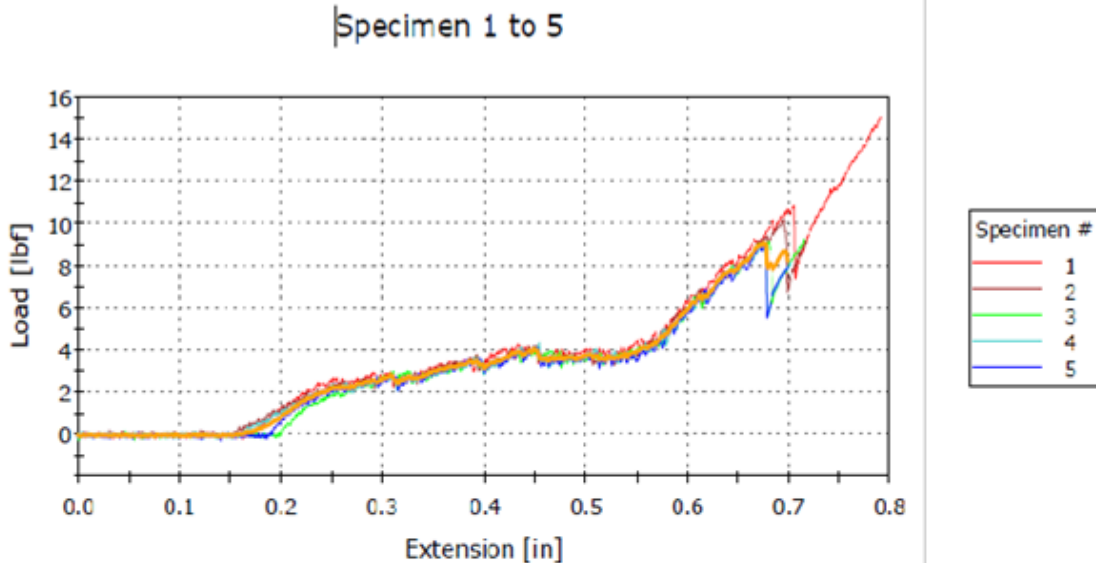


*Figure 149: Instron Setup for Force to Close Hand*

Figure 150 displays the Mathcad used to assess the point or force at which the hand was determined to be fully closed.

**Black Hand Gen 2 (2 Joint):  
Force Required to Close**



Raw Data Test Specimen #1:

Time	Extension	Load
(s)	(in)	(lbf)
84.6	0.70502	10.84196

Raw Data Test Specimen #4:

Time	Extension	Load
(s)	(in)	(lbf)
80.9	0.67418	9.1035

Raw Data Test Specimen #2:

(s)	(in)	(lbf)
83.2	0.69335	10.17861

Raw Data Test Specimen #5:

Time	Extension	Load
(s)	(in)	(lbf)
81	0.67502	9.02098

Raw Data Test Specimen #3:

Time	Extension	Load
(s)	(in)	(lbf)
81.5	0.67918	9.12121

Figure 150: Mathcad for Gen2 (Two-Segment) Model

Mathcad was then utilized to determine the distribution of the results to find the average and standard deviation found in Figure 151.

$$\text{ClosingForceGen2} := \begin{pmatrix} 10.84196 \\ 10.17861 \\ 9.121212 \\ 9.1035 \\ 9.02098 \end{pmatrix} \cdot \text{lb}$$

$$\text{mean}(\text{ClosingForceGen2}) = 9.653 \cdot \text{lb}$$

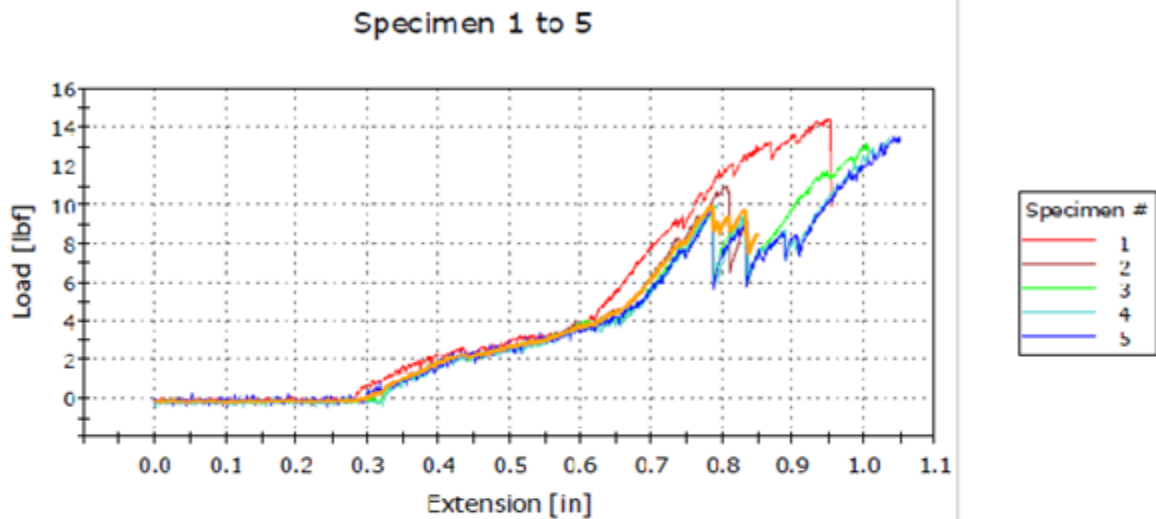
$$\text{Stdev}(\text{ClosingForceGen2}) = 0.818 \cdot \text{lb}$$

**Closing Force Distribution For Gen 2 (2Joint):  
9.6 +/- 0.8 lb**

*Figure 151: Mathcad for Gen2 (Two-Segment) Model Force to Close*

The generation 3 Model was also tested to determine the force necessary for the hand to fully close. The setup and distribution of the results can be found in Figure 152.

**Gen 3 Hand (2 Joint):**



Raw Data Test Specimen #1:

Time	Extension	Load
(s)	(in)	(lbf)
114	0.95002	14.32445

Raw Data Test Specimen #4:

Time	Extension	Load
(s)	(in)	(lbf)
124.074	1.03397	13.47534

Raw Data Test Specimen #2:

Time	Extension	Load
(s)	(in)	(lbf)
96.3	0.80252	10.97607

Raw Data Test Specimen #5:

Time	Extension	Load
(s)	(in)	(lbf)
125.7	1.04752	13.52229

Raw Data Test Specimen #3:

Time	Extension	Load
(s)	(in)	(lbf)
120.2	1.00168	13.19134

Figure 152: Mathcad for Gen3 (Two-Segment) Model Force to Close

Force Required to Close Final Model:

$$\text{ClosingForceGen3} := \begin{pmatrix} 14.32445 \\ 10.97607 \\ 13.19134 \\ 13.47534 \\ 13.52229 \end{pmatrix} \cdot \text{lb}$$

$$\text{mean}(\text{ClosingForceGen3}) = 13.098\text{-lb}$$

$$\text{stdev}(\text{ClosingForceGen3}) = 1.126\text{-lb}$$

Wrist is flexed at 20 Degrees

Fingers are Flexed at 60 Degrees at PIP

Fingers are Flexed at 100 Degrees at MIP

**Distribution of Closing Force Gen 3  
(2Joint): 13.1+/-1.1 lb**

Figure 153: Mathcad for Gen3 (Two-Segment) Model Force to Close

# Assembly Instructions

## Prosthetic Hand Parts:

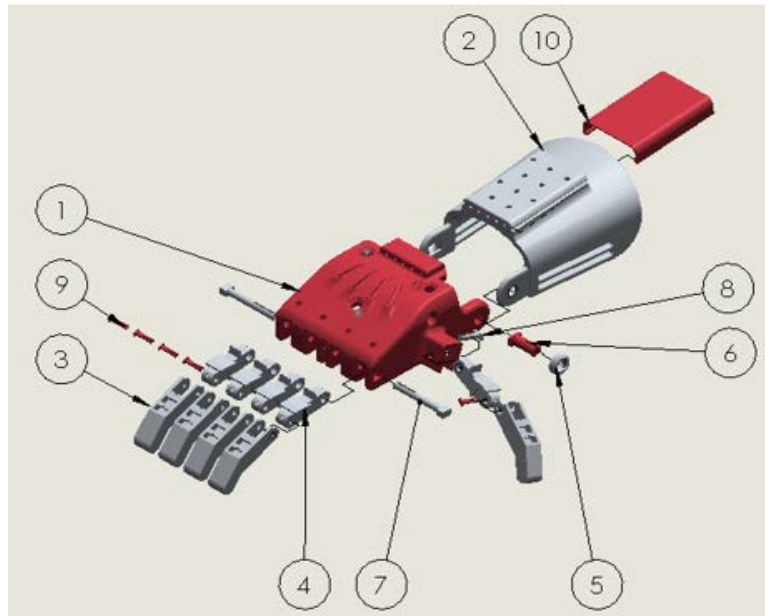











Figure 154: Exploded view of hand showing all the parts labeled with numbers

Table 23: Table of all the hand parts and quantities

ITEM NO.	DESCRIPTION	QTY.
1	Hand base	1
2	Gauntlet	1
3	Distal Finger	5
4	Proximal Finger	5
5	wrist pin cap	2
6	wrist pin long	2
7	Knuckle Pin	2
8	Thumb To Hand Pin	1
9	Distal to Proximal Pin	5
10	Gauntlet_cover	1






## Additional Hand Parts:

Table 24: Table of all the additional hand parts to complete the assembly

5ft of flexible elastic cord	
8ft of 90lb graded fishing line	
4ft of 2 inch wide double-side Velcro	
Micro gel fingertip grips (5)	
1ft Firm medical foam	
#8-32-1/2 screws (10)	
3/16-1/2 binding post screws (3)	
Leather (optional)	
M4-1/2 screws (13) for leather	

## Recommended Tools:

Table 25: Table of all the additional hand parts to complete the assembly

Phillips screwdriver – all the fasteners are Philips head	
Sharp knife – to remove raff and excess material	
Needle nose pliers – to remove raft, excess material, and for cable feeding	
Sandpaper (optional) – to remove any excess material causing any restriction in movement	
Lighter – to burn the ends of the cables to ensure easy feeding	

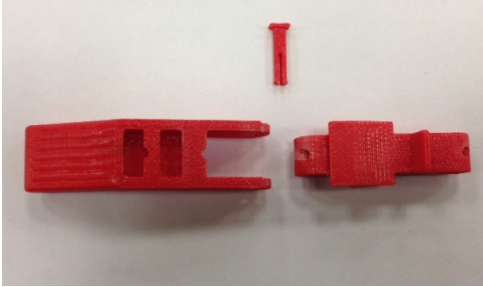
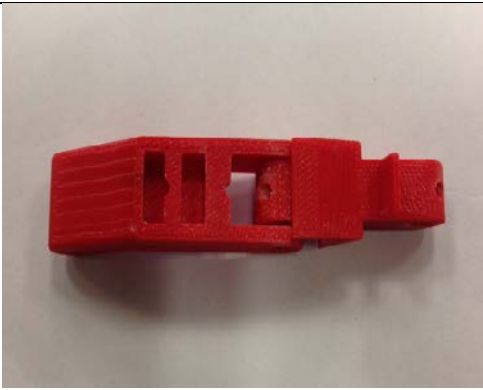
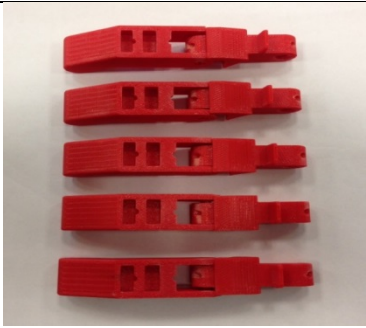
## Suggestions for hand assembly:

- Clean parts slowly and methodically
- Contains small parts (keep away from children and pets)
- Take your time to assemble
- Refer to instructions manual for any questions
- Be **Patient!**



## Step-by-step Instructions:

### Hand Assembly:

 <p>Figure 155: Parts comprising finger</p>	<p>The hand assembly begins with assembling the fingers first. In order to do this, gather one distal finger, one proximal, and one distal-to-proximal pin. Line up the holes and insert the pin ensuring that the square end of the pin ends up flush with the side of the finger.</p>
 <p>Figure 156: Completed finger for comparison</p>	<p>Once the finger has been assembled ensure that it moves relatively easy. It is possible for the finger to experience restrictive joint movement due to printing.</p>
 <p>Figure 157: Completed set of fingers</p>	<p>Once the first finger has been assembled, go ahead and assemble the remaining four fingers ensuring that they move freely at the joint pins.</p>

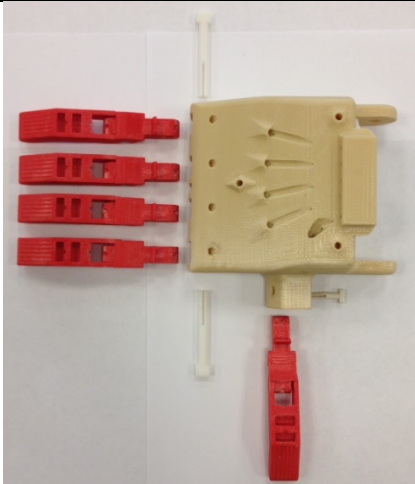


Figure 158: Parts needed for finger to hand base

After all the fingers have been assembled, they can be added to the hand base. The procedure for this is similar to the one used for the fingers. Use two knuckle pins for digits 1-4 and a thumb pin for the thumb. Again, ensuring that the pins are fully seated and flush with their respective sides.

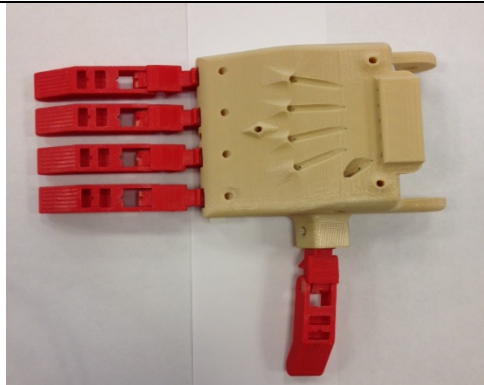


Figure 159: Completed finger and hand base

Once the fingers have been added to the hand base, ensure that they move freely without interference. The fingers should feel a little loose, that's okay.

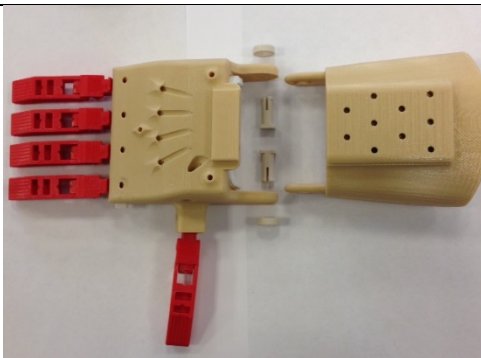


Figure 160: Parts needed for hand base to gauntlet

With the fingers assembled and attached to the hand base, it is now time to combine them with the gauntlet. This is done by lining up the holes of the hand base with those of the gauntlet and inserting the wrist pin from the inside of the hand outwards. A wrist pin cap is added to lock the knuckle pin to ensuring that it does not fall out during operation.

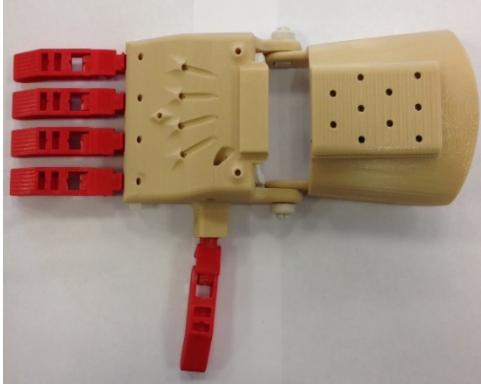


Figure 161: Complete 3D hand without tension

At this point, all the 3D printed parts that make up the hand are assembled together. The next step is to add the cabling.

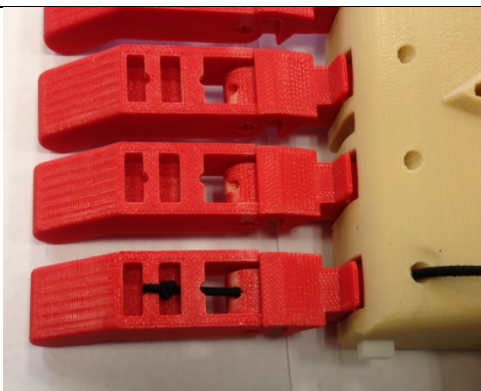


Figure 162: Return cable through finger

We start with the return cables, these cable are what allow the fingers to return to their normal position when the hand is not being actuated. Cut the 5 feet of elastic cable into 5 1 foot lengths. You may have to burn the ends with a lighter due to fraying cause by the cutting of the cables. Burning the ends just ensure that the cables will slide easily into the channels. Once the wires are cut, feed them through the holes by the knuckles and in through the top hole of the finger. Tie an enhanced clinch knot to the top bridge of the finger. Cut any excess cable.

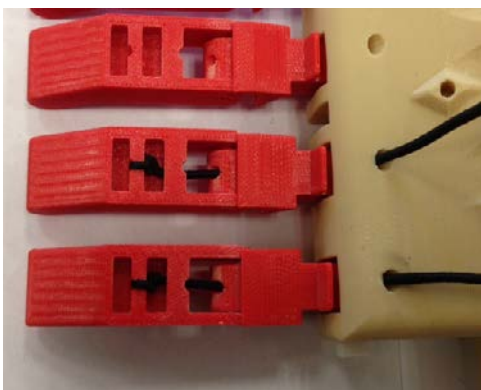
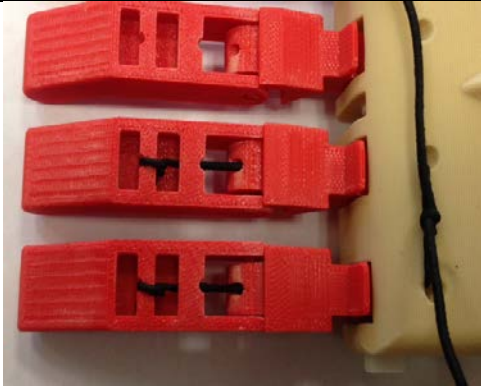


Figure 163: Return cable pair

Repeat the same procedure for another finger. Make sure that when the knots are tied they are secured tightly.



*Figure 164: Pair of fingers tied together*

Pull the cables tightly to provide tension on the fingers, ensuring that the fingers return in tandem. Do not tie the knots too tightly, this will reduce the finger's ability to return smoothly and increase the force needed to close the hand.

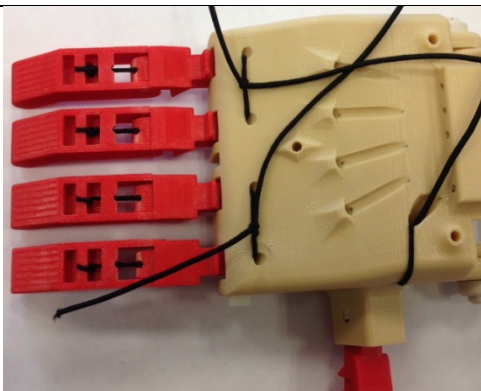


*Figure 165: All the return cables tied*

Repeat the same step for the remaining two fingers. The return cable for the thumb will be looped around several times around the hole feature and then securely tied with a double timber hitch knot. Ensure that all the fingers return in unison. Cut off excess cable.

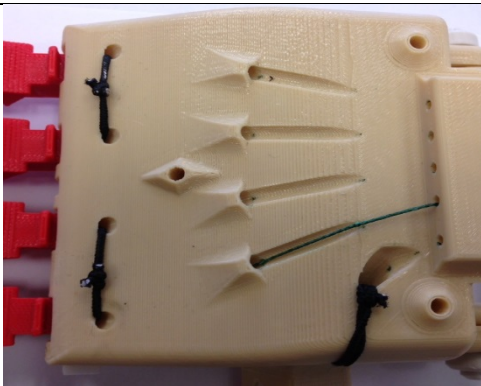


*Figure 166: Tension cable fed through top channel*

Once the return cable has been complete, the tension cable can resume. The cable is fed through the hole at the center of the hand base. Feed the cable through the bottom of the finger channel.

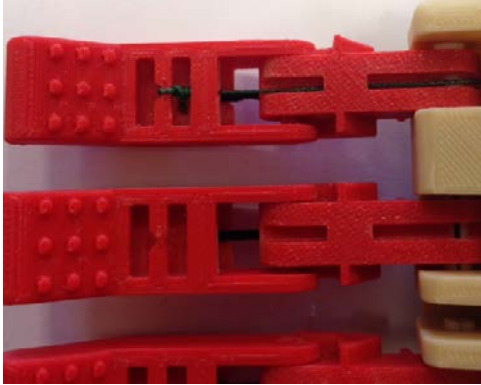


*Figure 167: Tension cable tied to finger with clinch knot*

Once the cable has reached the bridge, give the cable a little slack and tie the cable to the bridge utilizing an enhanced clinch knot.

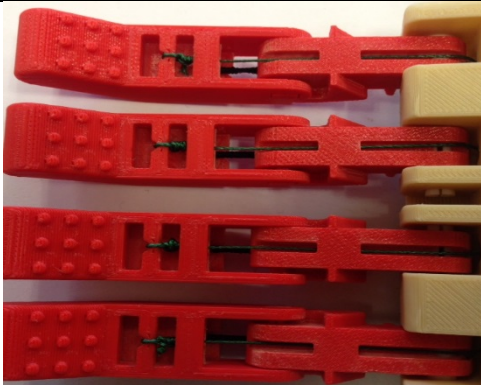


*Figure 168: All the fingers tied*

Repeat the process for all of the fingers. Ensure that all the cables are tight.

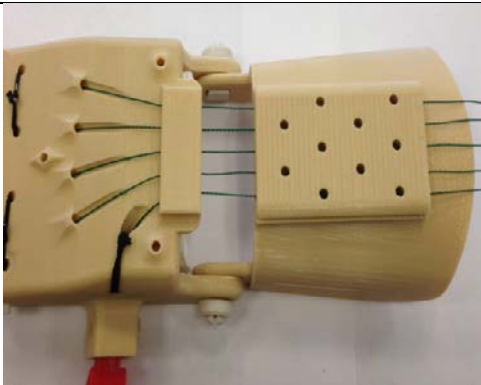


*Figure 169: Tension cables through hand base and gauntlet*

Feed the cable through the bridge atop the hand base and through the channels on the gauntlet tensioning device.

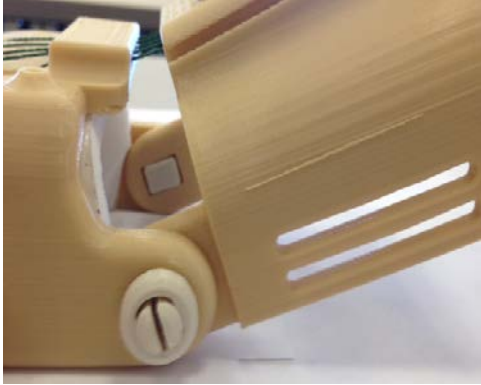


Figure 170: Example of pitch angle for gauntlet

Before tightening any screw for tensioning ensure that the gauntlet is oriented upward at around 20 - 30 degrees. Doing so will limit the possibility of the tensioning cable from having too much slack and potentially getting snagged on anything during daily activities which could cause injury or rip the cable out which would require the system to be re-tensioned.

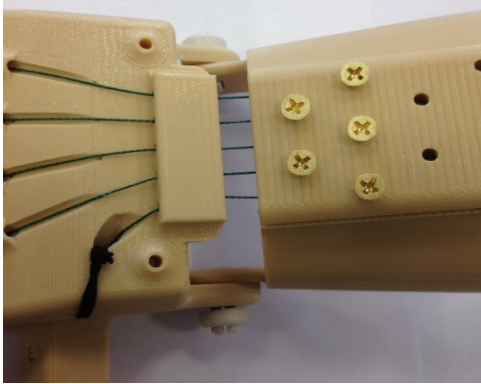


Figure 171: Tensioning the hand

To tension the hand, turn the screws in the clockwise direction using a Philips screwdriver. This will cause the screws to compress the cable creating tension on the cable which allows the user to flex or extend the wrist to create mechanical movement of the fingers. Ensure that the end result of the tensioning yield a simultaneous movement of all the fingers meaning that all the fingers move in unison. This step is the most critical in the assembly process. Take your time to ensure that the tensioning has been done correctly.

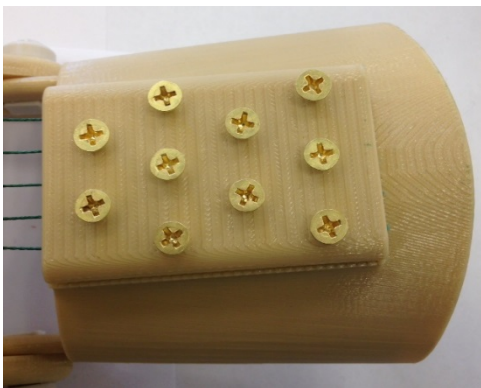
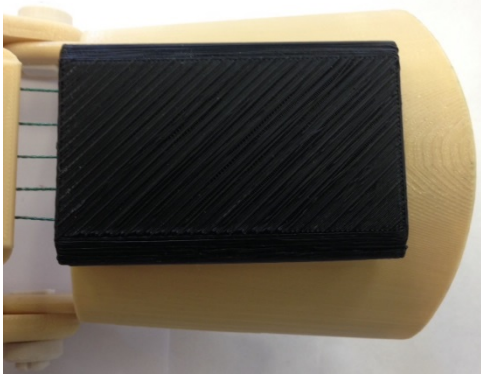


Figure 172: Tension hand with primary and secondary screws

After the hand has been tensioned, add the second set of machine screws. This second set is used for security in the case that the first set of screws strips causing the hand to lose its tensioning.



*Figure 173: Added Cover*

After the tensioning process has been complete, cover the screws with the gauntlet cover. The cover will protect the screws from getting caught on any times during daily activities which could cause injury.

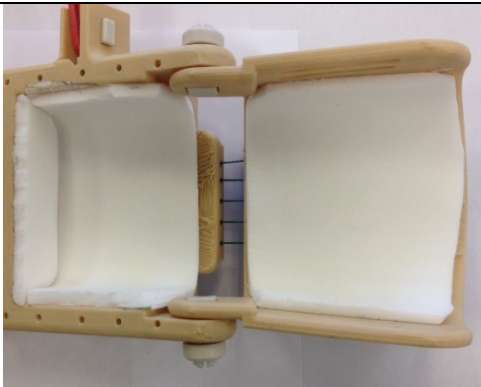


*Figure 174: Hand base and gauntlet with foam added*

Line the bottom of the hand and gauntlet with the firm medical foam. Make sure that the foam does not interfere with the slots on the gauntlet or the wrist pivot joints.

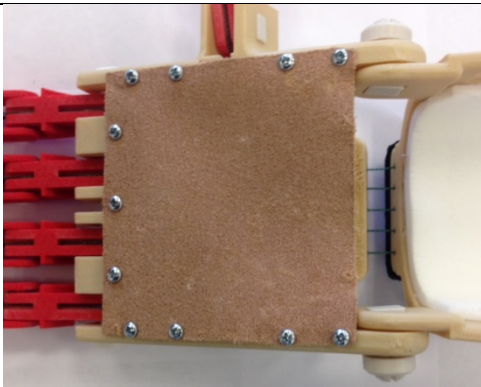


*Figure 175: Hand base with leather option*

Once the foam has been added, leather can be added to the hand base to provide the user a way to actuate the hand.

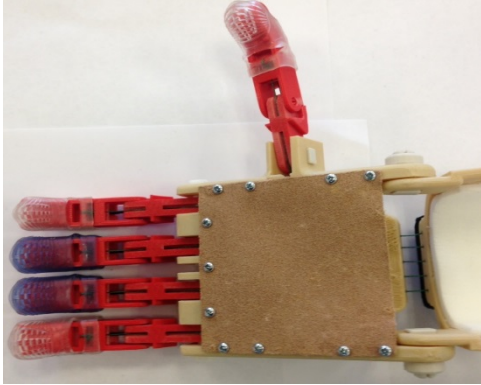


Figure 176: Hand with gel finger tips

After the leather is added, add the gel finger tips. The fingers give the hand a more dexterous feel and make the grabbing of items a lot simpler and more comfortable.

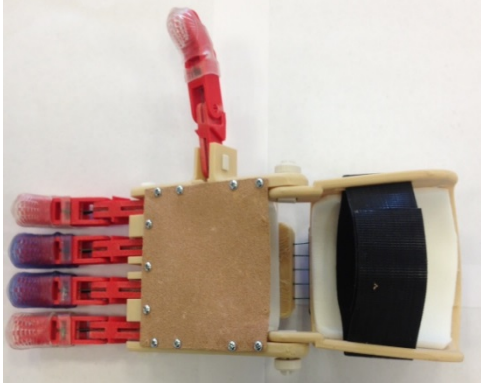


Figure 177: Hand with Velcro on gauntlet

Add the Velcro, the addition of the Velcro gives the user a means to attach the hand to themselves.

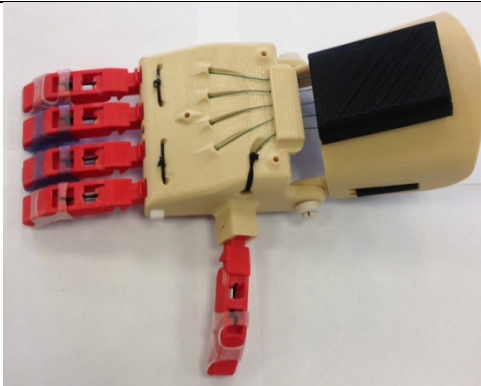


Figure 178: Completed 3D prosthetic hand

Congratulations you have fully assembled the hand!



### **Padding and Velcro Instructions:**

1. For the palm, cut firm medical padding and line the inside. Careful not to cover up pin joints.
2. Repeat step above for Gauntlet. Cut padding around the slots on the gauntlet to allow for Velcro attachment.
3. For the palm Velcro, cut an 8in length and a 5in length.
4. Align Velcro holes with the screw holes and cut holes to allow
5. Attach both Velcro pieces, 5in length vertically and 8in length horizontally to palm with screws.
6. For gauntlet, cut a 10in length. Slide one end through the top slot on both sides and through the bottom slot on both sides.
7. For gauntlet, cut a 10in length. Slide one end through the top slot on both sides and through the bottom slot on both sides

# Conclusion

## Prototype Assessment

Testing of the final prototype confirmed that the group was successful in completing the main objectives of the project. The prototype, shown in Figure 179, conforms to the previously laid out design specifications. After performing a series of tests, the prosthetic was able to carry groceries, hold a cell phone, hold and throw a tennis ball, and open doors. The prosthetic was not, however, able to hold a pen or pencil or use a zipper. This device is able to scale between 2.625 and 3.75in in terms of the width of hand that will wear it. Through a number of design iterations, printability, ease of assembly, tolerancing, and aesthetics were all improved.

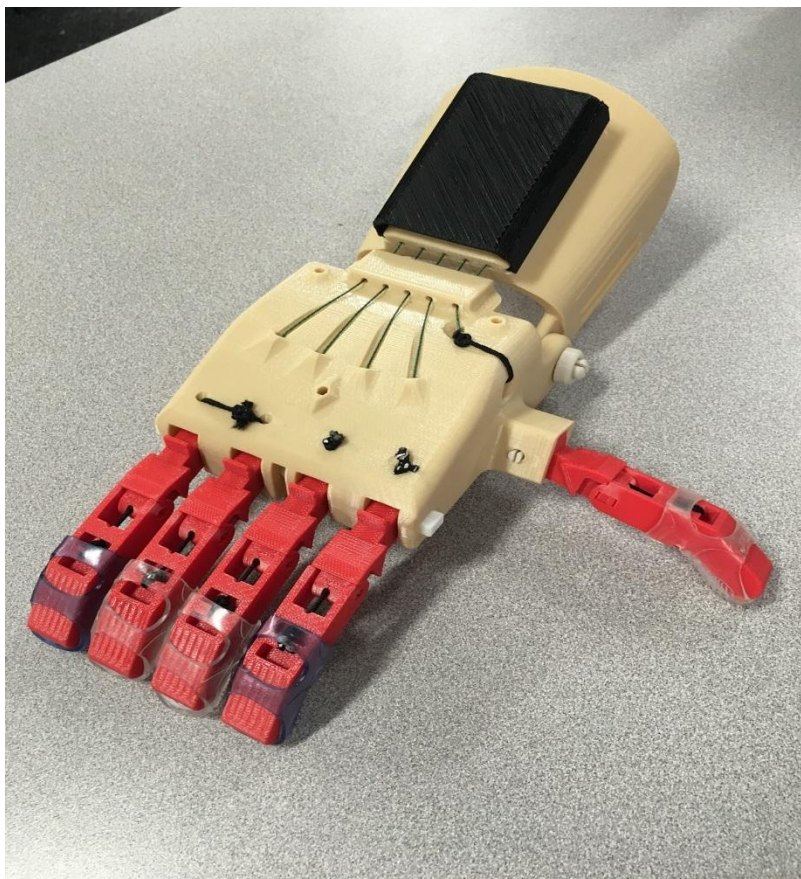


*Figure 179: Final Prototype*

## Future Work

There are various opportunities for future work on this design. Adding additional points of scaling would allow the user to more accurately size their prosthetic. Measurements of the length of the hand, size of the finger, width of the wrist, and forearm measurements could all be used to have perfect custom sizing, given the proper scaling algorithms. Increasing the range of functional scaling would also be useful, allowing for a wider variety of users and ages. Adding motors, sensors, and microcontrollers, independent finger motion could be achieved. This would allow for more realistic motion, as well as greater functionality.

# Appendices

## Appendix A: An Overview of Rapid Prototyping Processes

### SLA

Stereo lithography (SLA) is a process where an Ultraviolet (UV) light cures a liquid photopolymer one layer at a time to produce a 3D object<sup>iv</sup>, which is then immersed in a chemical bath to remove the uncured resin.

### SLS

Selective Laser Sintering (SLS) is an additive manufacturing technology which uses laser to trace and blend the powder layer by layer, until the part is complete.

### LOM

Laminated Object Manufacturing (LOM) is a process where layer fabrication starts by adhering the selected material laminates (paper, metal or plastic) stacked by layers and cut out to the shape of part using laser.

### FDM

Fused Deposition Modeling (FDM) is a process where a filament or thermoplastic polymer is heated and fused one layer at a time to fabricate a part.

### 3D Printing

3D Printing is a process where selective material was heated in nozzle and it deposits layer by layer to build a 3D object which is then toughened by UV light.

## MJP

MultiJet Printing (MJP) is a process just like 3D printing but which prints thin layers of UV curable liquid plastics and wax support materials to fabricate parts that are made from fully plastics.

## Appendix B: How to Change Hand Sizing and Save STL Files

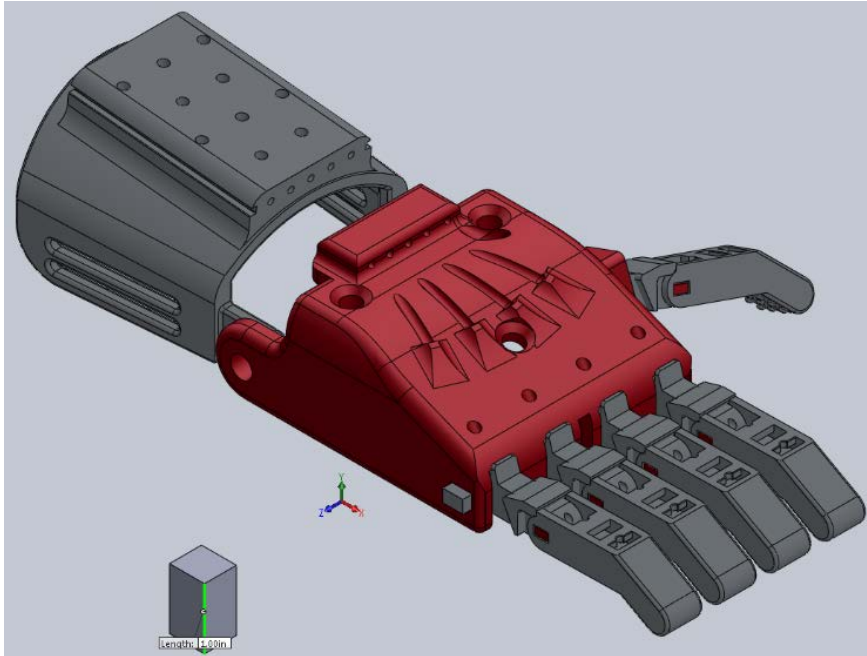


Figure 180: Full assembly of 2 Segment Hand

Here is the original size hand base, with an input hand width of 2.8 inches. The block is for scale. The block is 1 inch tall.

To scale and print your hand files, you must follow several steps.

Note: There will likely be a scaling issue when opening the assembly for the first time and if you change the configuration. Steps to fix this will be addressed later.

### Step 1: Open the Assembly.

Open Solidworks, and then open the 'Equation Assembly.SLDASM' file. Before proceeding, make sure to choose the finger design you would like. To do so, go to the configuration tab that is shown in Figure 181 and double click on the configuration you will be using.

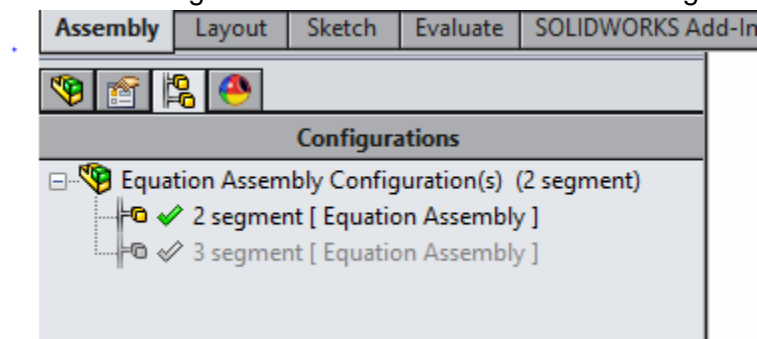


Figure 181: Step 1; Changing the Configuration

## Step 2: Opening the Equations Dialogue

To scale the files, you first need to open the main assembly. When you have the assembly file opened, click on the 'Tools' bar at the top, and then click 'Equations.' This will bring up a dialogue, shown in Figure 183, showing the global variables and equations being used by the program. Note that these values cannot be changed in the current menu, as they are referencing an external file.

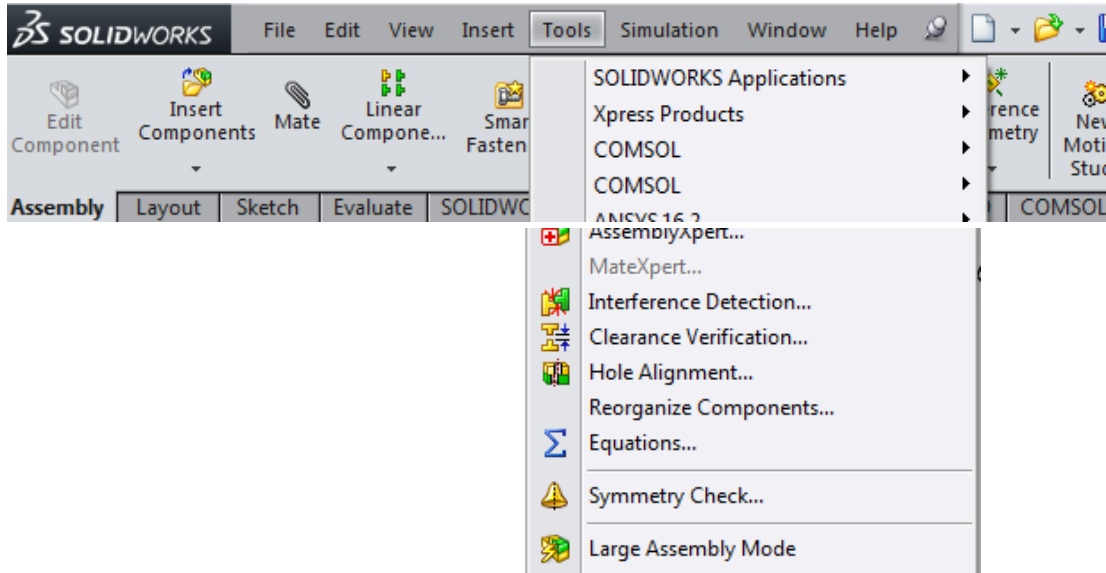


Figure 182: Step 2; Open the Equations Dialogue.

## Step 3: Opening the Equations Text File

Next, click on the 'open file' button, which is a yellow folder icon in the bottom right of the dialogue. This will open a text file with all of the variables and equations. Advanced users can edit these to make alterations if desired. Beginner users should avoid making any changes not specified in the instructions to prevent failures.

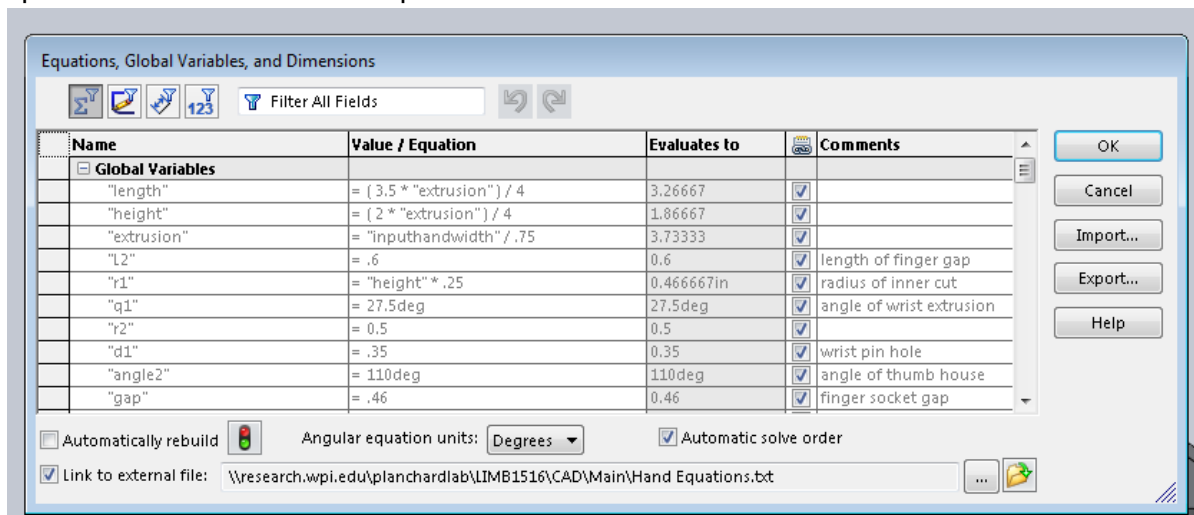


Figure 183: Step 3; Open the Equations Text File

## Step 4: Editing the Input Dimension

Edit the first dimension, 'inputhandwidth', to the width of your hand excluding your thumb. All scaling dimensions and features will reference this dimension directly or indirectly, so by modifying this value, the other values will change with it. Make sure to save the file before closing. The current version only allows scaling between a hand width of 2.8 inches and 3.75 inches. The two-segment finger can scale down to 2.6 inches. If your hand is thinner than the minimum size, you can print it at the minimum size and add extra padding. If your hand is wider than the maximum size, you will have to manually edit the parts.

```
Hand Equations - Notepad
File Edit Format View Help
["inputhandwidth"]=2.8 'Input the width of your hand
"length"= ( 3.5 * "extrusion" ) / 4
"height"= ( 2 * "extrusion" ) / 4
"extrusion"="inputhandwidth"/.75
"L2"= .6'length of finger gap
"r1"= "height" * .25'radius of inner cut
"q1"= 27.5deg'angle of wrist extrusion
"r2"= 0.5
"d1"= .35'wrist pin hole
"angle2"= 110deg'angle of thumb house
"gap"= .46'finger socket gap
"house"= 1'thumb housing position
"L1"= .35'rectangular pin cut length
"h1"= .2'rectangular pin cut width
"q2"= 45deg'reference angle
"h2"= .25'height of bridge
"d2"= .1'dia of bridge cables
"d0"=68deg'angle of cut'
"h3"= .8'thumb house height
"angle3"= 30deg'angle of fingers cabling
"d3"= .15deg'diameter of non-elastic cabling
"angle4"= 17deg
"d4"= .325'thumb cable hole size
"d5"= .3'thumb side cable hole size
"draftangle"= 12deg'draftangle of thumb cable
"angle5"= 140deg'angle of reference thumb cabling
"d6"= .18'diameter of elastic cable holes
"padding3"= .4'padding socket 3
"draftangle2"= 3deg
"padding4"= .3
"padding5"= .15
"fillet"= .05
"fillet1"= .1
"Fingerwidth"= "FingerLength" / 7
```

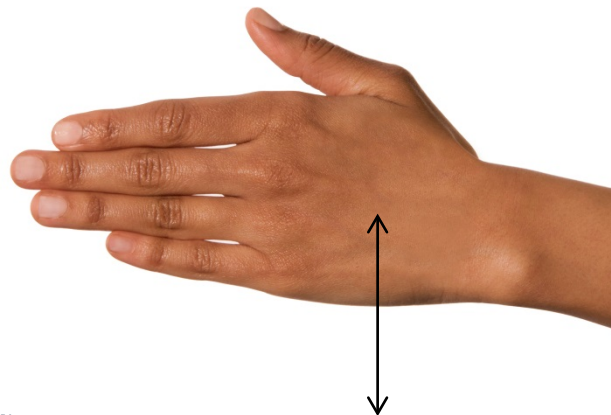


Figure 184: Step 4; Editing the Input Dimension<sup>xxxxv</sup>

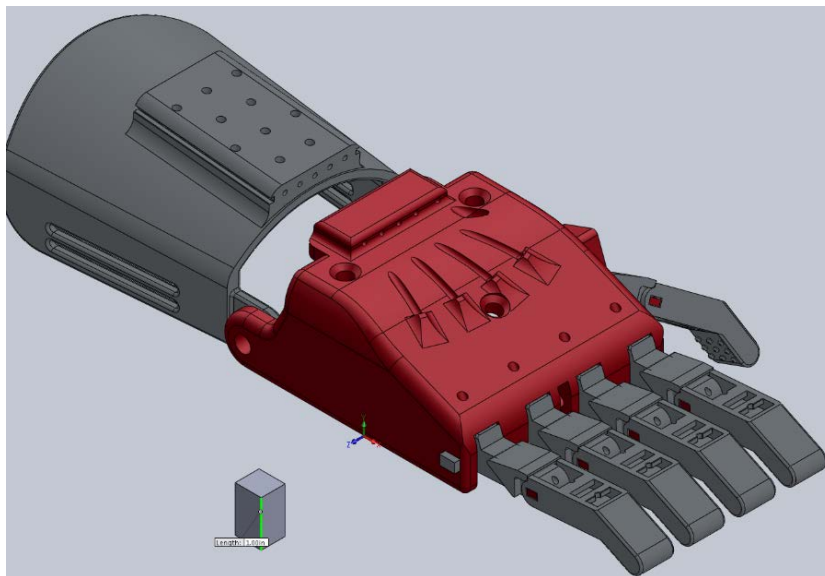


Figure 185: New Hand Size!

You now have your new size! Note the relative size of the reference block.



## Step 5: Save the Parts as STL Files

To save as STL files for printing, open each unique part. Then go to 'file', 'save as'. If prompted, choose the 'Save as' option. Go to the directory of your choosing, name the file as desired, and make sure to save as type: STL. You can then use this STL file to 3D print your part!

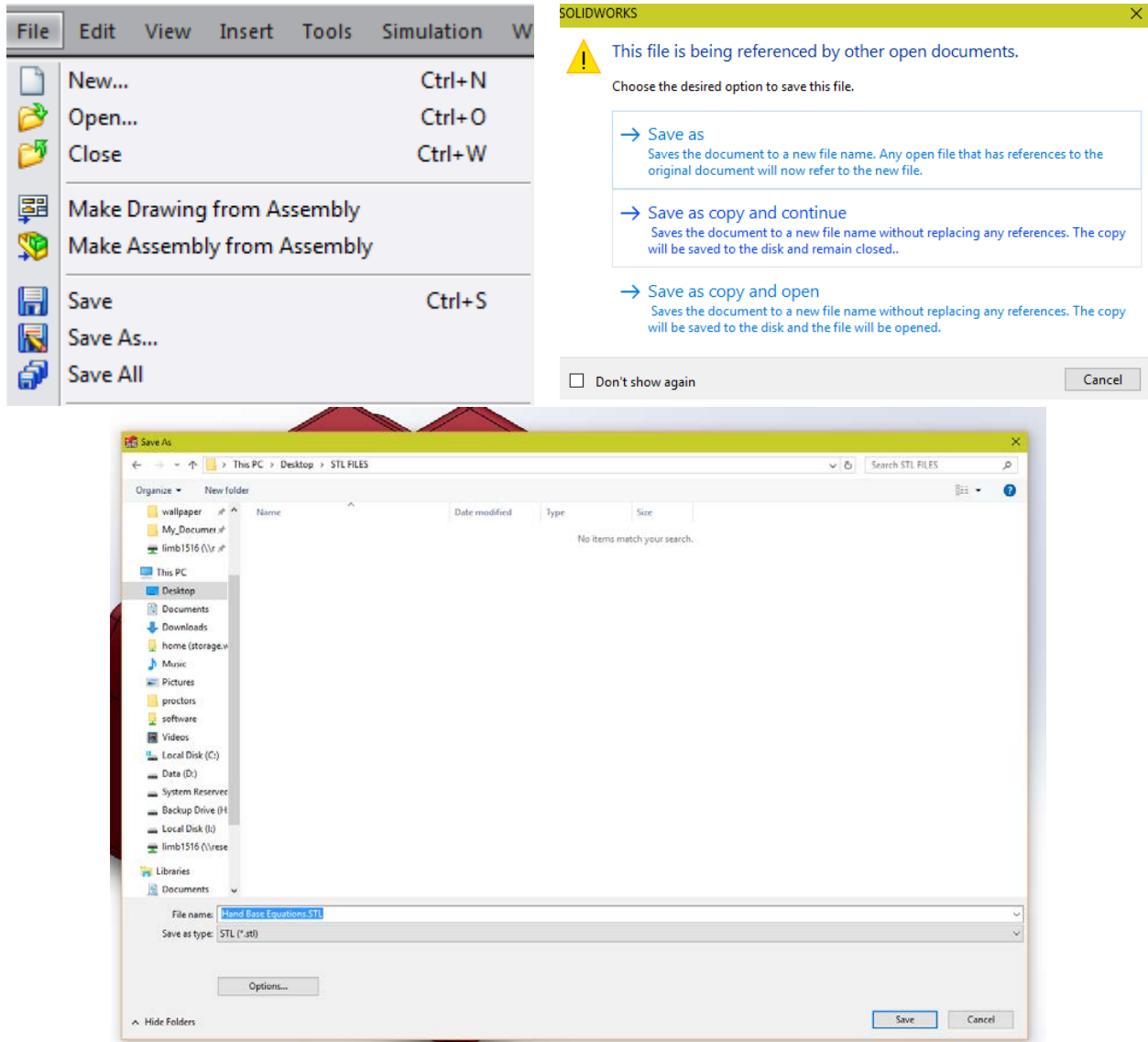
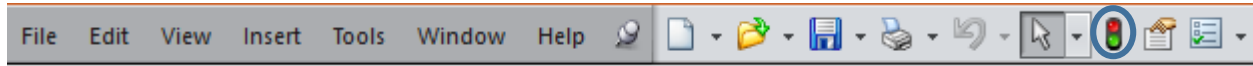


Figure 186: Step 5; Save as an STL

## Step 6: Fixing Scaling Issues (Not Always Applicable)

There is a known issue where using Pack and Go, zipping the folder, or changing the configuration of an assembly can temporarily remove the link between the equations file and the model. To fix this, you need to follow a few short steps. Keep in mind that while this problem will likely be fixed after the first time, it may be a recurring problem. Begin by changing the scaling

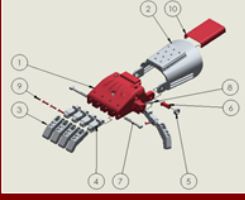
dimension to an arbitrary value within the allowable range (2.8 inches to 3.75 inches) by following steps 1 through 4. Then, open each individual part, rebuild by clicking the To fix this: Follow step open each file and rebuild them by clicking the traffic light icon shown in Figure 187. Then save and close each file. Go back to the main assembly and change the scaling dimension to the desired value. Your assembly should now scale properly.



*Figure 187: Fixing Potential Scaling Issues*

## Appendix C: Brochure

**Prosthetic Hand Parts:**



ITEM NO.	DESCRIPTION	QTY.
1	Hand base	1
2	Gauntlet	1
3	Distal Finger	5
4	Proximal Finger	5
5	wrist pin cap	2
6	wrist pin long	2
7	Knuckle Pin	2
8	Thumb To Hand Pin	1
9	Distal to Proximal Pin	5
10	Gauntlet cover	1

**Additional Hand Parts:**

- 5ft Flexible Elastic Cord
- #8-32-1/2 Screws (x10)
- 8ft of 90lb graded fishing line
- 4ft of 2" Wide Double Sided Velcro
- 3/16-1/2 Binding Post Screws (x3)
- Micro Gel Finger Tip Grips (x5)
- Leather (optional)
- M4-1/2 Screws (x13) (For Leather)
- Firm Medical Foam (12 inch length).

Figure 188: Outside Page of Brochure

**Scaling Instructions:**

1. Open the assembly files in SolidWorks.
2. While the assembly file is open, click on the 'Tools' bar at the top, and then 'Equations.'
3. Next, click on the 'open file' button. This will open a text file with all the variables and equations.
4. Edit the first dimension, 'inputhandwidth', to the width of your hand excluding your thumb.
5. To save the STL files for printing open each unique part. Then go to 'file', 'save as...'
6. When prompted, choose either 'Save as', or 'Save as copy and continue.'
7. Go to the directory of your choosing, name the file as desired, and make sure to save as type: STL.
8. You can then use this STL file to 3D print your part.

**Recommended Tools:**

- Phillips Screw Driver
- Sharp Knife
- Scissors
- Wire Cutters
- Needle Nose Pliers
- Sand Paper (Optional)

**Suggestions:**

- Clean Parts slowly and methodically
- Small parts (keep away from children and pets)
- Take time to assemble
- Be **PATIENT!**

## 3D Prosthetic Hand Assembly Instructions



**Designers:**

Sean Greene  
Dan Lipson  
Abimael Mercado  
Aung Heain Soe

<p>1</p>  <p>Assemble distal to proximal using pin</p>	<p>5</p>  <p>Should resemble image above</p>	<p>9</p>  <p>Repeat for a second finger</p>	<p>13</p>  <p>Feed tension cable through finger and tie using enhanced clinch knot</p>	<p>17</p>  <p>Tighten cables with machine screws. Ensure all fingers move simultaneously</p>	<p>21</p>  <p>Add leather and fasten with M4 -1/2 screws</p>
<p>2</p>  <p>Should resemble image above</p>	<p>6</p>  <p>Attach hand base with fingers to gauntlet using wrist pins</p>	<p>10</p>  <p>Tie excess return cables together providing tension. <b>Do not tie tight!</b></p>	<p>14</p>  <p>Repeat steps for all fingers</p>	<p>18</p>  <p>Once tensioned correctly, add second set of machine screws</p>	<p>22</p>  <p>Add gel finger tips</p>
<p>3</p>  <p>Assemble remaining fingers</p>	<p>7</p>  <p>Add wrist pin caps.</p>	<p>11</p>  <p>Repeat process for remaining fingers. Tie return cable for thumb through hole provided</p>	<p>15</p>  <p>Feed cables through gauntlet tension device channels</p>	<p>19</p>  <p>Add gauntlet cover</p>	<p>23</p>  <p>Cut 1-1/2" wide Velcro and feed through slots on gauntlet. Leave enough slack</p>
<p>4</p>  <p>Attach fingers to hand base using knuckle pins and thumb pin</p>	<p>8</p>  <p>Feed return cable from top of hand base through finger and tie to bridge of finger</p>	<p>12</p>  <p>Cut excess cable and discard</p>	<p>16</p>  <p>Angle gauntlet at 30 degrees before tensioning</p>	<p>20</p>  <p>Add padding to the inside of hand base and gauntlet</p>	<p>24</p>  <p>Congratulations! You have assembled the hand. Make adjustments as necessary. Enjoy!</p>

Figure 189: Inside Page of Brochure

## Appendix D: Mathcad Calculations

### Two Joint Finger Instron Testing Analysis

#### *symbols*

$\epsilon$  = Strain

$E$  = Young's Modulus

$K$  = Stress intensity

$N$  = Factor of Safety

$S_{uc}$  = Ultimate Compressive Strength

$S_y$  = Tensile Yield Strength

$S_{ys}$  = Shear Yield Strength

$U$  = Total Strain Energy

$\nu$  = Poisson's Ratio

$\sigma_1$  = Principal Stress

$\sigma_2$  = Principal Stress

$\sigma_3$  = Principal Stress

$\sigma$  = Modified-Mohr Effective Stress

$\sigma'$  = von Mises effective Stress

$w := 0.64in$

$t := 0.52in$

Factor of Safety = (2) (minimum)

(Non-critical component as failure would not result in serious injury or death.)

Factor of Safety [FS] = Actual Breaking Strength (lb)/Normal Working Load (lb)

In Tensile:

Figure 190: Nomenclature

*NormalWorkingLoad* := 71b  
*ActualBreakingStrength*<sub>1</sub> := 23.424181b +  
*ActualBreakingStrength*<sub>2</sub> := 70.663971b  
*ActualBreakingStrength*<sub>3</sub> := 57.351841b  
*ActualBreakingStrength*<sub>4</sub> := 41.147281b  
*ActualBreakingStrength*<sub>5</sub> := 47.667491b  
*ActualBreakingStrength*<sub>6</sub> := 37.449751b  
*ActualBreakingStrength*<sub>7</sub> := 68.647271b  
*ActualBreakingStrength*<sub>8</sub> := 54.471721b  
*ActualBreakingStrength*<sub>9</sub> := 67.413241b  
*ActualBreakingStrength*<sub>10</sub> := 50.29331b  
*ActualBreakingStrength*<sub>11</sub> := 39.098571b  
*ActualBreakingStrength*<sub>12</sub> := 50.870611b  
*ActualBreakingStrength*<sub>13</sub> := 50.140131b  
*ActualBreakingStrength*<sub>14</sub> := 37.363421b  
*ActualBreakingStrength*<sub>15</sub> := 71.327311b .....  
*ActualBreakingStrength*<sub>16</sub> := 77.543931b  
*ActualBreakingStrength*<sub>17</sub> := 33.488211b  
*ActualBreakingStrength*<sub>18</sub> := 44.048641b  
*ActualBreakingStrength*<sub>19</sub> := 36.029171b  
*ActualBreakingStrength*<sub>20</sub> := 60.691291b

$$FS_1 := \frac{ActualBreakingStrength_1}{NormalWorkingLoad} = 3.346$$

$$FS_2 := \frac{ActualBreakingStrength_2}{NormalWorkingLoad} = 10.095$$

$$FS_3 := \frac{ActualBreakingStrength_3}{NormalWorkingLoad} = 8.193$$

$$FS_4 := \frac{ActualBreakingStrength_4}{NormalWorkingLoad} = 5.878$$

Figure 191: Calculations of Factor of Safety

$$FS_5 := \frac{ActualBreakingStrength_5}{NormalWorkingLoad} = 6.81$$

$$FS_6 := \frac{ActualBreakingStrength_6}{NormalWorkingLoad} = 5.35$$

$$FS_7 := \frac{ActualBreakingStrength_7}{NormalWorkingLoad} = 9.807$$

$$FS_8 := \frac{ActualBreakingStrength_8}{NormalWorkingLoad} = 7.782$$

$$FS_9 := \frac{ActualBreakingStrength_9}{NormalWorkingLoad} = 9.63$$

$$FS_{10} := \frac{ActualBreakingStrength_{10}}{NormalWorkingLoad} = 7.185$$

$$FS_{11} := \frac{ActualBreakingStrength_{11}}{NormalWorkingLoad} = 5.586$$

---

$$FS_{12} := \frac{ActualBreakingStrength_{12}}{NormalWorkingLoad} = 7.267$$

$$FS_{13} := \frac{ActualBreakingStrength_{13}}{NormalWorkingLoad} = 7.163$$

$$FS_{14} := \frac{ActualBreakingStrength_{14}}{NormalWorkingLoad} = 5.338$$

$$FS_{15} := \frac{ActualBreakingStrength_{15}}{NormalWorkingLoad} = 10.19$$

$$FS_{16} := \frac{ActualBreakingStrength_{16}}{NormalWorkingLoad} = 11.078$$

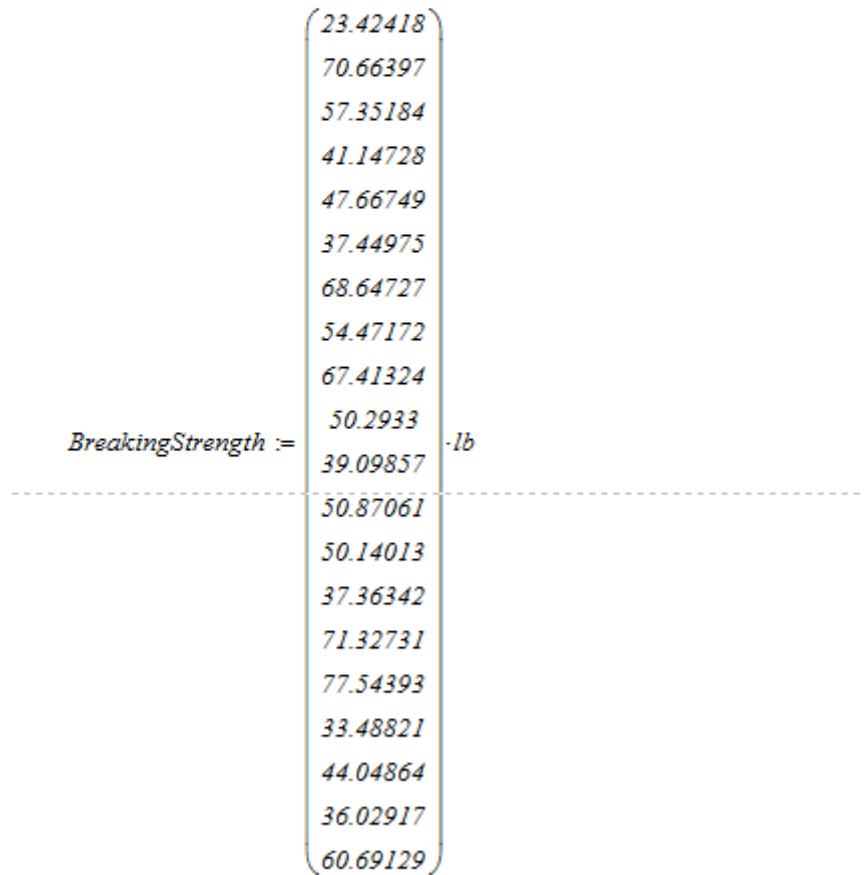
Figure 192: Calculations of Factor of Safety of Tensile Strength; Continued

$$FS_{17} := \frac{ActualBreakingStrength_{17}}{NormalWorkingLoad} = 4.784$$

$$FS_{18} := \frac{ActualBreakingStrength_{18}}{NormalWorkingLoad} = 6.293$$

$$FS_{19} := \frac{ActualBreakingStrength_{19}}{NormalWorkingLoad} = 5.147$$

$$FS_{20} := \frac{ActualBreakingStrength_{20}}{NormalWorkingLoad} = 8.67$$



$$mean(BreakingStrength) = 50.957 \cdot lb$$

$$mean := 50.957 \cdot lb$$

Figure 193: Calculations of Factor of Safety and Mean of Tensile Strength



$$FS_{21} := \frac{\text{mean}}{\text{NormalWorkingLoad}} = 7.28$$

$$\text{Stdev}(\text{BreakingStrength}) = 14.853 \cdot lb$$

$$\text{Stdev} = 14.853 \cdot lb$$

$$FS_{22} := \frac{\text{Stdev}}{\text{NormalWorkingLoad}} = 2.122$$

$$SEM := \frac{\text{Stdev}}{\sqrt{20}} = 3.321 \cdot lb$$

**Distribution (Mean+/-Stdev):**  
**Factor of Safety: 7.3 +/- 2.1**

Cyclic Loading Factors of Safety

$$w := 0.64 \text{ in} \quad t := 0.52 \text{ in}$$

Factory of Safety = (2) (minimum)

(Non-critical component as failure would not result in serious injury or death.)

Factor of Safety [FS] = Actual Breaking Strength (lb)/Normal Working Load (lb)

Test Samples were loaded at 15 pounds for 10 cycles before pulled to failure (fracture) in tension

$$\text{CyclicBreakingStrength}_1 := 17.49858 \cdot lb$$

$$\text{CyclicBreakingStrength}_2 := 27.96492 \cdot lb$$

$$\text{CyclicBreakingStrength}_3 := 39.99246 \cdot lb$$

$$\text{CyclicBreakingStrength}_4 := 30.77332 \cdot lb$$

$$\text{CyclicBreakingStrength}_5 := 47.48729 \cdot lb$$

$$\text{CyclicBreakingStrength}_6 := 54.55284 \cdot lb$$

$$\text{CyclicBreakingStrength}_7 := 37.26089 \cdot lb$$

$$\text{CyclicBreakingStrength}_8 := 73.49201 \cdot lb$$

$$\text{CyclicBreakingStrength}_9 := 57.23729 \cdot lb$$

$$\text{CyclicBreakingStrength}_{10} := 79.02111 \cdot lb$$

$$\text{CyclicBreakingStrength}_{11} := 59.39479 \cdot lb$$

$$\text{CyclicBreakingStrength}_{12} := 60.53239 \cdot lb$$

Figure 194: Calc. of Standard Deviation of Tensile Strength and Data of Cyclic Loading

$$FS_{23} := \frac{CyclicBreakingStrength_1}{NormalWorkingLoad} = 2.5$$

$$FS_{24} := \frac{CyclicBreakingStrength_2}{NormalWorkingLoad} = 3.995$$

$$FS_{25} := \frac{CyclicBreakingStrength_3}{NormalWorkingLoad} = 5.713$$

$$FS_{26} := \frac{CyclicBreakingStrength_4}{NormalWorkingLoad} = 4.396$$

$$FS_{27} := \frac{CyclicBreakingStrength_5}{NormalWorkingLoad} = 6.784$$

$$FS_{28} := \frac{CyclicBreakingStrength_6}{NormalWorkingLoad} = 7.793$$

$$FS_{29} := \frac{CyclicBreakingStrength_7}{NormalWorkingLoad} = 5.323$$

$$FS_{30} := \frac{CyclicBreakingStrength_8}{NormalWorkingLoad} = 10.499$$

$$FS_{31} := \frac{CyclicBreakingStrength_9}{NormalWorkingLoad} = 8.177$$

$$FS_{32} := \frac{CyclicBreakingStrength_{10}}{NormalWorkingLoad} = 11.289$$

$$FS_{33} := \frac{CyclicBreakingStrength_{11}}{NormalWorkingLoad} = 8.485$$

$$FS_{34} := \frac{CyclicBreakingStrength_{12}}{NormalWorkingLoad} = 8.647$$

Figure 195: Calculations of Factor of Safety of Cyclic Loading

$$\text{BreakingStrength2} := \begin{pmatrix} 17.49858 \\ 27.96492 \\ 39.99246 \\ 30.77332 \\ 47.48729 \\ 54.55284 \\ 37.26089 \\ 73.49201 \\ 57.23729 \\ 79.0211 \\ 59.39479 \\ 60.53239 \end{pmatrix} \cdot \text{lb}$$

Cyclic Testing: Safety Factors

$$\text{mean}(\text{BreakingStrength2}) := 48.76732333 \text{ lb}$$

$$\text{meanCyclic} := 48.76732333 \text{ lb}$$

$$FS_{35} := \frac{\text{meanCyclic}}{\text{NormalWorkingLoad}} = 6.967$$

$$\text{stdev}(\text{BreakingStrength2}) := 18.6558952 \text{ lb}$$

$$\text{stdevCyclic} := 18.6558952 \text{ lb}$$

$$FS_{36} := \frac{\text{stdevCyclic}}{\text{NormalWorkingLoad}} = 2.665$$

$$SEM2 := \frac{\text{stdevCyclic}}{\sqrt{12}} = 5.385 \text{ lb}$$

**Distribution (Mean+/-Stdev):**  
**Factor of Safety: 6.9 +/- 2.7**

Figure 196: Calc. of Factor of Safety, Mean and Standard Deviation of Cyclic Loading

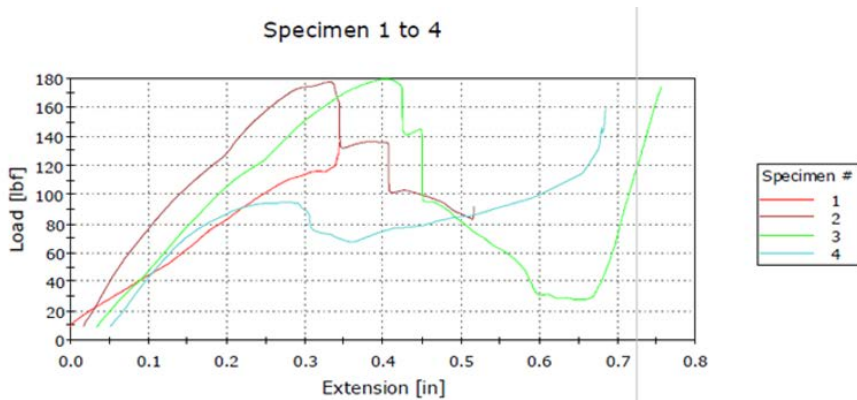


Figure 197: Compression Testing of Two-Segment Fingers

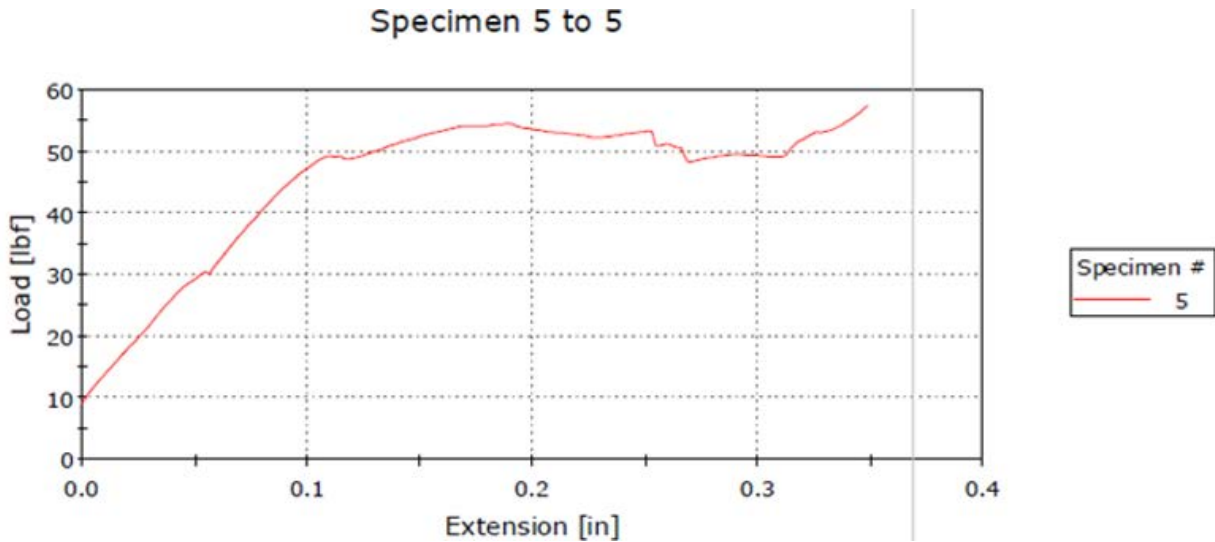


Figure 198: Compression Testing of Two-Segment Finger: Specimen #5

During compression testing, 5 samples were used and subjected to compressive loads until failure. During testing the instron uniaxial testing device failed to recognize the failure or fracture points of each sample. Visually inspecting the graph the points of failure can be extrapolated. Values were estimated for safety factor calculations in compression.

$$\text{CompressionBreakingStrength}_1 := 130lb$$

$$\text{CompressionBreakingStrength}_2 := 175lb$$

$$\text{CompressionBreakingStrength}_3 := 175lb$$

$$\text{CompressionBreakingStrength}_4 := 95lb$$

$$\text{CompressionBreakingStrength}_5 := 50lb$$

$$FS_{37} := \frac{\text{CompressionBreakingStrength}_1}{\text{NormalWorkingLoad}} = 18.571$$

$$FS_{38} := \frac{\text{CompressionBreakingStrength}_2}{\text{NormalWorkingLoad}} = 25$$

Figure 199: Data and Calculations of Factor of Safety of Compression Testing

$$FS_{39} := \frac{CompressionBreakingStrength_3}{NormalWorkingLoad} = 25$$

$$FS_{40} := \frac{CompressionBreakingStrength_4}{NormalWorkingLoad} = 13.571$$

$$FS_{41} := \frac{CompressionBreakingStrength_5}{NormalWorkingLoad} = 7.143$$

$$CompressionBreaking := \begin{pmatrix} 130 \\ 175 \\ 175 \\ 95 \\ 50 \end{pmatrix} lb$$

Compression Testing: Safety Factors

$$mean(CompressionBreaking) := 125lb$$

$$FS_{42} := \frac{mean(CompressionBreaking)}{NormalWorkingLoad} = 17.857$$

$$stdev(CompressionBreaking) := 53.73546315lb$$

$$FS_{43} := \frac{stdev(CompressionBreaking)}{NormalWorkingLoad} = 7.676$$

$$SEM3 := \frac{stdev(CompressionBreaking)}{\sqrt{5}} = 24.031 \cdot lb$$

Figure 200: Calc. of Factor of Safety, Mean and Standard Deviation of Compression Testing

**Distribution (Mean+/-Stdev):**  
**Factor of Safety: 17.9 +/- 7.7**

Tensile Testing Results for 3 Joint Finger  
 Sampes used in testing: 4

$$TensileBreakingStrength_1 := 29.17256lb$$

$$TensileBreakingStrength_2 := 32.46377lb$$

$$TensileBreakingStrength_3 := 24.31022lb$$

$$TensileBreakingStrength_4 := 15.03853lb$$

Figure 201: Data of Compression Testing

$$FS_{44} := \frac{TensileBreakingStrength_1}{NormalWorkingLoad} = 4.168$$

$$FS_{45} := \frac{TensileBreakingStrength_2}{NormalWorkingLoad} = 4.638$$

$$FS_{46} := \frac{TensileBreakingStrength_3}{NormalWorkingLoad} = 3.473$$

$$FS_{47} := \frac{TensileBreakingStrength_4}{NormalWorkingLoad} = 2.148$$

$$TensileBreakingStrength := \begin{pmatrix} 29.17256 \\ 32.46377 \\ 24.31022 \\ 15.03853 \end{pmatrix} lb$$

Tensile: Safety Factors (3 Joint Fingers)

$$\underline{\underline{mean(TensileBreakingStrength)}} := 25.24627 lb$$

$$FS_{48} := \frac{mean(TensileBreakingStrength)}{NormalWorkingLoad} = 3.607$$

$$\underline{\underline{stdev(TensileBreakingStrength)}} := 7.58468204 lb$$

$$FS_{49} := \frac{stdev(TensileBreakingStrength)}{NormalWorkingLoad} = 1.084$$

$$SEM4 := \frac{stdev(TensileBreakingStrength)}{\sqrt{4}} = 3.792 \cdot lb$$

**Distribution (Mean+/-Stdev):**  
**Factor of Safety: 3.6 +/- 1.1**

Figure 202: Calc. of Factor of Safety, Mean and Standard Deviation of Tensile Strength

# Works Cited

---

- i "The Future is Here: 3D Printed Prosthetics." Dealing With Different. Accessed December 16, 2015. <http://dealingwithdifferent.com/3d-printing-prosthetics>.
- ii "ABOUT US." Enabling The Future. 2014. Web. 26 Jan. 2016. <http://enablingthefuture.org/about/>.
- iii Woods, Sean. "Designer Digits." ShowMe. Popular Mechanics, Feb. 2013. Web. 15 Feb. 2016. <http://showme.co.za/lifestyle/designer-digits/>
- iv "Rapid Prototyping: An Overview." EFunda: The Ultimate Online Reference for Engineers. Accessed December 16, 2015. [http://www.efunda.com/processes/rapid\\_prototyping/intro.cfm](http://www.efunda.com/processes/rapid_prototyping/intro.cfm).
- v "3D Printing History: The Free Beginner's Guide." 3D Printing Industry. Accessed December 16, 2015. <http://3dprintingindustry.com/3d-printing-basics-free-beginners-guide/history/>.
- vi "The History of Stereo lithography (SLA) : InTech Industries | Rapid Prototyping." InTech Industries | Rapid Prototyping. Accessed December 16, 2015. <http://www.intechrp.com/the-history-of-stereolithography-sla/>.
- vii "Rapid Prototyping & Manufacturing: Fundamentals of Stereo lithography - Paul Francis Jacobs." Google Books. Accessed December 16, 2015. [https://books.google.com/books?hl=en&lr=&id=HvcN0w1VyxwC&oi=fnd&pg=PA1&dq=history+rapid+prototyping&ots=SsG2OT-OSJ&sig=YNIHPUfRifs\\_KKsi5QTknI9sgKo#v=onepage&q=history%20rapid%20prototyping&f=false](https://books.google.com/books?hl=en&lr=&id=HvcN0w1VyxwC&oi=fnd&pg=PA1&dq=history+rapid+prototyping&ots=SsG2OT-OSJ&sig=YNIHPUfRifs_KKsi5QTknI9sgKo#v=onepage&q=history%20rapid%20prototyping&f=false).
- viii "Rapid Prototyping Techniques, Selective Laser Sintering, 3D Printing & FDM Prototype Mumbai." Rapid Prototyping, Medical Models, Vacuum Casting & 3 D Printing - Protosys Technologies. Accessed October 16, 2015. <http://www.protosystech.com/rapid-prototyping.htm>.
- ix "MultiJet Printing Quickparts." 3D Systems. Accessed November 13, 2015. <http://www.3dsystems.com/quickparts/prototyping-pre-production/multijet-printing-mjp>.
- x "The StL Format | Fabbers.com." Historical Resource on 3D Printing | Fabbers.com. Accessed October 14, 2015. [http://www.fabbers.com/tech/STL\\_Format](http://www.fabbers.com/tech/STL_Format).
- xi "Pros and Cons of Additive Manufacturing." Composites Manufacturing Magazine. Accessed October 24, 2015. <http://compositesmanufacturingmagazine.com/2014/10/pros-cons-additive-manufacturing/>.
- xii "The FAA Cleared the First 3D Printed Part to Fly in a Commercial Jet Engine from GE." GE Reports. Accessed November 26, 2015. <http://www.gereports.com/post/116402870270/the-faa-cleared-the-first-3d-printed-part-to-fly/>.
- xiii "3-D Printer Uses Metal To Make Custom Rib Cage For Cancer Patient: Shots - Health News: NPR." NPR.org. Accessed September 29, 2015. <http://www.npr.org/sections/health-shots/2015/09/15/440361621/engineers-create-a-titanium-rib-cage-worthy-of-wolverine>.
- xiv The Peachy Printer - The First \$100 3D Printer & Scanner. Accessed November 12, 2015. <http://www.peachyprinter.com/>.

- 
- xv "X line 2000R by Machines - Concept Laser" Concept Laser. Accessed October 18, 2015. <http://www.conceptlaserinc.com/machines/>.
- xvi O&P Virtual Library | Orthotics & Prosthetics Journals, Books and Reference Material. Accessed October 29, 2015. [http://www.oandplibrary.org/al/pdf/1955\\_02\\_022.pdf](http://www.oandplibrary.org/al/pdf/1955_02_022.pdf).
- xvii "Enabling the Future – e-NABLE" e-NABLE. Accessed October 18, 2015. <http://enablingthefuture.org/>.
- xviii "Endoskeletal Prosthetic Hand." Office of Rehabilitation Research & Development. Accessed November 28, 2015. <http://www.rehab.research.va.gov/jour/98/35/4/doshi.htm>.
- xix Talon Hand 2.0 (now 2.7) by Profbink - Thingiverse." Thingiverse - Digital Designs for Physical Objects. Accessed November 18, 2015. <http://www.thingiverse.com/thing:229620>.  
"Talon Hand 2.X by e-NABLE." e-NABLE. Accessed November 18, 2015. <http://enablingthefuture.org/upper-limb-prosthetics/talon-hand/>.  
"Interview with Peregrine by e-NABLING the Future." e-NABLE. Accessed November 18, 2015. <http://enablingthefuture.org/upper-limb-prosthetics/talon-hand/>.
- xx "Low-Cost 3D-Printed Dextrus Hand Could Transform Amputees' Lives Low-Cost 3D-Printed Dextrus Hand Could Transform Amputees' Lives – Inhabitat - Sustainable Design Innovation, Eco Architecture, Green Building." Inhabitat | Design For a Better World!. Accessed October 14, 2015. <http://inhabitat.com/low-cost-3d-printed-dextrus-hand-could-transform-amputees-lives/dextrus-hand-5/>.  
"The Open Hand Project - Dextrus." The Open Hand Project - Home. Accessed November 13, 2015. <http://www.openhandproject.org/dextrus.php>.
- xxi "Osprey Hand." Enabling The Future. 2015. Web. 12 Jan. 2016. <http://enablingthefuture.org/osprey-hand/>.
- xxii "Phoenix Hand." Enabling The Future. 2015. Web. 12 Jan. 2016. <http://enablingthefuture.org/phoenix-hand/>.
- xxiii "k-1 Hand." Enabling The Future. 2015. Web. 12 Jan. 2016. <http://enablingthefuture.org/k-1-hand/>.
- xxiv "Material Reference by J. J. Short Associates, Inc." J. J. Short Associates, Inc. Accessed October 23, 2015. <http://www.jjshort.com/Rubber-Properties.php>.
- xxv STRATASYS | ABS Reference Material. Accessed October 29, 2015. <http://www.nrri.umn.edu/NLTC/ABS07.pdf>.
- xxvi "PLA monomer (Polylactic Acid) by MATBASE." MATBASE. Accessed November 18, 2015. <http://www.matbase.com/material-categories/natural-and-synthetic-polymers/agro-based-polymers/material-properties-of-polylactic-acid-monomere-pla-m.html#properties>.
- xxvii Stephens, Brent (November 2013). "Ultrafine particle emissions from desktop 3D printers". Atmospheric Environment 79: 334–339.
- xxviii "Frequently Asked Questions About PLA Earth-Friendly Products." Welcome to the Store. Accessed November 15, 2015. <http://www.lollicupstore.com/PLA-FAQ.htm>.



---

xxxix "Bioplastics – Study: Market, Analysis, Trends | Ceresana." Ceresana | Marktstudien Für Industrie, Chemie & Kunststoffe. Accessed October 13, 2015.

<http://www.ceresana.com/en/market-studies/plastics/bioplastics/>.

xxx "The Difference between ABS and PLA for 3D Printing by Luke Chilson- ProtoParadigm" ProtoParadigm. Accessed October 18, 2015. <http://www.protoparadigm.com/news-updates/the-difference-between-abs-and-pla-for-3d-printing/>.

xxxixi Tobuya 3D Printer. Web. 5 Mar. 2016. <http://tobuya3dprinter.com/wp-content/uploads/2014/03/da-vinci-1-3d-printer-review.jpg>

xxxixii Javelin Tech. Web. 2 Mar. 2016. [http://www.javelin-tech.com/3d-printer/wp-content/uploads/2013/06/printer\\_dimension\\_1200\\_alt.jpg](http://www.javelin-tech.com/3d-printer/wp-content/uploads/2013/06/printer_dimension_1200_alt.jpg).

xxxixiii "Makerbot Replicator 2X - LabFab." *LabFab*. Web. 23 Jan. 2016. <http://www.labfab.fr/makerbot-replicator-2x/>.

xxxixiv "Sindoh 3DPrinter." Sindoh 3DPrinter. Web. 26 Mar. 2016. <http://3dprinter.sindoh.com/Product3Dwox>

xxxixv WorldWhiteWeb. Web. 20 Apr. 2016. <http://www.worldwhiteweb.net/images/hands/human-hand.jpg>